UAB
Universitat Autònoma de Barcelona

Regulation of the mitotic exit in eukaryotic cells

Alberto Zurita Carpio

Regulation of the mitotic exit in eukaryotic cells

Alberto Zurita Carpio

Biophysics Unit

Department of Biochemistry and Molecular biology

School of Medicine

Universitat Autònoma de Barcelona

2023

Universitat Autònoma de Barcelona

School of Medicine

Department of Biochemistry and Molecular Biology

Biophysics Unit

Regulation of the mitotic exit in eukaryotic cells

A thesis submitted in conformity with the requirements for the degree of Doctor in Biochemistry, Molecular Biology and Biomedicine

Autonomous University of Barcelona

January 2023

Ph.D. Candidate

Alberto Zurita Carpio

Thesis supervisor

Dr. David G. Quintana

To my parents, for always believing in me

Abstract

In eukaryotic cells, mitosis is the cell cycle phase in which the replicated chromosomes are segregated (anaphase) and the cell is physically divided into two daughter cells at the mitotic exit (cytokinesis). Multiple controls operate to prevent the occurrence of mitotic exit before the completion of chromosome segregation, which would result in genomic instability and aneuploidy, conditions that fuel malignant transformation.

A critical control layer is enforced by the Mitotic Cyclin Dependent Kinase activity (M-Cdk1). The release from the nucleolus to the cytosol of the Cdc14 phosphatase, which counteracts M-Cdk1 phosphorylation activity, is essential to trigger mitotic exit. Null mutations in Cdc14 or in the Mitotic Exit Network (MEN), responsible for the controlled release of Cdc14, arrest cells after anaphase, unable to undergo cytokinesis. Therefore, one or more M-Cdk1/Cdc14 substrates are critical to block a premature mitotic exit.

Using the model eukaryotic organism *Saccharomyces cerevisiae*, we devised an experimental approach to identify the minimal set of substrates through which M-Cdk1 blocks premature cytokinesis. Cells over-expressing an inducible copy of the hyperstable mitotic cyclin *clb2ΔN* mutant permanently arrest after anaphase, unable to undergo mitotic exit. Therefore, cells carrying non-phosphorylatable alleles of the critical M-Cdk1/Cdc14 substrates should be able to enter mitotic exit in the presence of sustained high M-Cdl1 activity.

In this thesis, we show that a strain carrying non-phosphorylatable alleles of the MEN kinases Cdc15 and Mob1-Dbf2 partially overrides the control of M-Cdk1 activity, as the kinases localise prematurely to the Spindle Pole Bodies, the sites for MEN activation. Despite bypassing such control, cells under sustained high M-Cdk1 activity fail to release Cdc14 to the cytosol and mitotic exit does not occur. These observations point to at least an additional critical M-Cdk1 target upstream in the MEN pathway.

Contents

1. Introduction

1.1. The eukaryotic mitotic cell cycle

The mitotic cell cycle is the biological process through which a cell duplicates its genetic material and distributes it equally to give place to two identical daughter cells. The mitotic cell cycle is a complex and tightly regulated process and has been historically divided into four distinct phases based on the gross chromosomal events that occur in the cell[1]: (1) the G1 (for Gap 1) phase includes the biological processes that a cycling cell undergoes to prepare for a round of DNA replication, namely reaching an adequate mass and expressing genes essential for chromosome replication. (2) In S phase, the cell undergoes the bulk of chromosome replication. (3) During G2 phase the cell undergoes a transcription wave required for mitosis. (4) Finally, during M phase, chromosomes are condensed, and one complete set of chromosomes is segregated into opposite cell poles. At the end of M phase, the cell splits to give place to two daughter cells, through a process termed cytokinesis.

1.2. The *Saccharomyces cerevisiae* eukaryotic model organism

Yeasts, particularly the budding yeast *Saccharomyces cerevisiae (S. cerevisiae),* have been used as an experimental model to study the eukaryotic cell cycle for decades. The critical biological processes and controls are conserved to humans[2].

Many are the advantages of working with budding yeast. *S. cerevisiae* was the first eukaryotic organism to be completely sequenced[3]. The entire genome information and databases are available in the *Saccharomyces Genome Database* (SGD, www.yeastgenome.org), allowing the fast design of genomic manipulation strategies.

In this regard, despite wild *S. cerevisiae* switches from diploid to haploid state, laboratory strains have been modified to remain stably haploid, which halves the requirements for genomic modification. Furthermore, budding yeast readily integrates DNA fragments by homologous recombination, which greatly facilitates

site-directed integration of deletion cassettes, promoter replacement or in-frame tags. Integration clones are easily selected either through antibiotic resistance markers or through several nutrient autotrophy markers. Laboratory strains have been conveniently modified for several auxotrophies.

Also, *S. cerevisiae* cells develop a small protuberance (bud) throughout the course of the cell cycle, which becomes the so-called *daughter* cell upon division. Conveniently, bud emergence and growth correlate with progression through the cell cycle, which allows for easy monitoring of the cell phase using light microscopy. Also, because the bud size is always smaller than the mother cell body, both *mother* and *daughter* cells can be easily distinguished under the microscope (figure 1.1).

As another advantage, the doubling time of *S. cerevisiae* is short compared to mammalian cells (around 90 minutes in complete medium at 30ºC).

Last, but not least, most growth media are inexpensive compared with the media required to grow mammalian cells. In addition, the ability to grow under different medium compositions allows one to take advantage of two reliable promoters which modify gene expression: the strong *GAL* promoter, which positively expressed proteins under its control in the presence of galactose[4], and the *MET3* promoter, repressed by the presence of methionine[5,6].

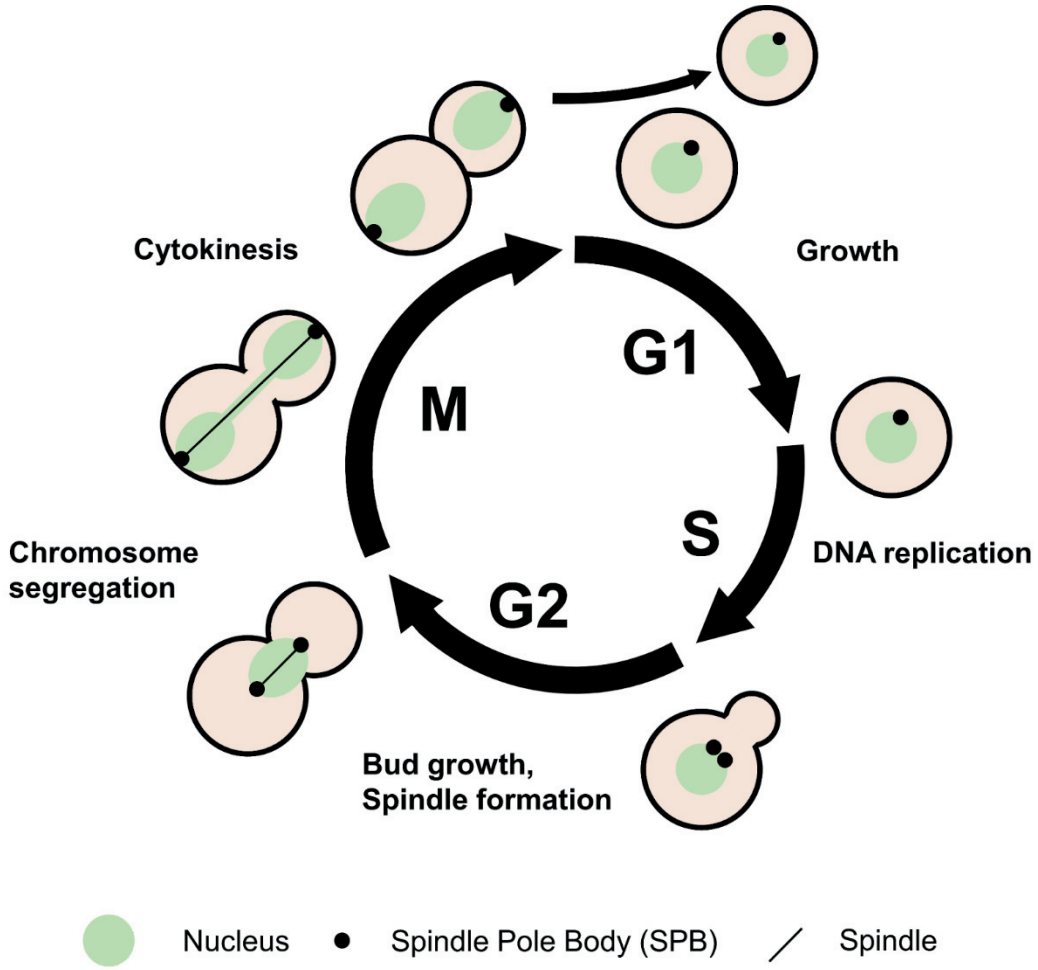

Figure 1.1. The Saccharomyces cerevisiae cell cycle.

1.3. Eukaryotic cell cycle control

Cell cycle progression is highly regulated to ensure that genetic information is preserved. Loss of genomic integrity results in loss of viability and generation of genomic instability[7]. Genomic instability is the leading force that in higher eukaryotes drives malignant transformation.

An alteration of the orderly process of events during the cell cycle, either by premature entry into replication, chromosome segregation before replication is complete, or cytokinesis before chromosome segregation is finished, results in either loss of viability or viability with loss of genomic integrity[8].

Current knowledge of eukaryotic cell cycle regulation reveals four major modes of control.

First, the sequence of critical cell cycle events is unidirectional and irreversible[9]. Such directionality is based on the regulated expression and destruction of the critical activities and substrates required at each given time of the cell cycle[10]. An initial cell cycle event, called the Restriction point (R point) in mammalian cells and START in budding yeast, commits cells to one round of mitotic division cycle. For a cell to cross the R point, pro-proliferative signalling must prevail, and the cell must have reached a critical mass that ensures it will be able to support a round of division[11]. After crossing the R point, cells trigger a program of interdependent transcriptional waves. Each wave produces the proteins required for the subsequent cell cycle phase and to enable the next transcriptional wave[12].

Two of the modes of control ensure that each critical event occurs once and only once per cycle. One, cell-cycle regulated kinase activities are essential both to trigger specific cell cycle events, and also to inhibit licensing factors from reloading[13]. The other, essential phase-specific factors and cell cycle inhibitors are timely targeted for destruction by the ubiquitin-proteasome system[14,15]

Finally, a fourth major control mode exists in the form of *feed-forward* surveillance mechanisms, better known as checkpoints[16]. Checkpoints are signal transduction mechanisms that monitor different key cell cycle events and ensure that, whenever a problem that threatens genomic integrity is detected, the cell cycle is halted to give the cell time for correction. An example of this is the Spindle Position Checkpoint, which blocks mitotic exit until the two divided nuclei are fully segregated into the bodies of the future daughter cells (section 1.4.4.1. below).

1.3.1. Cyclin-dependent kinases (CDKs)

Cell cycle progression is driven by highly conserved kinase proteins called Cyclin-Dependent Kinases (CDKs)[17]. CDKs were first discovered as part of the Cell Division Cycle (CDC) family in the groundbreaking genetic screens in *Saccharomyces cerevisiae* and *Schizosaccharomyces pombe* performed respectively by Lee

Hartwell[18] and Paul Nurse[19]. They were later renamed CDKs at the Cold Spring Harbor Symposium on Cell Cycle in 1991[20].

Although six different CDK paralogs are present in budding yeast[21], Cdk1, expressed from the *CDC28* gene, is the single essential CDK that drives all the main processes throughout the cell cycle[22–24]. In yeast, Cdk1 is constitutively expressed, and its regulation depends on the expression or degradation of the different cyclins to which Cdk1 binds. In higher eukaryotes, however, different CDK paralogs act on specific phases of the cycle (figure 1.2)

CDKs phosphorylate serine or threonine residues that are followed by a proline[25]. Such activity is dependent on the binding of an activating subunit called cyclin[10]. Different phase-specific cyclins confer the different levels of specific activity required to progress through the different cell cycle phases, and also a certain extent of substrate specificity[26–31]

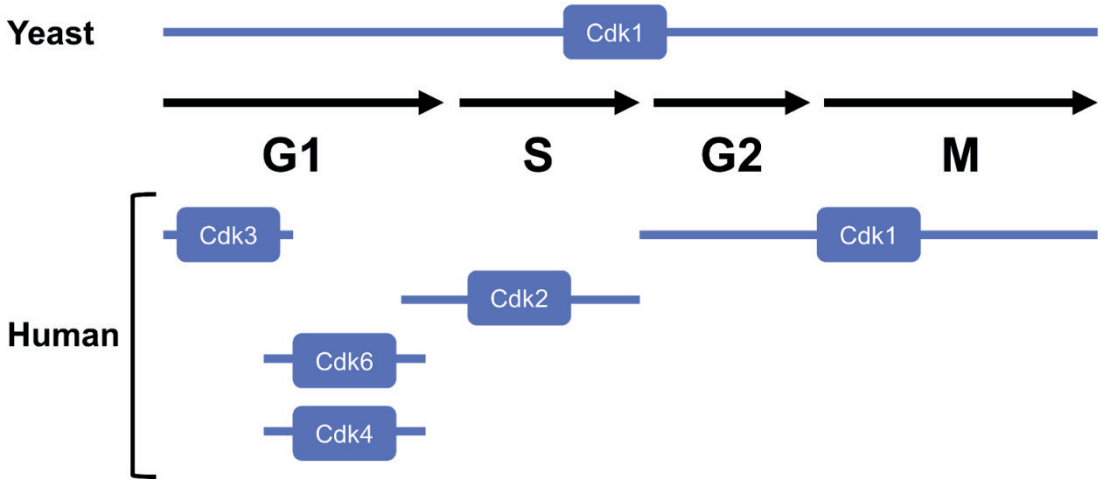

Figure 1.2. Cyclin-Dependent Kinases in humans and yeast. In yeast, only one CDK, Cdk1 (*CDC28*) is responsible for all the events of the cell cycle. In human cells, however, different CDKs are active at different points of the cell cycle.

1.3.2. Cyclins

Cyclins are activator subunits of CDKs. Cyclins were discovered in sea urchin embryos by Tim Hunt as proteins that appeared and disappeared in a phase-specific manner in the embryonic mitotic cell cycle upon egg fertilisation[10]. Nine different

cyclins are present in budding yeast, which are categorised according to the phase of the cycle in which they are present: three G1-specific cyclins (Cln1-3) and six B-type cyclins (Clb1-6)[32,33].

Cln3 is a protein present from G1 until the G2/M phase[34]. During early G1, Cln3-Cdk1 complexes remain sequestered at the endoplasmic reticulum bound to Whi7[35]. When cells progress through G1 and grow in mass, accumulation of the J chaperone Ydj1 outcompetes Cln3-Cdk1, which is thus released[36]. Nuclear Cln3-Cdk1 activates the transcription factors MBF and SBF that define START[37].

Late G1 cyclins Cln1 and Cln2, and S-phase cyclins Clb5 and Clb6 are among the pool of proteins that are expressed upon START[38,39]. Accumulation of Cln1,2-Cdk1 activity eventually targets the S-phase Cyclin-Dependent Kinase Inhibitor Sic1 for destruction[40], thus releasing the Clb5,6-Cdk1 activity that defines the entry into S-phase and triggers DNA replication[38,41].

In yeast, G2 cyclins Clb3 and 4 play an accessory role and are dispensable[42,43].

Finally, M phase cyclins Clb1 and Clb2, expressed in G2 phase under the SFF-driven transcriptional wave[44,45], are both responsible for triggering mitosis and blocking premature cytokinesis[46–48].

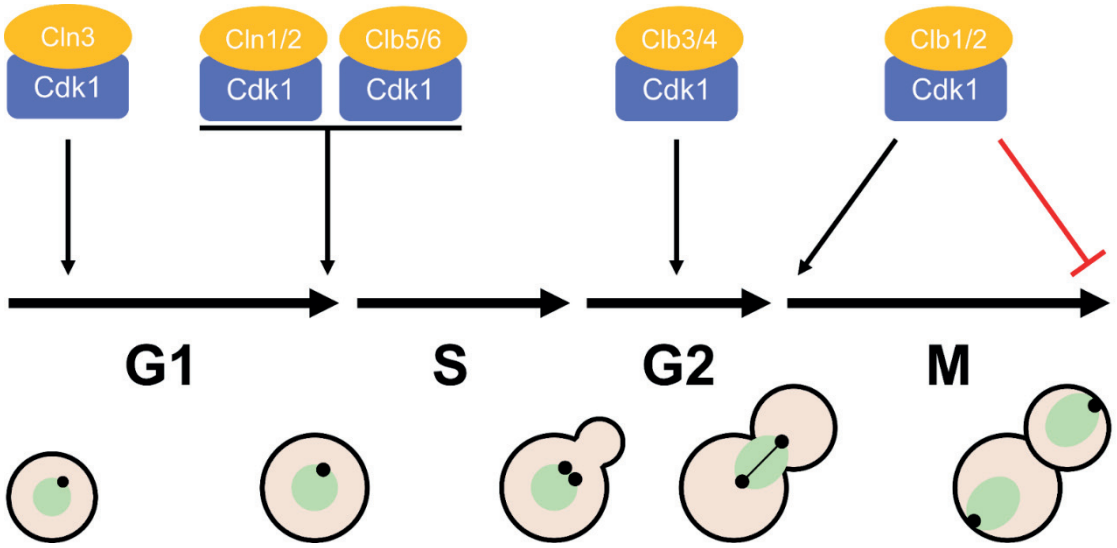

Figure 1.3. Cyclins in S. cerevisiae during the cell cycle.

1.3.3. Regulation of Cdk1 activity

Cdk1 levels remain constant throughout the cell cycle[49]. However, the catalytic Cdk1 subunit is inactive without several modifications.

CDK activity requires a specific activatory phosphorylation to grant cyclin binding. Cdk1 is phosphorylated by the CDK-Activating Kinase Cak1 at the conserved Threonine 169 (T169) on the T-loop, which is required for cyclin binding[50,51]. Puzzlingly, Cak1 activity is constant throughout the cell cycle[52].

Cdk1 can also be negatively regulated through different mechanisms: the binding of CDK inhibitors (CKIs) and the downregulation of CDK activity by inhibitory phosphorylation.

In G1 phase, the CKI Sic1 prevents premature S-Cdk1 activation[53]. Sic1 is expressed at the very last transcriptional wave in the cell cycle, driven by SWI5 in telophase[40]. Sic1 specifically blocks Cdk1 activity associated with Cb1-6 cyclins (S, G2, M), but not Cdk1 activity associated with Cln1-3 cyclins (G1)[53]. As cells progress through the post-START G1 phase, accumulation of Cln1,2-Cdk1 activity eventually targets Sic1 for destruction[40], thus releasing the Clb5,6-Cdk1 activity that defines the entry into S-phase and triggers DNA replication[54,55].

Finally, Cdk1 phosphorylation at the conserved tyrosine 19 (Y19) by the Swe1 kinase specifically inhibits mitotic Cdk1 (M-Cdk1) activity[56,57], with no effect on S phase Cdk1 (S-Cdk1). Swe1 mediates the cell cycle arrest elicited by the DNA damage checkpoint, which blocks the segregation of damaged or incompletely replicated chromosomes[56].

1.3.4. Regulation of cyclins

Except for Cln3, which is constitutively expressed at regular levels throughout the cell cycle, cyclins are regulated by regulated expression and destruction. Each particular cyclin is expressed before the phase where it is needed, and it is then destroyed once its activity would affect further cell cycle progression.

1.3.4.1. Transcriptional regulation

The expression of cyclins is mediated by the coordination of different transcriptional waves, which allow for the expression of the factors necessary to undertake each step of the cell cycle (1.3.5.). Each transcriptional wave is also responsible for preparing the next one. Coordinated with the timely destruction of both cyclin and other elements of the cell cycle machinery, these two elements confer the cell cycle unidirectionality.

Sensibly, expression of *CLN3*, the G1 cyclin responsible to trigger the cell cycle programme by allowing the cells to cross START[58–60] is responsive to nutrient availability[61]. In contrast to the rest of the cyclins, Cln3 expression is not cell cycle regulated[34,62]. When nutrients are available, Whi3 sequesters at the endoplasmic reticulum both the *CLN3* mRNA and the Cdk1 protein during early and mid-G1[63–65]. Cell progression through G1 involves growth in mass, which results in the accumulation of the J chaperone Ydj1. Ydj1 binding to Whi3 results in the release of *CLN3* mRNA and Cdk1[36]. Assembled Cln3-Cdk1 translocates to the nucleus, where it phosphorylates and inactivates the transcriptional repressor Whi5, thus freeing the transcription factors MBF (Mlu I Cell-Cycle Box Binging Factor) and SBF (Swi4/6 Cell-cycle Box Binding Factor) that unleash START[66,67].

CLN1 and *CLN2* are expressed upon START by transcription factor SBF and MBF[68,69]. Cln1 and Cln2 are unstable proteins, as they are constantly targeted for destruction by the SCF^{Cdc4} (Cln1) and the SCF^{Grr1} (Cln1 and Cln2) ubiquitin ligases[70]. Such targeting is dependent on the Cdk1 phosphorylation of both cyclins[71] Their presence is, therefore, dependent on active expression and translation.

CLB5 and *CLB6* are also transcribed during START, under MBF[72,73]. Interestingly, the presence of Clb6 protein is short-lived, as it is targeted for proteasome degradation during early S phase by the ubiquitin-ligase SCF^{Cdc4} [74]. The reasons for such an early elimination are not elucidated. Clb5 is targeted by proteasome degradation later in mitosis, by ubiquitin-ligase APC^{Cdc20} and APC^{Cdh1} [75,76] (Anaphase Promoting Complex).

CLB3 and *CLB4* transcription occurs at the end of S phase, under the Hcm1 transcription factor[77], and remain present until the end of the cell cycle, when both are targeted for destruction by the APC[78–80].

CLB1 and *CLB2* transcription occurs at the end of S-phase, under the transcriptional wave driven by SFF[77]. Clb1 and Clb2 levels build up until metaphase, when levels peak and so does M-Cdk1 activity. At the metaphase-anaphase transition, activation of the ubiquitin ligase APC^{Cdc20} promotes a partial reduction in the levels of both mitotic cyclins[81]. At the exit of mitosis, the APC^{Cdh1} ubiquitin ligase is responsible for the complete elimination of Clb cyclins[82–85].

1.3.4.2. Regulation by polyubiquitin-proteasome degradation

Mitotic cyclins are recognised by the E3 ubiquitin ligase APC^{Cdc20} (see section 1.4.2.2 below) through a consensus recognition sequence called destruction box (D box) located at their N-terminus[84,85]. Thus, in a finely tuned negative feedback loop, high M-Cdk1 activity in metaphase activates the APC^{Cdc20}. In turn, the APC^{Cdc20} partially decreases the mitotic cyclin complement, to adjust the M-Cdk1 activity to the level required for accurate anaphase[86].

The Clb2 N-terminus contains two additional recognition sequences, termed KEN boxes because of the presence of Lysine, Glutamic and Asparagine[87] KEN boxes are specifically recognised by the E3 ubiquitin ligase APC^{Cdh1} which, among other targets, fully terminates Clb cyclins at the end of mitosis[81] (figure 1.4).

The fact that mitotic cyclins are regulated by sequence recognition at their N-termini, allows for the creation of hyperstable mutants by deletion of the N-terminus[88,89].

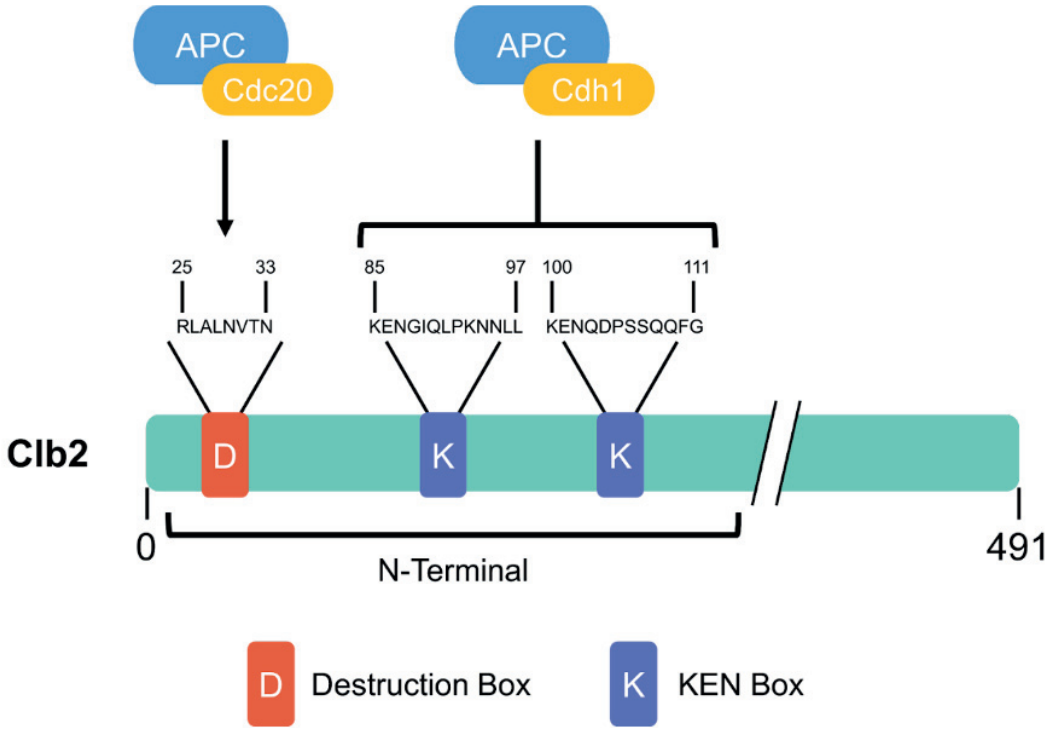

Figure 1.4. Clb2 regulation by the APC. During anaphase, APC^{Cdc20} ubiquitinates Clb2 at its D-box, which decreases Clb2 levels by half. This decrease, together with the release of Cdc14, results in the activation and relocalisation of Cdh1, which binds to the APC to form active APC^{Cdh1}. APC^{Cdh1} ubiquitinates Clb2 at its two KEN boxes, eliminating the cyclin at the mitotic exit.

1.3.5. Two coupled oscillators drive the cell cycle

The transcriptional oscillator set off at START feeds the cyclin-dependent kinase oscillator by expressing the different waves of phase-specific cyclins. In turn, the different phase-specific Cdk1 activities trigger START and ensure the robustness of the subsequent transcriptional waves[90]. Finally, the Cdk1 activities target the different cyclins for destruction via ubiquitin ligase-proteasome.

Thus, in G1, once the cell achieves a critical mass[36], Cln3-Cdk1 inactivates the transcriptional repressor Whi5[67], the yeast analogue of mammalian pRB. Whi5 is a repressor of the expression of genes regulated by transcription factors SBF (Swi4/6 cell-cycle box Binding Factor) and MBF (Mlu I cell-cycle box binding factor), a heterodimer of Mbp1 and Swi6[73,91,92]. SBF is responsible for the expression of G1 cyclins Cln1 and Cln2[93], while MBF is responsible for the expression of S phase

cyclins Clb5 and Clb6[55]. A third transcription factor, Hcm1, is expressed as well during this first wave[94].

During S phase, Hcm1 is responsible for the expression of the elements of SFF (Swi Five Factor), the transcription factor responsible for the next transcriptional wave. Later in the cell cycle, SFF promotes the expression of mitotic cyclins Clb1 and Clb2, as well as the final transcription factors involved in the cell cycle, Ace2 and Swi5[95,96].

Ace2 and Swi5 promote the expression of G1 genes, as well as Sic1[97]. Sic1 inhibits Clb-Cdk1 when S phase cyclins start accumulating in post-START during G1, thus avoiding premature initiation of replication[53].

Destruction of cyclins is mediated through regulated ubiquitination by the ubiquitin-proteasome system. Two essential ubiquitin-ligase complexes exist in yeast: SCF (Skp1, Cullin, F-Box) and the APC (Anaphase Promoting Complex)[84,98]. SCF is active throughout the cell cycle and is regulated by the phosphorylation of its potential substrates. Most of its substrates are dependent on Cdk1 itself, such as Sic1[99]. The APC, however, is activated by M-Cdk1 activity during the M phase[100] and targets all substrates containing specific consensus sequences, such as the destruction boxes (D box) found at the N-terminal region of Clb1 and Clb2[85].

1.4. Control of Mitosis in *Saccharomyces cerevisiae*

1.4.1. Regulation of mitotic onset

Mitosis entry is promoted by Cdk1 bound to mitotic cyclins Clb1 or Clb2 (M-Cdk1). During M phase, duplicated chromosomes are condensed, and positioned in the centre of the cell, and the two sister chromatids are segregated into each of the future descendant cells[101]. Sister chromatid segregation is achieved through a microtubule structure termed mitotic spindle, which attaches a protein structure located at the centrosome of each chromosome, the kinetochore, to another structure located at each pole of the cell, the centrosome, called Spindle Pole Body (SPB) in budding yeast. The spindle then pulls the chromatids towards each centrosome, allowing for

a balanced separation of DNA. While in higher eukaryotes the nuclear envelope is disassembled during this process, in budding yeast the nuclear envelope remains intact throughout mitosis, stretching and enlarging as required during chromosome segregation.

The M phase can be subdivided into five distinct stages, based on the changes in the nucleus and cytoskeleton morphology (figure 1.5): prophase, prometaphase, metaphase, anaphase, and telophase.

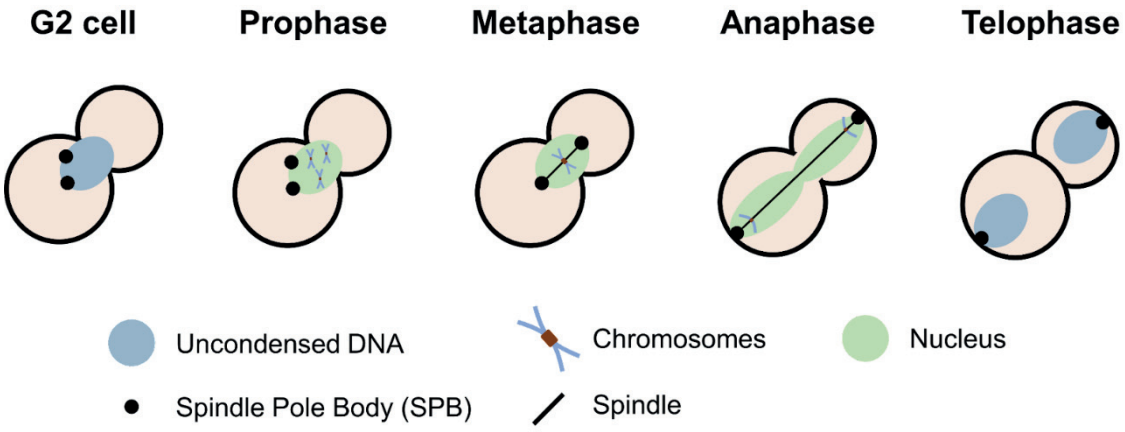

Figure 1.5. M phase main events in S. cerevisiae. During prophase, replicated chromosomes condense and kinetochores assemble. In higher eukaryotes, the nuclear envelope is then disassembled, and centrosomes are duplicated and located at the pole of each daughter cell. Due to the lack of nuclear envelope disassembly in budding yeast, the SPBs are attached to the nuclear envelope. Later, in prometaphase, chromosomes continue condensing and the nucleus migrates to the centre of the cell. Also, during prometaphase, the mitotic spindle starts attaching to the chromosomes at the kinetochores. Metaphase is achieved once all chromosomes are positioned at the centre of the cell and centromeres attach to the spindle with each chromatid pair under bipolar tension. Premature chromosome segregation is prevented by the cohesion of sister chromatids (see the section about APC^{Cdc20}).

Once metaphase is completed, cells enter anaphase, during which sister chromatid cohesion is lost and chromosome segregation takes place. Once chromosome segregation is completed, cells enter telophase. During telophase, the mitotic spindle starts disassembling, chromosome decondensation begins and the nuclear envelope reappears in higher eukaryotes. After mitosis is completed (karyokinesis, separation

of nuclei) the cell splits in two (cytokinesis, separation of two cells). During cytokinesis plasma ingression takes place, dividing the cytoplasm into two daughter cells.

1.4.2. Regulation of the metaphase to anaphase transition

During prometaphase, compacted, sister chromatids are bound together by cohesin, a highly conserved structure formed by proteins Smc1, Scc1 and Scc3. At the centromere of each chromatid, the kinetochore structure is formed, which connects chromosomes with spindle microtubules.

Kinetochores are complex structures consisting of multiple copies of at least 50 unique components[102]. The two sister chromatids are attached through the kinetochores to a spindle microtubule connected to each of the Spindle Pole Bodies (SPBs), in an amphitelic (bi-polar) orientation[103]. Guided by these microtubules, chromosomes migrate to the two cell poles later in anaphase.

Once all chromosomes are attached to the spindle, with sister chromatids under bi-oriented tension, the so-called Spindle Assembly Checkpoint (SAC, see below) inactivates, allowing the activation of the APC^{Cdc20} ubiquitin ligase.

APC^{Cdc20} targets Pds1/securin for destruction via the proteasome. Pds1/securin is an inhibitor of Esp1/separase, which now activates. The essential substrate of Esp1/separase is the cohesin subunit Scc1[104,105]. Loss of cohesion frees the sister chromatids from each other, which can now migrate to opposite poles.

1.4.2.1. The Spindle Assembly Checkpoint (SAC)

Monitoring amphitelic chromosome attachment is crucial to preserve genomic integrity. A key player is the Spindle Assembly Checkpoint (SAC), a surveillance mechanism that targets Cdc20 and negatively regulates its ability to activate the APC, thus preventing premature entry into anaphase.

In yeast, the SAC works through the formation of a Mitotic Checkpoint Complex (MCC), which contains three SAC proteins, Mad2, Mad3 and Bub3, as well as Cdc20. The MCC binds to the APC and inhibits its activity[106]. Other SAC components, such as Mad1, Bub1, MPS1 or Ipl1 (Aurora-B in higher eukaryotes) amplify the SAC signal and rate of MCC formation[107–110]

During prometaphase, Cdc20 and the SAC proteins Mad1 and Mad2 concentrate at unattached kinetochores, promoting the dynamic formation of MCC complexes that keep APC^{Cdc20} inhibited. Attachment of the kinetochores to the microtubules results in the release of SAC components Mad1 and Mad2, thus abolishing the formation of MCC complexes. This results in the release of Cdc20[111], which is now able to assemble the functional ubiquitin ligase APC^{Cdc20}.

Although MCC formation is decreased as chromosomes are attached to microtubules, a single unattached kinetochore is enough to keep the SAC active and block entry into anaphase[112]. Also, because microtubule-kinetochore attachment depends on stable bi-oriented tension[113,114], which in turn depends on the amphitelic attachment of sister chromatids, the SAC also indirectly monitors that sister chromatids are under bi-oriented tension.

Finally, additional mechanisms exist to fix incorrect attachment of kinetochores to the SPBs, such as when the two kinetochores in a chromosome are attached to the same SPB (syntelic attachment), which is fixed by the Ipl1/Aurora-B kinase. In tensionless kinetochores, Ipl1 phosphorylates the kinetochore protein Ndc80, which results in the dissociation of the kinetochore-microtubule interaction, allowing for the attachment to a microtubule of the correct spindle pole[115–117].

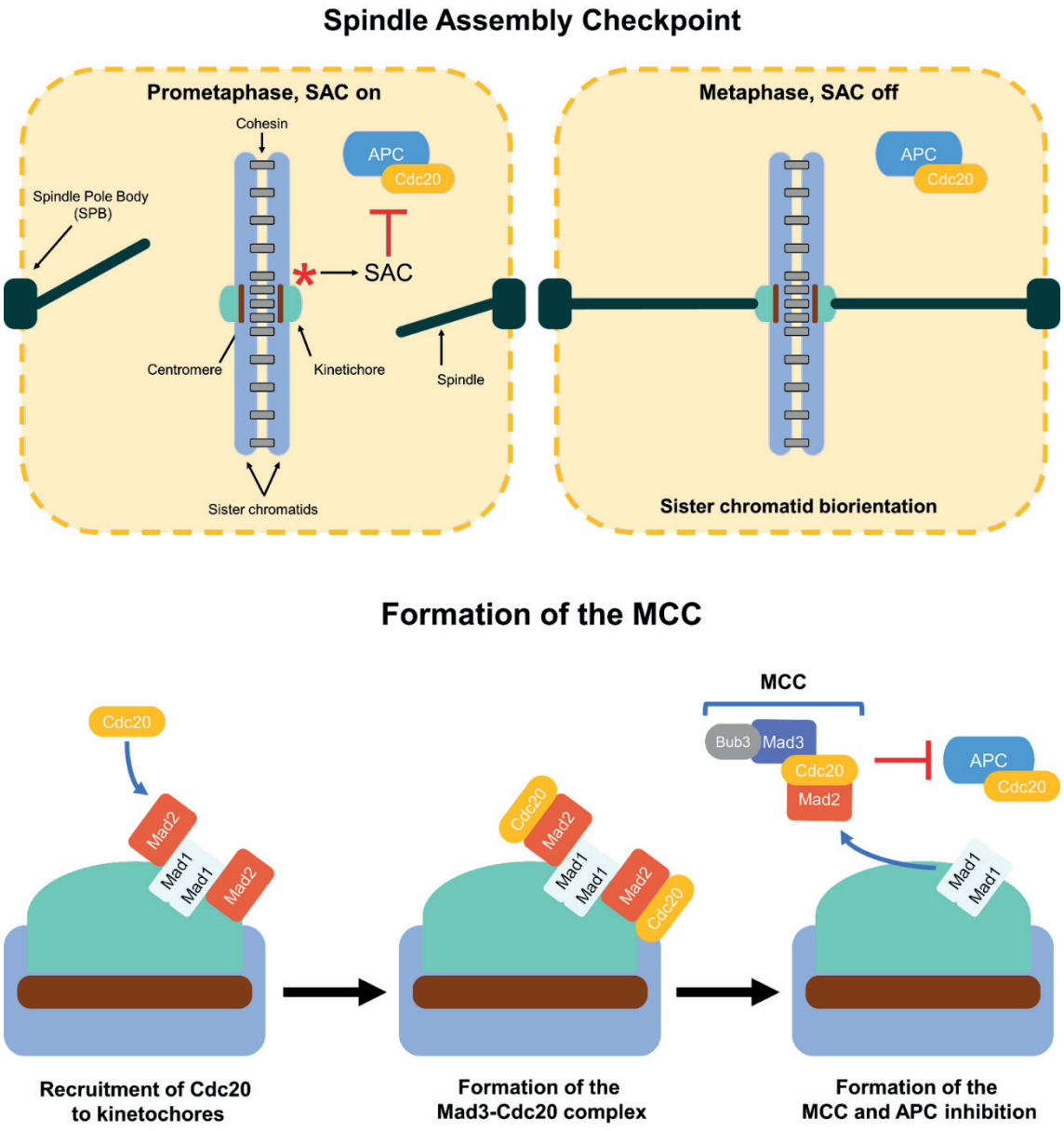

Figure 1.6. The Spindle Assembly Checkpoint.

1.4.2.2. The Anaphase Promoting Complex (APC)

The Anaphase Promoting Complex (APC) is the E3 ubiquitin ligase responsible for the metaphase-to-anaphase transition[118]. The APC is responsible for the polyubiquitination (and subsequent degradation via proteasome) of key proteins involved in mitosis. In yeast, this large macromolecular complex consists of at least 13 subunits and, much like Cdk1, is regulated by the binding of a partner which confers activity and substrate specificity: During metaphase, the APC binds to Cdc20

and promotes degradation of Pds1[118], as well as a reduction in the levels of Clb cyclins[48].

The essential role of APC^{Cdc20} is to promote the degradation of Pds1/securin that blocks anaphase onset[118]. During an unperturbed cell cycle, Cdc20 protein levels accumulate from late S phase, peaking in early mitosis[119]. Once the Spindle Alignment Checkpoint deactivates, Cdc20 is released from the MCC and binds to APC, thus forming an active ubiquitin ligase.

At the time of mitotic exit, the MEN released Cdc14 activates Cdh1 by phosphorylation[120]. APC^{Cdh1} completes Clb cyclin degradation[81,83], which resets the cell cycle. In addition, APC^{Cdh1} targets for destruction Cdc20[82] and mitotic kinase Cdc5[121], contributing to the relocalisation of Cdc14 to the nucleolus.

1.4.2.3. Esp1/separase

Esp1/separase is a caspase-like cysteine protease. Its role in cleaving the cohesin subunit Scc1 is an essential step for sister chromatid separation. Esp1 protein is present throughout the cell cycle[122]. Once Esp1 cleaves Scc1, spindle elongation pulls the SPBs to the poles, connected to the SPBs through astral microtubules, thus segregating sister chromatids, which defines anaphase[104].

A second role of Esp1 during anaphase is the cleavage of the spindle midzone and kinetochore-associated protein Slk19[123,124]. Slk19 cleavage is required for the stabilisation of the spindle during elongation and facilitates chromosome bipolar attachment[124–127].

Esp1 is also responsible for the transient release of the Cdc14 phosphatase in anaphase from the nucleolus to the nucleoplasm (see the FEAR section in 1.4.3 next below)[123,128,129].

Esp1 is inhibited by the chaperone Pds1/securin. Phosphorylation of Pds1 by Cdk1 activity promotes Esp1/Pds1 complex formation and translocation to the nucleus [130]. Esp1 activation requires M-Cdk1 phosphorylation [131] and the elimination of Pds1 by APC^{Cdc20} [105,118]

Additional negative control of Esp1 activity is constituted by Slk19 and phosphatase PP2A^{Cdc55}. M-Cdk1 reverts such inhibition[131]

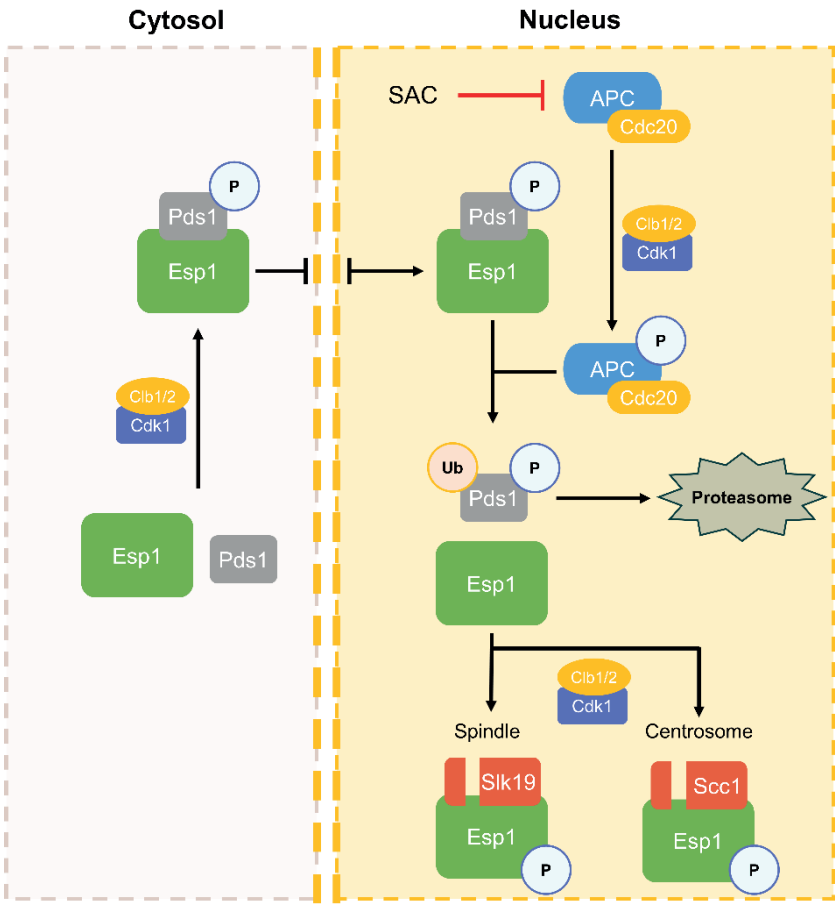

Figure 1.7. Regulation of Esp1/separase during the metaphase to anaphase transition. During the G2 phase, Esp1 is inhibited by binding to Pds1. Phosphorylation of Pds1 by M-Cdk1 promotes both its binding to Esp1 as well as its translocation to the nucleus. During metaphase, once the SAC is satisfied, the APC^{Cdc20} complex is formed and activated by the phosphorylation of several of its elements by M-Cdk1. Subsequently, the active APC^{Cdc20} ubiquitinates Pds1, targeting it for destruction through the proteasome, releasing Esp1. Finally, Esp1 cleaves Scc1/securin, as well as the kinetochore-associated protein Slk19, triggering anaphase.

1.4.3. Progression through Anaphase: The FEAR network

Upon entry into anaphase, subsequent mitotic events depend on the balance of activities from the M-Cdk1 kinase and the Cdc14[120,132]. Cdc14 is an essential phosphatase responsible to revert the bulk of M-Cdk1 phosphorylations. Both the downregulation of M-Cdk1 activity, and the release of Cdc14 from the nucleolus, occur in two times[133,134].

The first M-Cdk1/Cdc14 adjustment occurs upon anaphase onset, resulting in the transient release of Cdc14 from the nucleolus into the nucleoplasm by the so-called FEAR (cdc **F**ourteen **Ea**rly **R**elease) network[133]. FEAR release of Cdc14 requires the phosphorylation of the nucleolar anchor protein Net1 by the M-Cdk1 and Cdc5 mitotic kinases[135–138] During metaphase, the high M-Cdk1 activity is counteracted on Net1 by phosphatase $PP2A^{Cdc55}$. Upon entry into anaphase, the release of Esp1 (see section 1.4.2.3 above) leads to the inhibition of $PP2A^{Cdc55}$ mediated by the Esp1, Slk19 and Zds1/2 proteins[139,140]. Finally, M-Cdk1 phosphorylates Net1 to enable the release of Cdc14 to the nucleoplasm[123,128,129] and the SPBs[141], where the control of mitotic exit sits.

The FEAR release of Cdc14, although dispensable for the yeast mitotic cell cycle[142], is responsible for sharpening the metaphase to anaphase transition, correcting rDNA segregation, spindle stabilisation, spindle midzone assembly and the timely Mitotic Exit Network (MEN) activation (see section 1.4.4.2 below)[143–146]. The subjacent mechanisms involve the dephosphorylation of nuclear and SPB targets common to M-Cdk1 and Cdc14, as discussed in section 1.4.4.2 below.

In metaphase, phosphorylation of Pds1 by M-Cdk1 promotes the binding to Esp1, which is thus kept inhibited by the chaperone[122]. In parallel, M-Cdk1 phosphorylates the mitotic polo-like kinase Cdc5, promoting its activity[128,147]. Cdc5 phosphorylates Net1 at key sites that are necessary to prime the M-Cdk1 phosphorylation sites on Net1[148,149]. However, despite the high M-Cdk1 activity present in metaphase, Net1 is kept hypophosphorylated by the $PP2A^{Cdc55}$ phosphatase, which locally overcomes the M-Cdk1 activity at the nucleolus[140,150]. In this manner, Cdc14 remains sequestered at the nucleolus through metaphase.

Several mechanisms have been identified that regulate the activation of FEAR upon entry into anaphase (figure 1.8). First, a fraction of the Cdc55 is exported to the cytosol through a still unknown mechanism and kept in the cytosol by proteins Zds1 and Zds2. This mechanism effectively lowers the $PP2A^{Cdc55}$ activity at the nucleolus[140,151]. Second, active Esp1/separase, bound to Slk19, inhibits $PP2A^{Cdc55}$ by a still unknown mechanism that does not involve protein cleavage[129,131]. Third, the above reductions in $PP2A^{Cdc55}$ activity at the nucleolus allow M-Cdk1 activity to prevail. M-Cdk1 phosphorylation of Cdc55 results in further $PP2A^{Cdc55}$ inhibition[150]. Additionally, M-Cdk1 activity also phosphorylates the nucleolar protein Spo12, which antagonises the FEAR inhibitor Fob1[152]

In all, the kinase/phosphatase balance shifts towards M-Cdk1, which is now able to phosphorylate the Net1 anchor, resulting in the release of Cdc14 to the nucleoplasm[136] and also to the SPBs [148,149].

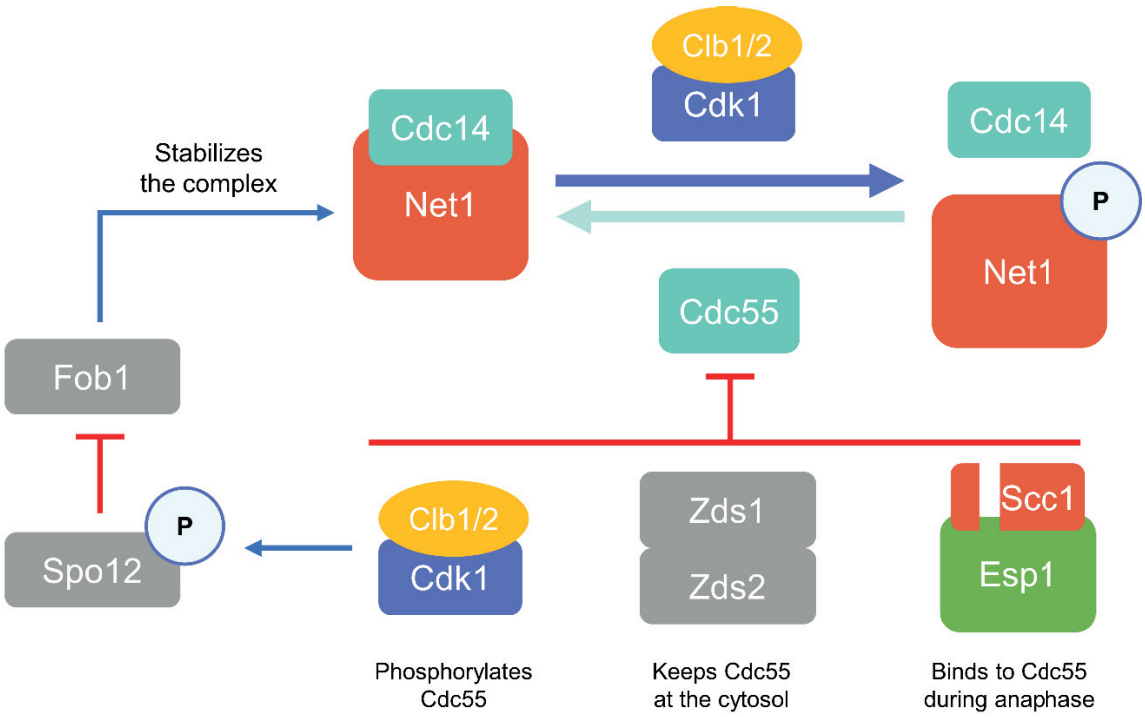

Figure 1.8. The FEAR network.

1.4.4. Control of the Anaphase-Cytokinesis transition

1.4.4.1. The Spindle Position Checkpoint (SPOC)

A surveillance mechanism, the Spindle Orientation Checkpoint (SPOC) blocks mitotic exit until both SPBs reach the cell cortex at the opposite cell poles, thus preventing the inheritance of an unbalanced chromosome complement.

The critical SPOC target is the monomeric Ras-like GTPase protein Tem1, which is the upstream-most member of the Mitotic Exit Network (MEN, see next section below). Tem1 is a highly mobile protein that locates at both SPBs, preferentially at the bud-directed SPB during anaphase[153,154].

G-proteins require an external Guanine nucleotide Exchange Factor (GEF), to promote the exchange of GTP for GDP and activate the pathway; and a GTPase Activating Protein (GAP), to promote the hydrolysis of the GTP and inactivate the signalling. The GAP complex Bfa1/Bub2 keeps Tem1 inhibited at the SPBs[155,156]. In anaphase, Bfa1/Bub2 re-localises exclusively to the SPB that will enter the daughter cell (dSPB)[157].

During a misaligned anaphase, localisation of the dSPB in the mother body places it in contact with the mother cell cortex, which is coated with Kin4, a kinase that precludes the inactivation of Bub2-Bfa1[158–160]. As a result, the cell remains arrested before cytokinesis until the spindle position defect is corrected[161].

In a correctly culminated anaphase, spindle elongation along the mother–daughter axis places the dSPB in contact with the daughter cell cortex, which is coated with Lte1, resulting in the inactivation of Bfa1/Bub2 and the activation of Tem1. Lte1 also inhibits Kin4 by binding, preventing its association with the dSPB[162,163]. Despite Lte1 being a GEF-like protein, no GEF activity has been observed[164]. In contrast, Tem1 singularly displays high intrinsic nucleotide exchange activity[165,166].

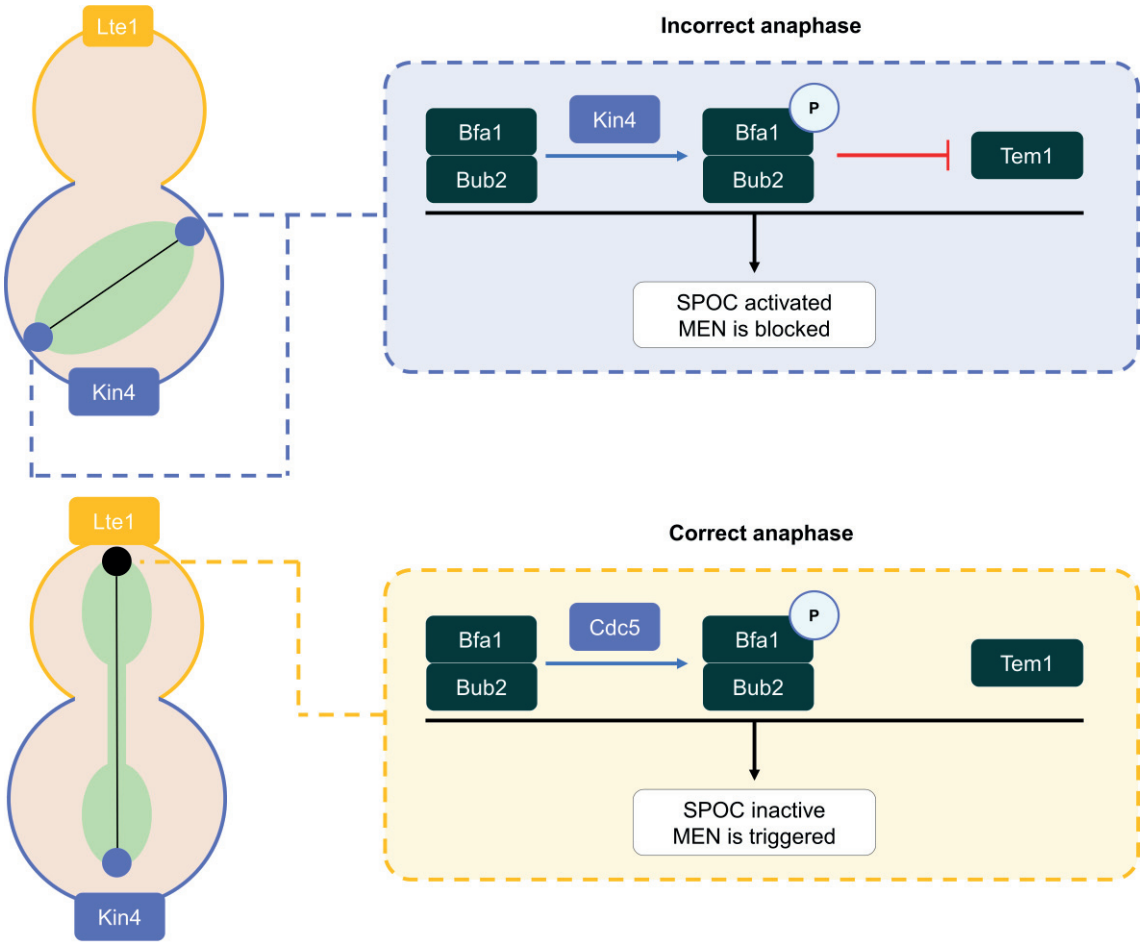

Figure 1.9. The Spindle Position Checkpoint (SPOC). In the event of either an incorrect or incomplete anaphase elongation, both Spindle Pole Bodies (SPBs) contact the mother cell cortex, which is coated with kinase Kin4. Kin4 is then recruited at the SPBs and phosphorylates the GAP element Bfa1, keeping it active. During a correct anaphase, the bud-directed Spindle Pole Body (SPB) becomes out of reach to Kin4 once it crosses the bud neck, and Bfa1/Bub2 is inhibited by Cdc5 once anaphase is complete. Lte1, which coats the bud cortex, contributes to Kin4 inactivation at said SPB.

1.4.4.2. The Mitotic Exit Network checkpoint (MEN)

A second and final M-Cdk1/Cdc14 adjustment occurs upon Mitotic Exit Network (MEN) activation, triggering cytokinesis and the end of the cell cycle.

The MEN is a RAS-like GTPase-driven signalling cascade, the yeast equivalent to the Hippo pathway in mammalian cells. Much like the FEAR network is involved in the transient release of Cdc14 to the nucleoplasm, the MEN pathway triggers the stable release of Cdc14 to the cytosol[120,132,167–170]. This event is essential for mitotic exit, as Cdc14 is responsible for the dephosphorylation of key M-Cdk1 substrates required for cytokinesis and cell separation[134].

The whole cascade is triggered and regulated at the outer plaque of the Spindle Pole Bodies[148,168,171] Once anaphase is completed, Tem1 activation (see preceding section) promotes recruitment and activation of kinase Cdc15[172]. Cdc15 phosphorylates the SPB scaffolding protein Nud1, creating a docking site for the essential MEN kinase Mob1-Dbf2[173]. Subsequently, Cdc15 phosphorylates Dbf2, required for Mob1-Dbf2 kinase activation[174]. In addition, phosphorylation of Dbf2 at the N-terminal, presumably by Cdc15 as well, masks an NES signal, allowing the accumulation of active Mob1-Dbf2 at the nucleus[148].

The Dbf2 kinase has a paralog, Dbf20, that can also bind to Mob1[175]. Despite that Mob1 is essential[176], neither the individual deletion of Dbf2 nor Dbf20 is lethal. The double *dbf2 dbf20* mutant, however, is inviable[175], suggesting that Dbf20 may partially replace Dbf2. However, *dbf2* null mutant cells display a remarkable mitotic delay phenotype (hence termed ***d****umb****b****ell* ***f****ormation* mutant), whereas *dbf20* null cells grow normally[175] and get the *dbf* name based on homology to Dbf2.

Critically, active, nuclear Mob1-Dbf2 can reach the nucleolus, where it phosphorylates Net1, resulting in the release of Cdc14[148]. Net1 phosphorylation of Net1 requires the priming phosphorylation by polo-like kinase Cdc5, which occurs early in metaphase[148,149]. Mob1-Dbf2 phosphorylation also masks an NLS signal in Cdc14[169]. In consequence, contrary to the FEAR-driven release of Cdc14, the MEN-driven release allows Cdc14 to localise to the cytosol, where it dephosphorylates critical cytokinesis targets in the Ingression Progression Complex (IPC), such as Iqg1[177], Chs2[178,179], Inn1 and Cyk3[179], which then re-localise to the site of cell division, and the APC activator Cdh1[120,132]. Upon activation, the ubiquitin ligase

APC^{Cdh1} targets mitotic cyclins for destruction via the proteasome, thus terminating M-Cdk1 activity[82].

Activated Mob1-Dbf2 also relocalises to the site of cell division, where it triggers AMR contraction through the phosphorylation of IPC proteins Hof1[180] and Chs2[181–183]

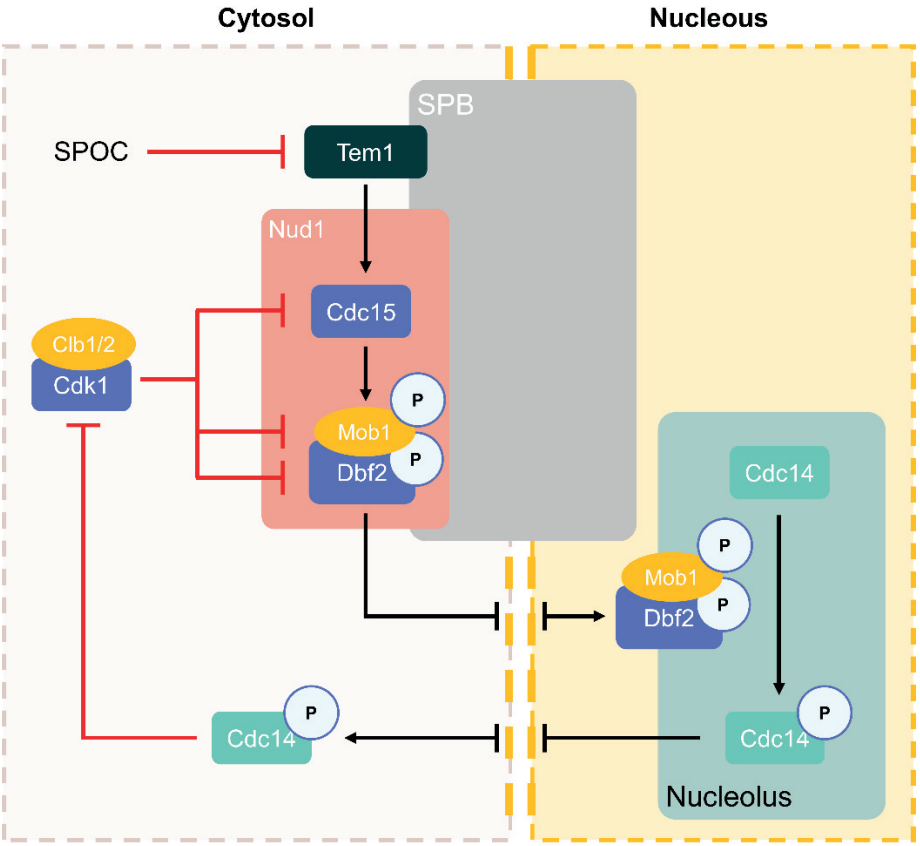

Figure 1.10. The MEN pathway.

As described in the preceding section, MEN activation requires a completed, bipolar anaphase, as monitored by the Spindle Position Checkpoint (SPOC). Only then, the G-protein Tem1, the upstream most element in the MEN pathway, is turned on.

A second layer of control is under the M-Cdk1 kinase. M-Cdk1 has been shown to phosphorylate and inhibit Cdc15 and Mob1[184]. During anaphase, APC^{Cdc20} promotes a partial degradation of mitotic cyclin Clb2, lowering the overall activity of M-Cdk1 to around half its original peak activity in metaphase[89]. Such a decrease might shift the phosphorylation/dephosphorylation balance in favour of the Cdc14 phosphatase released by FEAR, which might thus trigger MEN activation. In support of such a

scenario, FEAR-released Cdc14 localises to the SPBs[141] suggesting it may locally prevail over M-Cdk1 on the shared MEN substrates.

An apparent conundrum results from the fact that the MEN proteins are known to localise to the outer plaque of the SPBs[148], whereas FEAR releases Cdc14 to the nucleus, not the cytosol. In that sense, cells modified to conditionally restrict Cdc14 localisation to the nucleus fail to complete cytokinesis[185]. However, in studies with unmodified Cdc14 in cells where MEN is suppressed, despite Cdc14 remaining mostly nuclear, enough is still able to translocate to detectable levels to the outer plaque of the SPBs, where it partially dephosphorylates Cdc15[128]. Also, in a similar approach, Cdc14 localisation to the SPB is shown to be dependent on Bub2, which is also at the outer plaque[141]. Finally, the genetic interactions between FEAR and MEN components[186] also support that FEAR-released Cdc14 reaches the cytoplasmic side of the SPB, albeit at a level that goes undetected by fluorescence microscopy approaches. In all, despite that Cdc14 phosphorylation by the MEN kinase Mob1-Dbf2 is required for the bulk of Cdc14 to freely localise to the cytosol, enough FEAR-released Cdc14 seems to reach the SPB outer plaque.

A second conundrum derived from this model is the dispensability of FEAR[125,142]. A possible explanation can be inferred from unpublished observations in our laboratory, showing that cells can adapt to the block by Clb2 overexpression, eventually dividing. Cells are again blocked at the subsequent mitosis until they adapt again. This observation suggests that APC^{Cdc20} continues to decrease mitotic cyclin levels in arrested cells, eventually overriding the requirement for the FEAR-dependent release of Cdc14.

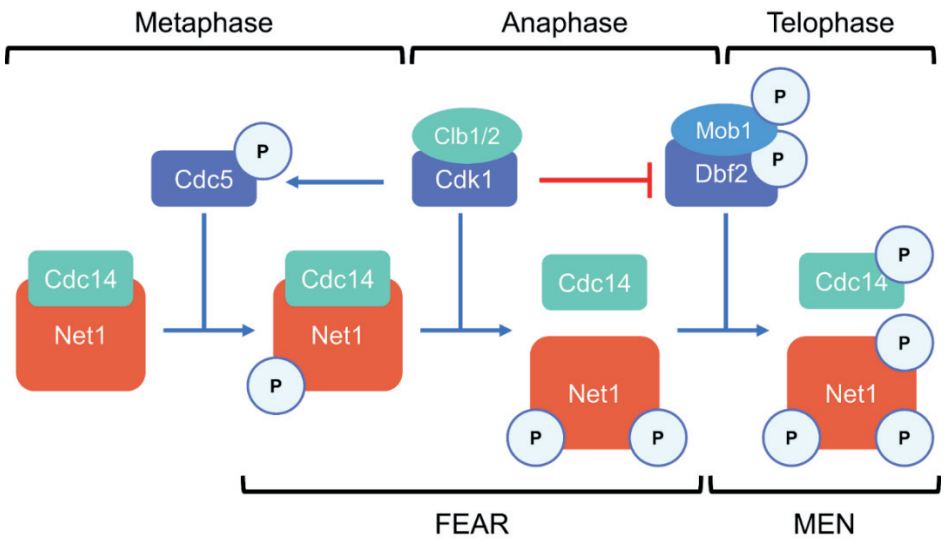

Figure 1.11. Cdc14 regulation through the FEAR and MEN pathway.

1.4.4.3. Essential roles of Mob1-Dbf2 in cytokinesis

Mob1 is essential for cytokinesis[176]. In addition to its role as effector kinase in the MEN pathway (see section 1.4.4.2. above), Mob1-Dbf2 plays further downstream roles in mitotic exit.

Mob1-Dbf2 localises to the site of cell division upon MEN activation[187], where it promotes the formation of the primary septum by phosphorylation of the chitin synthase Chs2 by Mob1-Dbf2[183]. Full contraction of the actomyosin ring and formation of the primary septum at cytokinesis depend on each other[188].

Despite such critical roles, the only essential role for the Dbf2 kinase as a downstream effector or the MEN pathway is likely to be the cytosolic release of Cdc14 (see section 1.4.4.2.). We base this vision on experiments with a Cdc14 mutant that cannot be sequestered in the nucleolus, which renders Dbf2/Dbf20 dispensable[189].

1.4.5. Control of Cytokinesis

Once anaphase has satisfactorily culminated and the SPOC allows MEN activation, the cell can enter cytokinesis and mitotic exit. At the end of cytokinesis, plasma membranes separate the two descendant cells.

In budding yeast, a scaffolding structure, the septin ring, works as a scaffold for the separation process. In addition, Primary Septum (PS) synthesis and the contraction of the Actomyosin Ring (AMR) are coupled[188,190–199]. Actomyosin ring (AMR) contraction is responsible for the invagination of the plasma membrane that culminates in the individualisation of the two descendant cells.

1.4.5.1. The septin ring

Septins are a family of GTP-binding proteins that assemble into cytoskeletal filaments. They consist of protein chains formed by five proteins: Cdc3, Cdc10, Cdc11, Cdc12 and Shs1[200], four of which were already described by Lee Hartwell back in the 1970s as proteins that, when mutated, cause a terminal phenotype of failed cytokinesis[18]. Septins polymerise together to form filaments and bind end to end, generating a ring around the bud neck[201].

The septin ring is the first structure that appears at the division site, during the G1/S transition[202]. Recruitment to the bud site is mediated by the activation of the small GTPase Cdc42[203]. Septins are assembled in two closely-bound rings that form an ‘hourglass structure’ at the bud site that is essential for cell division[204]. During this process, the septin-associated protein Bni5 contributes to the formation of the septin network by crosslinking septin filaments[205]. Septins function not only as scaffolding structures for other elements of the cytokinesis machinery to be recruited, but also as a permeability barrier at the plasma membrane, thus contributing to the asymmetric distribution of proteins between mother and daughter cells, which is crucial for the correct regulation of cytokinesis[206–208].

At the onset of cytokinesis, the two septin rings split and separate, in a process that is visible through fluorescent microscopy[209]. Separation of the septin rings allows for the formation of the PS, and always precedes AMR assembly and contraction (figure 1.12).

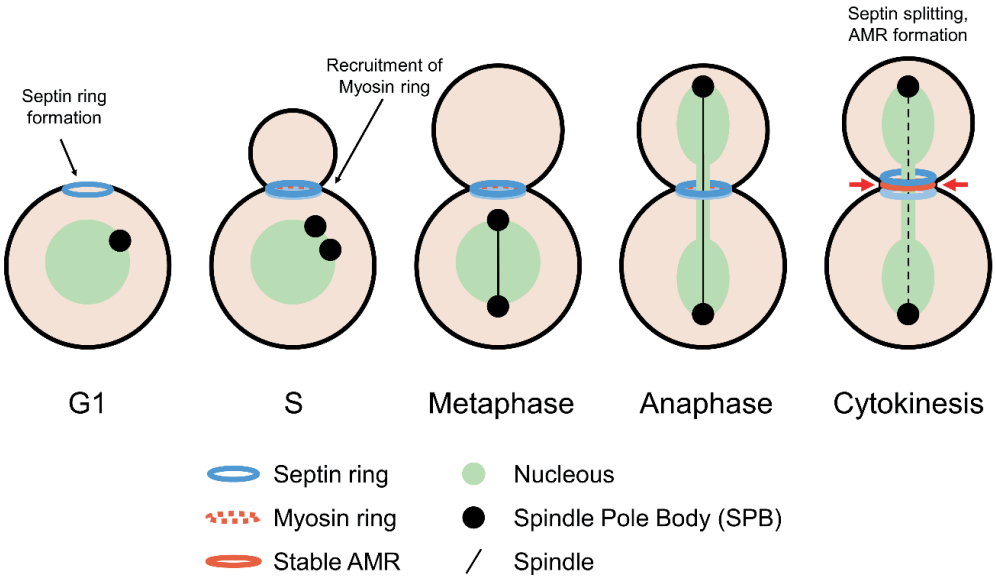

Figure 1.12. Septin ring formation and splitting. Adapted from **Meitinger & Palani, 2016**

1.4.5.2. Assembly of the Actomyosin Ring (AMR)

The contractile Actomyosin Ring (AMR, also termed CAR) is the driver of plasma membrane constriction during cytokinesis. The AMR is formed by the type-II myosin heavy chain, Myo1, and its light chain, Mlc1[195]. An essential protein, Iqg1, is required for AMR stabilisation and recruitment of F-actin[177], after which the AMR is completely assembled and proceeds to contract.

The AMR is assembled in sequential order throughout the cell cycle. Myo1 is recruited at the nascent bud site during the G1/S transition, creating a myosin ring[210], which is kept at the bud through the septin-binding protein Bni5 [209]. Before mitotic exit, Myo1 is mobile at the bud neck. In mitosis, Mlc1 arrives at the bud neck and recruits Iqg1[210]. Iqg1 stabilises the myosin ring and recruits F-actin, creating the contractile actomyosin ring[177,211]. AMR contraction is coupled with cell wall formation[190,191].

1.4.5.3. Septa formation

The Primary Septum (PS) is a chitin ring surrounding the bud neck, synthesised during AMR contraction[212]. It allows for the production of the cell wall during AMR constriction and is essential for full cell separation in budding yeast[188]. The AMR acts as a scaffold to recruit and stabilise the necessary elements for PS formation[199].

Chitin-synthase protein Chs2 is the main responsible for PS formation[191]. Chs2 is recruited at the bud neck from its regular localisation at the Endoplasmic Reticulum (ER) by the change of balance between the M-Cdk1 and the Cdc14 activities[178,179,196,213]. Chs2 activation requires the presence of Inn1 and Cyk3, which are recruited to the bud neck shortly after the septin ring split[179,197]. The F-Bar protein Hof1, localised at the mother side of the bud neck during G2, migrates to the middle of the bud neck as well just *before* such splitting[214]. Together, these elements compose the so-called Ingression Progression Complex (IPC)[194]. Chs2 is phosphorylated by the MEN kinase Mob1-Dbf2, which promotes Chs2 relocation in the bud neck region[183,215,216].

The primary septum is then covered on both sides, forming the secondary septa, the work of 1,3-beta-glucan synthases Fks1 and Fks2[217,218] and chitin synthase Chs3[191]. Each secondary septum eventually becomes part of one of the new cells' independent walls.

Finally, the primary septum is hydrolysed by chitinase Cts1[219], after which the mother and daughter cells become independent.

A summary of the whole process is depicted in figure 1.13.

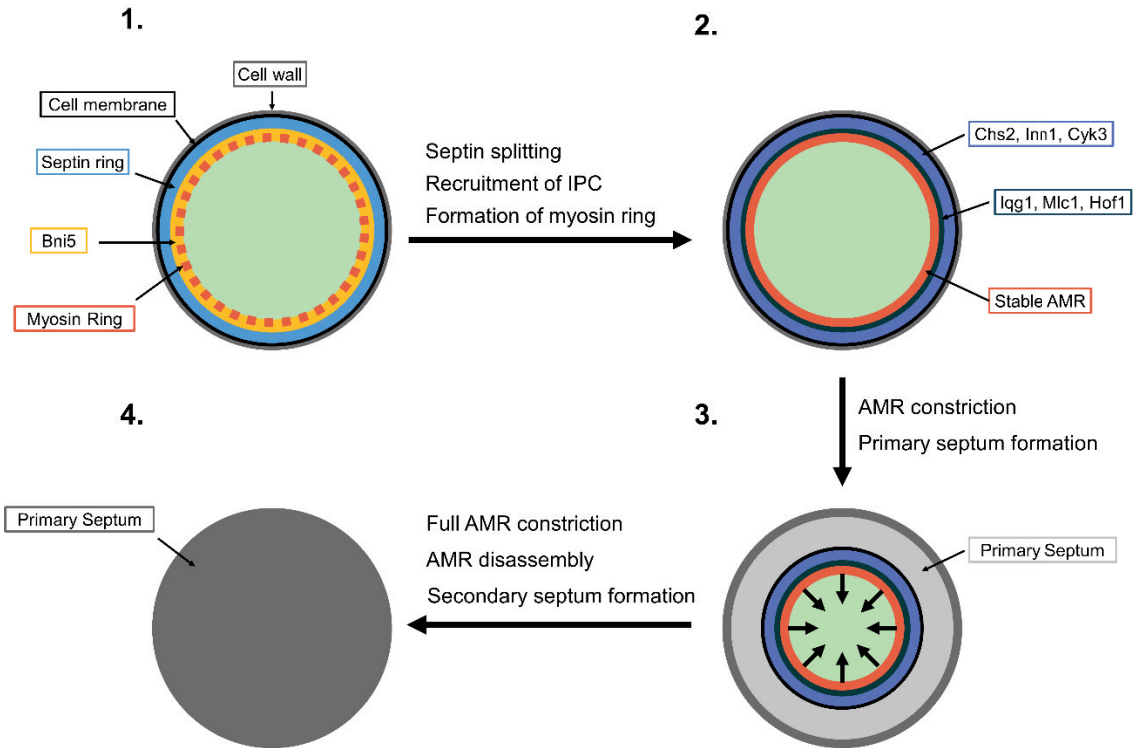

Figure 1.13. Actomyosin ring and primary septum formation. Adapted from **Meitinger & Palani, 2016**

1.5. Defining the essential role of M-Cdk1 to block premature cytokinesis

Cytokinesis is the final event in the eukaryotic cell cycle, in which a parental cell separates the cytoplasm with plasma membrane, thus defining two independent daughter cells. As shown above, cytokinesis is tightly controlled to ensure that the division program does not initiate until chromosome segregation is completed. Premature cytokinesis causes chromosome breakage and aneuploidy, due to abscission before chromosome segregation is complete[220]. On the other hand, delayed cytokinesis may result in regression of the cleavage furrow, leading to bi-nucleate, genomically unstable cells[221–223]. Both scenarios involve genomic instability and aneuploidy, conditions that fuel malignant transformation[7,224]

Many of the events in cytokinesis and mitotic exit are negatively regulated by M-Cdk1 activity, such as the activation of MEN kinases Cdc15 and Mob1[184], the relocalisation of cytokinesis factors to the site of cell division, such as Iqg1[177], Chs2[178,179], Inn1 and Cyk3[179], and the licensing of the APC activator Cdh1[120,132,225]. Conversely, M-Cdk1 inhibition, either by using the analogue-sensitive mutant *cdk1-as*[226,227] or by overexpression of *sic1ΔN,* a hyperstable mutant of the Clb-CDK inhibitor[228], result in premature mitotic exit.

Providing further support, conditional mutants of Cdc14, the phosphatase that reverts the bulk of M-Cdk1 phosphorylation at the mitotic exit, arrest with a completed unable to enter cytokinesis[22,185,229].

Finally, expression of hyperstable forms of the mitotic cyclins arrests cells in telophase with two separated nuclei (karyokinesis) but unable to divide[88,89,230].

In all, the above observations indicate a key role for M-Cdk1 in the regulation of cytokinesis. Therefore, the very same activity that drives cells into mitosis and promotes chromosome segregation, elegantly blocks the occurrence of premature cytokinesis. A similar control operates in S phase, where S-Cdk1 triggers DNA replication, and prevents re-replication by inhibiting the re-assembly of chromosomal pre-replication complexes[231].

Although the essential role of the APC and the MEN pathway in countering M-Cdk1 activity to promote cytokinesis is therefore well established, the exact substrates phosphorylated by M-Cdk1 involved in the process are unknown.

We hypothesise that one or more critical M-Cdk1 substrates prevent premature cell division.

The objective of this thesis is to identify the minimal set of essential M-Cdk1 targets that prevent premature entry into cytokinesis.

2. Materials and Methods

2.1. Yeast techniques

2.1.1. *Saccharomyces cerevisiae*

This thesis has used the budding yeast *Saccharomyces cerevisiae* as an experimental model for the cell cycle. All strains were from the W303 genetic background [232]. Haploid cells mating type Mat-a were used (W303-1a). To avoid the spontaneous generation of MAT-α haploid cells (W303-1b) and diploid cells, the heterothallic HO gene is mutated in this background. In most strains, to allow for a tighter G1 synchronisation using α-factor, the *bar1* gene was deleted.

2.1.2. Yeast Growth conditions

For general use, yeast strains were grown in regular YP media (1% Yeast Extract, 2% Peptone) and later supplemented with 2% carbon source (D for glucose, Raf for raffinose, Gal for galactose). Glucose was used for optimal yeast growth, while raffinose and galactose were used for *GAL1* promoter induction when needed. YP media was sterilised by autoclaving.

For yeast strains carrying the *MET3-CDC20* mutation, by which cells deplete essential protein Cdc20 in the presence of methionine, as well as microscopy experiments, yeast was grown in Synthetic Complete media (SC, 0.17% Yeast Nitrogen Base without amino acids and ammonium sulphate (BD, 233520), 0.5% ammonium sulphate as a nitrogen source, and Supplement Mixture -Met Drop-Out (Formedium, DCS0111) supplemented with 2% carbon source (glucose or else, see above) and 40 µg/ml Adenine. Concentrated stocks of all these elements were filtered using 0,2 µm filters and added to the remaining autoclaved media when its temperature was down to 50ºC.

For selection purposes, in which a particular strain had auxotrophy for either Adenine, Histidine, Tryptophan, Leucine or Uracil, a Supplement Mixture -6aa Drop-Out (Formedium, DCS1519) was used instead. SCD media was later supplemented with the necessary auxotrophic requirements using concentrated sterilised stocks to

achieve the following final concentration: 20 µg/ml Uracil, Tryptophan, Histidine and Methionine; 40 µg/ml Adenine; and 100 µg/ml Leucine.

For counter-selection of the URA3 auxotrophy, a special media containing 1 mg/ml of 5-Fluorotic Acid (5-FOA, Formedium, 5FOA05) in SCD supplemented with 50 µg/ml Uracil media was used. For antibiotic selection plates in YPD, media was supplemented with either 200 µg/ml Geneticin (Formedium, G4181), 100 µg/ml Nourseothricin (Sigma-Aldrich, 74667) or 350 µg/ml Hygromycin B (Ibian, ant-hg-1). For antibiotic selection plates using SCD media, however, 0.1% Glutamic Acid was used instead of ammonium sulphate as a nitrogen source and 600 µg/ml Geneticin, 100 µg/ml or 600 µg/ml Hygromycin B was used for selection. The antibiotics were added when the temperature of the autoclaved media was down to 50ºC in a water bath.

2.1.3. Cell synchronisation

To synchronise yeast cells in pre-start G1, the mating pheromone α-factor (Lifetein) was added to exponentially growing cells at 50 ng/ml in *bar1*Δ cells or *5 µg/ml* on BAR1 cells for a doubling time (i.e. around 90 minutes in rich media, 30ºC and wild-type genotype). Cells were periodically checked under the light microscope to determine the budding index and the appearance of a pear-shaped (shmoo) morphology. Budding indexes of <5% were the condition for acceptable synchronisation. To release cells from the G1 arrest, cells were washed twice in media without α-factor and finally resuspended in the pheromone-free media. α-factor was added to the media from filter-sterilised, concentrated stocks in deionised water with 8% methanol stored at -80ºC for long-term storage, and -20ºC for short-term storage.

To synchronise cells in metaphase, cells were made *MET3-CDC20*. Since the sole copy of the *CDC20* gene is under the control of the *MET3* promoter in these strains, Cdc20 expression is induced in the absence of methionine in the media and repressed in the presence of the amino acid. Thus, cells growing in SC media lacking methionine (SC-Met) were synchronised in metaphase adding 4mM methionine to the media. Cells were periodically checked under the light microscope to determine the Dumbbell Index. Acceptable synchronisations required a Dumbbell Index of

>90%. For the synchronous release from the metaphase arrest, cells were washed 3 times using SC media lacking methionine and released in the appropriate media.

To synchronise cells in strains lacking the *MET3-CDC20* mutation, Nocodazole (LKT labs, N5409) was added to 5 µg/ml. Nocodazole depolymerises tubulin, blocking spindle assembly and arresting cells at the G2/M transition. To avoid cells escaping from the arrest, an extra 2.5 µg/ml was added every 90 minutes until the acceptable >90% Dumbbell Index was achieved. To release cells from Nocodazole arrest, cells were washed twice and transferred to media without Nocodazole. Nocodazole was added from concentrated stocks, diluted in pure DMSO, and stored at -20ºC.

2.1.4. Over-expression of the *GAL1* promoter

The hyperstable mitotic cyclin *clb2ΔN* mutant, which lacks the first 120 amino acids of its N-terminus, was subcloned into an integrative vector downstream of the galactose inducible *GAL1* promoter.

To induce over-expression of the *GAL1* promoter, cells were grown to mid-exponential phase in media supplemented with 2% raffinose. Cells were then pulled down and resuspended in fresh media supplemented with 2% Galactose. For correct over-expression of *GAL1-clb2ΔN* gene, cells needed to grow in Galactose media for at least 45 minutes.

In some strains, however, the *ADGEV* gene was integrated to allow for rapid estradiol induction of the *GAL1* promoter in glucose media. The *ADGEV* (*ADH1-Gal4-hER-VP16*) transcription factor carries, under the constitutive *ADH1* promoter, the chimeric protein from the fusion of the DNA binding domain of the Gal4 transcription factor, the hormone binding domain of the human estrogen receptor, and the transactivation domain of the herpes virus protein VP16 [233] The ADGEV protein remains inactive in the cell until estradiol is added. Upon activation, the chimeric transcription factor drives transcription of the genes under the GAL promoter, regardless of the carbon source present in the media. For correct over-expression from the *GAL1* promoter, β-estradiol (was added to 36 µM for at least 30 minutes. β-estradiol (Sigma, E2758) was added from concentrated stocks, diluted in absolute ethanol and stored at -20ºC.

2.1.5. Induction of protein degradation using Auxin-Inducible Degron (AID)

The Auxin-inducible degron (AID) technology allowed us to conditionally deplete a protein of interest by the addition of 3-Indole acetic acid (IAA) to the media. AID strains were generated by the C-terminal tagging of the protein of interest with the degron using the plasmid collection from Morawska and Ulrich[234]. AID strains also need a copy of the *Oryza sativa* F-box protein *TIR1,* which we integrated with a constitutive *ADH1* promoter. The OsTir1 F-box protein is activated upon auxin binding and assembles a functional ubiquitin-ligase complex in yeast cells. In the presence of auxin, the F-box OsTir1 targets proteins carrying the AID degron sequence, which are then polyubiquitinated and destroyed via proteasome[234–236]

To allow for correct protein depletion, IAA was added to 5mM in YP media or 1mM in SC media for at least 30 minutes. In plates, IAA was added from concentrated stocks, diluted in DMSO and stored at -20ºC.

2.1.6. Yeast transformation

The protocol used is adapted from the classical alkaline cations methods[237] and is based on the generation of pores in the cell wall and the subsequent transformation by heat shock.

Around $1x10^8$ of exponentially growing cells were harvested and washed twice with deionised water and washed a third time with a LiAc/TE mix (100 mM Lithium Acetate pH 7.5, 10mM Tric-HCl pH 7.5, 1 mM EDTA). The cell pellet is then resuspended in 25 µl of LiAc/TE mix and 2 µg of the integrative DNA (PCR product or plasmid) are added, as well as 5 µl of ssDNA at 10 mg/ml. Salmon Sperm ssDNA acts as a carrier of the DNA used to transform, enhancing the yield of the protocol [238]. To further enhance the DNA contact with the cells, 300 µl of 50% Polyethylene glycol 3350 diluted in the same LiAc/TE solution are added to the mix as a crowding agent. This mix was incubated for 30 minutes at 30ºC.

After the incubation, DMSO is added to a final 10% concentration (v/v) and cells are heat shocked at 42ºC for 15 minutes and 1 minute on ice. Finally, transformed cells are spun down, the LiAc/TE/PEG/DMSO mix supernatant is discarded, and the pellet

is resuspended in 200 µl of synthetic complete media without any auxotrophic markers. This suspension is plated in different selective media plates and incubated for around 72 hours at 30ºC.

Resistant clones are streaked in a new selective plate to avoid false positives and the transformation is then checked by at least one preferred method: if no antibody or tag is available or sequencing is needed, by PCR of the genomic DNA of the clone; if the transformation DNA encodes for a protein with a C-terminal tag, by Western Blot of whole cell extracts; and if the transformed product encodes for a fluorescent protein, by checking its signal under a fluorescent microscope.

2.1.6.1. Deletion of yeast genes

To delete a gene in *S. cerevisiae*, its entire Open Reading Frame (ORF) was replaced by a selection marker in a one-step transformation process[239]. We integrated a PCR product containing said selection marker flanked by 45-60 base pairs (bp) annealing with both ends of the gene's ORF. Competent cells transformed with the PCR product replace the original sequence of the gene with the resistance marker by homologous combination of its 3' tails.

The PCR product was obtained from custom oligos that include the said 45-60 nucleotides (nt) at its 3' tail and 18-21 nt at the 5' tail, which anneal to the plasmid containing the desired marker. We used plasmids from the pFA6a collection[240] and the pRS collection[241] as templates for the PCR. The deletion process is depicted in figure 2.1.

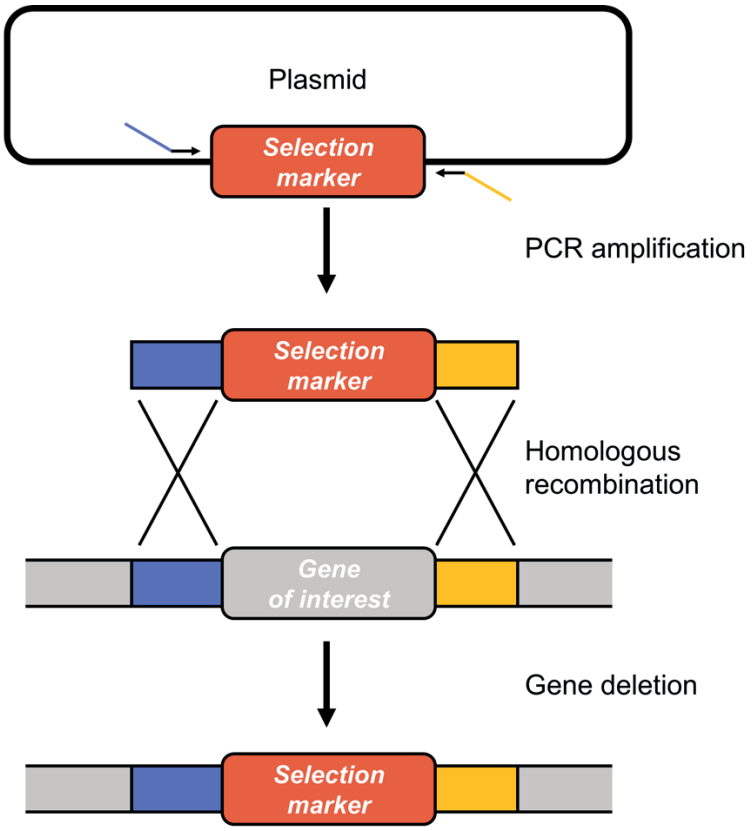

Figure 2.1. The principle of gene deletion.

2.1.6.2. C-terminal tagging of yeast genes

To tag a protein in *S. cerevisiae*, be it for Western Blot analysis or Microscopy analysis, we tagged the C-terminal of its gene. The strategy used was similar to the one described for gene deletion. In short, a PCR product is generated using a vector carrying the DNA sequence coding for the tag of interest, and a resistance marker. The PCR product is then transformed into competent yeast cells, which integrate the sequence at the end of its gene by homologous recombination.

The oligos used to amplify the vector plasmid contained on their 3' tail the last 45-60 nt of the gene of interest minus the STOP codon and the following 45-60 nt immediately after the STOP codon. On their 5' tail, the oligos included the 18-21 nt needed for annealing to the vector plasmid (figure 2.2). The plasmids used for tagging were from the pYM collection[242].

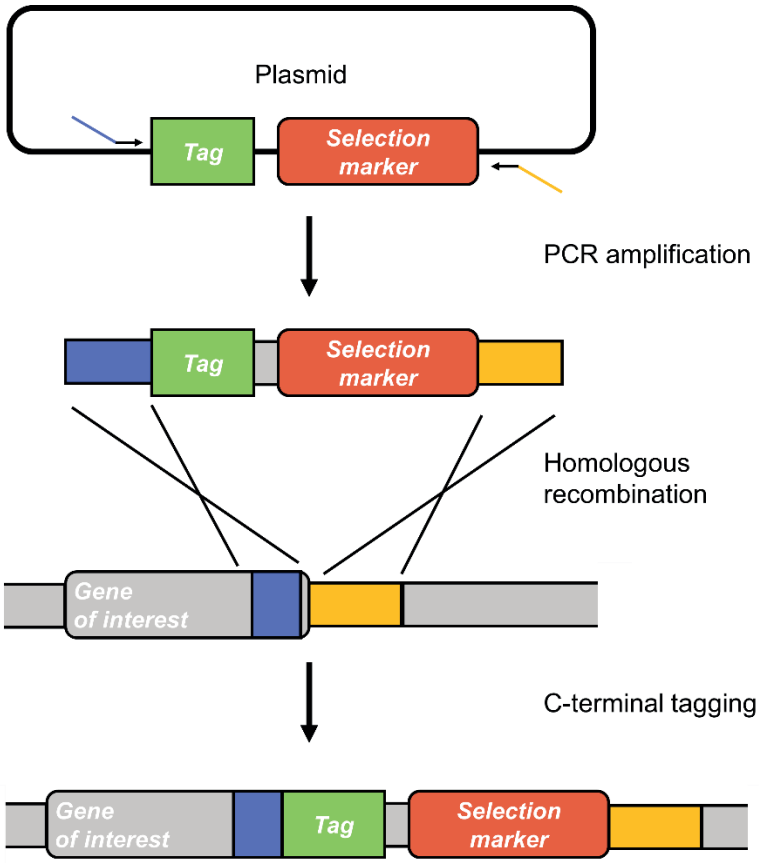

Figure 2.2. The principle of C-terminal tagging

2.1.7. Frozen yeast stocks

Genetically modified yeast strains were stored frozen in 30% glycerol. A single positive colony of the strain of interest is grown overnight in selective media at 30ºC. 800 µl of the overnight culture was mixed with 800 µl of sterile 60% glycerol in a cryogenic tube and stored in a -80ºC freezer.

2.2. Bacterial techniques

2.2.1. Bacteria Growth conditions

For *Escherichia coli* growth, LB (*Luria Broth*) media containing 1% tryptone, 0,5% Yeast Extract and 0,5% sodium chloride was used, supplemented with 50-75-100 µg/ml Ampicillin when needed. Psi-broth media for DH5α competent cells preparation consisted of 2% tryptone, 0,5% Yeast Extract and 0,5% MgSO4·7H2O, adjusted to pH 7.6. Both media were sterilised by autoclaving.

For solid media, the same components described for all liquid media were used, supplemented with 2% agar to the autoclaved mix.

2.2.2. *Escherichia coli* competent cell preparation

For cloning and long-term storage of plasmid DNA, we transformed competent DH5α *E. coli* cells. DH5α competent cells were prepared by a chemical method based on rubidium chloride. This reagent weakens the cell wall and prepares cells for transformation with heat shock.

To prepare competent cells, a 20 ml LB culture is inoculated with a single DH5α colony previously woken up in a regular LB plate and incubated overnight at 37ºC 200 RPM. The next morning, 2 ml of saturated culture is inoculated into 200 ml of PSI-broth (see 2.2.1). The culture is grown at 37ºC until the optical density at 550 nm is around 0.48. Next, the culture is chilled on ice water for 15 minutes and cells are spun down at 4000 g for 4 minutes at 4ºC in a refrigerated centrifuge using chilled sterile centrifuge bottles.

After discarding the supernatant, cells were resuspended in 80 ml of pre-chilled, sterile TfbI media (30 mM potassium acetate, 100 mM rubidium chloride, 10 mM calcium chloride, 50 mM manganese chloride, 15% glycerol). Cells were spun down again as before to remove the TfbI media and the cell pellet was resuspended in 8 ml of pre-chilled, sterile TfbII media (10 mM MOPS, 75 mM calcium chloride, 10 mM rubidium chloride, 15% glycerol). Competent cells were incubated for 15 minutes on

ice and transferred to sterile Eppendorf tubes, 120 µl each, and frozen using liquid nitrogen for quick storage at -80ºC.

2.2.3. *Escherichia coli* competent cell transformation with plasmid DNA

To transform plasmid DNA, either from a miniprep or a ligation after cloning, competent DH5α *E. coli* cells stored at -80ºC were thawed on ice for 15 minutes. A maximum of 50 ng of DNA in a volume no larger than 10 µl was added to competent cells and the mix was incubated on ice for 30 minutes. Cells were then submitted to heat shot at 42ºC for 90 seconds and 1 minute on ice to allow for DNA intake. After this, 1 ml of LB was added to the mix and cells were allowed to recover at 37ºC for 1 hour.

After incubation, transformed cells were tap spun to remove the excess media and 2 LB plates supplemented with 50 µg/ml Ampicillin were seeded with different concentrations of the transformed cells. Plates were incubated overnight at 37ºC and a few of the resistant clones were processed for plasmid DNA extraction (2.3.2.) and stored at -80ºC if positive (2.2.4.)

If plasmid DNA came from a cloning ligation, transformed cells were plated in white-blue LB selection plates (LB plates supplemented with 75 µg/ml Ampicillin, 40 µg/ml X-GAL, 0.1 mM IPTG). All plasmid vectors used for our constructs possess a Multiple Cloning Site (MCS) within the α subunit coding region of the *LacZ* gene, one of the two essential subunits for the β-galactosidase enzyme. Thus, plasmid constructs used in this study harbour a truncated form of the *LacZ* gene. Since DH5α cells used for transformation only have the complementary Ω fragment of the β-galactosidase, positive clones for the insertion of a gene of interest inside the MCS would render DH5α cells unable to convert X-Gal to a coloured product.

Therefore, when using white-blue selection plates, only white colonies were chosen for further checking.

2.2.4. Frozen bacterial stocks

E. coli cells carrying a construct of interest were also stored frozen in 30% glycerol. A colony carrying the plasmid was inoculated in 5 ml LB media supplemented with 50 µg/ml Ampicillin and incubated at 37ºC overnight. 800 µl of overnight culture was mixed with 800 µl of sterile 60% glycerol stock in a cryogenic tube and stored in a -80ºC freezer.

2.3. Molecular biology techniques

2.3.1. Yeast genomic DNA extraction

We used the extraction of genomic DNA by glass-bead beating in phenol/chloroform, followed by DNA precipitation in isopropanol.

Single colonies were inoculated in 5 ml liquid media cultures and incubated O/N at 30ºC, 200RPM. In the morning, 1 ml of saturated culture was harvested and transferred into a screw-cap vial. Cells were spun down by centrifugation at 1000 g for 1 minute and the media was discarded. Cells were resuspended in 400 µl of lysis buffer (100 mM NaCl, 10 mM Tris-HCl pH 8.9, 1 mM EDTA, 0,1% (w/v) SDS) by vortexing. Around 400 µl of acid-washed glass beads (0.5 mm diameter) were added to the cell suspension and the vial was vortexed at maximum power for 90 seconds, breaking the cell walls.

Next, 400 µl of phenol/chloroform/isoamyl alcohol (25:24:1) was added to the lysate and vortexed again as before, to dechromatinise the chromosomal DNA and extract it with the aqueous layer. The mix was spun down at 14.000g for 3 minutes and the top aqueous layer was transferred to a fresh screw-cap vial, to re-extract again exactly as before, to increase the purity of the DNA. After the second extraction, the aqueous solution was transferred to a regular Eppendorf tube.

To precipitate the DNA, a volume of isopropanol was added to the extract and the sample was mixed by inversion and incubated on ice for 15 minutes. Chromosomal DNA was then recovered by centrifugation at 14.000 g for 20 minutes at room

temperature. The DNA pellet was washed twice with 70% ethanol and dissolved in 50 µl of TE buffer supplemented with RNase A to remove the co-purified RNA (10 mM Tris-HCl pH 8.0, 1 mM EDTA, 10 µg/ml RNase A). For PCR, 1 µl of genomic DNA prep was used as a template.

2.3.2. Plasmid DNA extraction

To extract DNA, Epoch Life Science Inc EconoSpin® All-In-One DNA/RNA Mini Spin Columns were used.

A single E. Coli colony containing the desired plasmid DNA was inoculated in 5 ml of LB media supplemented with Ampicillin and incubated at 37ºC 200 RPM O/N. The next morning, 1 mL of the culture is transferred to an Eppendorf tube and spun down at 10.000 g for 1 min. Media was discarded and the cell pellet was resuspended in 250 µl of MX1 buffer (50 mM Tris-HCl pH 8.0, 10 mM EDTA, 100 µg/ml RNase A). Then, 250 µl of MX2 buffer (0.2 M NaOH, 1% SDS) is added, and the solution is mixed by inversion and incubated at room temperature for 5 minutes, until the solution becomes clear. Finally, 350 µl of MX3 buffer (4 M guanidine hydrochloride, 0,5 M sodium acetate pH 4.2) are added, mixed by inversion and centrifuged at 12.000 g for 10 minutes.

The supernatant containing the DNA is then transferred to the column and spun down at 1500 g for 1 minute to trap the DNA in the column. The column is then washed twice by passing 500 µl of WS buffer (10 mM Tris-HCl pH 7.5, 80% Ethanol) through the column at 12.000 g for 1 minute. Finally, to elute the DNA onto a new Eppendorf tube, we incubated the column for 5 minutes with 50 µl of EB buffer (10 mM Tris pH 8.5) or deionised water and spun down the DNA at 12.000 g for 1 minute.

DNA presence and quantity were estimated by Ethidium Bromide agarose gel electrophoresis.

2.3.3. Agarose gel electrophoresis

Agarose gel electrophoresis allows for the separation of linearised DNA molecules according to their size. For this thesis, we used it commonly to verify DNA products used for *S. cerevisiae* transformation (2.1.6.), as well as DNA purification and check for cloning purposes (see 2.3.6. and 2.3.7.).

To prepare the gels, we heated 50 ml of TAE buffer (50 mM Tris-HCl pH 8.5, 2 mM EDTA) supplemented with 0,5%-1% (w/v) agarose in a microwave and poured the mix in an agarose gel casting tray. To stain the DNA, we added 0.5 µg/ml Ethidium Bromide (EtBr). EtBr intercalates double-stranded RNA or DNA and emits a fluorescent signal under UV light 25-fold brighter over the background. To run the gel electrophoresis, gels were installed on a gel running tank full of TAE buffer and ran at 80-90 V for the time needed for correct DNA separation (usually around 50 minutes).

DNA samples were loaded using commercial 6x DNA gel loading dye. To determine both the size and quantity of the different DNA fragments in the gel, samples were run alongside the appropriate amount of 1 Kb DNA ladder (New England Biolabs, N3232).

2.3.4. Polymerase Chain Reaction (PCR)

Polymerase Chain Reaction (PCR) was used to amplify DNA from plasmid DNA or *S. cerevisiae* genomic DNA for either yeast transformation, plasmid cloning and check or to check yeast transformation clones. We used two different polymerases according to their purpose: for cloning, transformation, site-directed mutagenesis and sequencing, we used Phusion High-Fidelity DNA polymerase (New England BioLabs, M0530); for simple, efficient and inexpensive DNA amplification for plasmid and strain checks, we used GoTaq DNA polymerase (Promega, M3001).

PCRs were performed using a thermocycler, and reactions were typically 50 µl. All PCR reaction products were kept on ice before use and at -20ºC freezer for long-term storage.

For Phusion polymerase reactions, the following PCR reaction mix and thermocycler profile were used:

- Phusion PCR reaction mix, prepared on ice, for 50 µl:
    - 10 µl of 5x DNA Polymerase Buffer. We used HF Buffer most of the time, and GC Buffer for difficult genomic templates
    - 4 µl of dNTP mix, at 2.5 mM each, for a final concentration of 200 µM each
    - 2 µl of the oligo mix (12.5 µM each), for a final concentration of 0.5 µM each
    - Between 0.1-1 µl of DNA template
    - 0.3 µl of Phusion Polymerase
    - Deionised water to 50 µl, added before the polymerase to avoid any primer degradation caused by the 3' → 5' exonuclease activity

- Phusion PCR thermocycler profile:
- Denaturation: 45 seconds at 98ºC
- 28 cycles:
    - Denaturation: 5 seconds for plasmid DNA, 10 seconds for genomic DNA, at 98ºC
    - Annealing: 10 seconds at an appropriate Annealing Temperature (Ta) for each reaction, ranging between 50 and 70ºC according to the New England BioLabs Tm calculator (https://tmcalculator.neb.com/#!/main). Effective Ta used was lowered when DMSO was added to the mix, at 0.6ºC for every % (v/v) of DMSO.
    - Amplification: 15 seconds/Kb for plasmid DNA and 30 seconds/Kb for genomic DNA, plus 10 extra seconds, at 72ºC
- Final amplification: 4 minutes at 72ºC

For the GoTaq polymerase reaction, the following setup was used instead:

- GoTaq polymerase PCR reaction mix, prepared on ice, for 50 µl:
    - 10 µl of 5x DNA Polymerase Buffer. We used green dye GO buffer to streamline gel agarose electrophoresis check
    - 5 µl MgCl2 at 25 mM (final concentration 2.5 mM)
    - 4 µl of dNTP mix, at 2.5 mM each, for a final concentration of 200 µM each
    - 1.5 µl of each oligo at 5 µM, for a final concentration of 0.15 µM each
    - Between 0.1-1 µl of DNA template
    - 0.3 µl of GoTaq polymerase
    - Deionised water to 50 µl, added before the polymerase

- GoTaq polymerase thermocycler profile:
- Denaturation: 2 minutes at 94ºC
- 30 cycles:
    - Denaturation: 30 seconds at 94ºC
    - Annealing: 30 seconds at 55ºC
    - Amplification: 1 minute/Kb at 72ºC
- Final amplification: 7 minutes at 72ºC

2.3.5. Oligo design

To amplify any DNA template, we designed both forward and reverse oligos surrounding the desired sequence to amplify, with particular sequences according to their use. Although manual design using SerialCloner 2.6 (http://serialbasics.free.fr/Serial_Cloner.html) or SnapGene viewer (https://www.snapgene.com/snapgene-viewer) was common, we also used Primer-Blast[243] to streamline the process. In general, all designed oligos included the following features:

- Sequence annealing to the template was 19-21 bases long, with a Melting Temperature (Tm) between 52 to 75ºC and had between 40-60% GC content. For every couple of oligos designed (forward and reverse) in a reaction, both Tm had to be as similar as possible (a maximum of 3ºC apart was allowed).
- No significant overall dimers were detected with the software.
- To allow for a stronger 3' annealing, the 3' end two base pairs on the oligo were either G or C.

Additional to the aforementioned features, designed oligos included the following sequences depending on their use:

- If the amplified DNA was used for cloning using classic enzyme digestion/ligation strategy (see 2.3.6), the 5' tails of the oligos included an overhang sequence containing the desired enzyme consensus sequence, as well as 3-6 random nucleotides to improve digestion efficiency.
- If the amplified DNA was used to integrate a particular sequence in the *S. cerevisiae* genome by yeast transformation (see 2.1.6.), a 5' overhang between 45-60 nucleotides annealing to the target region of the genome was included for each oligo. This would allow for the correct integration, replacement or deletion of genes in the region of interest by homologous recombination.

2.3.6. Plasmid cloning through restriction enzyme digestion and ligation

To introduce a particular gene inside the MCS region of a plasmid vector, a PCR of the full ORF from a genomic DNA template, including at least 500 bp upstream the ORF to include the wild-type promoter if needed, was performed. The PCR product is purified using the Epoch Columns. The resulting DNA product concentration was estimated using agarose gel electrophoresis.

Around 5 µl of vector plasmid and the purified PCR product are digested, in parallel, with the restriction enzymes chosen for the cloning, in 20 µl reactions each. We generally used New England Biolab enzymes with adequate incubation times and temperatures provided by the company. The vector plasmid 5' ends were also

dephosphorylated using Thermosensitive Alkaline Phosphatase (TSAP, Promega, M9910) to prevent plasmid re-circularisation. To perform the dephosphorylation, 5 U of TSAP (and 2.5 µl its correspondent buffer) were added to the vector plasmid digestion and incubated at 37ºC for 15 minutes. To inactivate the enzyme, the digestion is incubated for another 5 minutes at 65ºC. Both digestions are checked again by agarose gel electrophoresis to ensure full linearisation as well as to estimate the final concentration.

Finally, a ligation reaction using T4 DNA ligase (NEB, M0202S) was performed. The final volume used for this reaction was 10 µl and the vector and insert were added at a 1:3 ratio, to facilitate the reaction. The reaction mix was incubated at 16ºC overnight. As a ligation control, a separate reaction including only the vector is performed as well. After *E. coli* transformation of both ligation products, transformed cells were plated in white-blue LB selection plates (2.2.1). The number of colonies in the control ligation plate allowed for an estimation of false positives.

To check for positive clones, individual white colonies were inoculated into 5 ml of LB supplemented with 50 µg/ml Ampicillin and incubated at 37ºC overnight for plasmid DNA extraction (2.3.2.). A sample of the resulting minipreps was digested with the same restriction enzymes used in the cloning and analysed through agarose gel electrophoresis (2.3.3.). Positive clones were those showing two bands of the right size vs one corresponding to the empty vector.

2.3.7. Plasmid cloning through Gibson assembly

With this method[244], molecular cloning is achieved in a single isothermal mix that combines three reactions: a 5' exonuclease generates long overhangs, a polymerase fills in the gaps of the annealed single-strand regions, and a DNA ligase seals the nicks of the annealed and filled-in gaps. We used this method to subclone constructs based on the pRS backbone into new vector plasmids for which the standard digestion/ligation strategy was complicated or unavailable. To perform the assay, we used the Gibson Assembly Master Mix (NEB, E2611S)

The insert DNA fragment is amplified from a donor construct by PCR with a pair of oligos consisting of 19-21 nt homologous to the fragment to be amplified, also homologous to the recipient DNA. A parallel PCR using complementary oligos was performed on the recipient DNA to linearise it.

Both PCR products were purified using Epoch Columns and their concentration was estimated using agarose gel electrophoresis. 300 ng of insert DNA and 100 ng of recipient plasmid were mixed with 10 µl of 2x Gibson cloning master mix and water to a total of 20 µl. The reaction mixture is incubated at 50°C for 30 minutes and chilled down on ice for 10 minutes. Finally, 2 µl of ligation mixture is transformed into *E. coli* and checked like the classic digestion/ligation strategy (2.3.6.)

2.4. Biochemical techniques

2.4.1. Yeast whole cell protein extracts using LiAc/NaOH method

Protein whole cell extracts from yeast were obtained adapting a method described by Zhang et al. 2011[245]. The method is based on using highly concentrated Lithium Acetate (LiAc) to turn the cell wall completely leaky and denaturalise proteins with a base, to later resuspend them with Laemmli Loading Buffer (LLB).

At least $5x10^7$ cells were collected in Eppendorf tubes, keeping them on ice until cells are spun down at 1500 g for 1 minute in a refrigerated Eppendorf centrifuge. After removing the supernatant, the cell pellet was resuspended in 500 ul of pre-chilled 2 M LiAc and incubated on ice for 5 minutes. The sample was then centrifuged again at 1500 g for 1 minute in a refrigerated Eppendorf centrifuge and the LiAc was removed. Pellet was then resuspended in 500 µl of pre-chilled 0.4 N NaOH and incubated on ice for 5 minutes.

Finally, the sample was spun down again, the supernatant was removed and the pellet was resuspended in the appropriate amount of 1x LLB, at a density of $5x10^5$ cells/µl. Samples were boiled for 3 minutes at 95ºC, spun down the non-solubilised material and between 5 to 20 µl of the sample were loaded for SDS-Polyacrylamide gel electrophoresis (2.4.2).

2.4.2. SDS-Polyacrylamide gel electrophoresis (SDS-PAGE)

SDS denaturing Polyacrylamide Gel Electrophoresis (PAGE) was used to resolve proteins from whole cell extracts according to size[246]. A resolving gel containing either 7.5%, 10% or 12% (v/v) total acrylamide (37.5:1 acrylamide-bis acrylamide ratio, PanReac AppliChem, A4989) in 370 mM Tris pH 8.8, 0,1% SDS was cast in 1.5 mm thick glass plates. Resolving gels were topped with a 4% acrylamide stacking gel in 125 mM Tris pH 6.8, 0,1% (w/v) SDS. To allow for acrylamide polymerisation, 0,1% (w/v) ammonium persulphate (APS) and 0,1% (v/v) N,N,N',N'-Tetramethylethylenediamine (TEMED, Sigma, T9281) was added to each mix immediately before transfer to the glass plates.

To visualise in which region across the gel we would find our protein of interest during the run, two different pre-stained molecular markers were used:

- Prestained Protein Molecular Weight marker, Thermo Scientific (26612) for routine strain check
- Precision Plus Protein Standards Dual Color, Bio-Rad, (161-0374) for key experiments

To run protein samples on the acrylamide gels, gels were immersed in Running Buffer (25 mM Tris, 192 mM Glycine, 0.1% SDS (pH8.3-8.6) and run first at 80 volts (V) for 20 minutes (constant voltage) using a Power-Pac Basic (Bio-rad) to allow for the protein samples to linearise all the protein in a sharp, single band. After that, gels with a particular acrylamide concentration were run at different times and voltages depending on the protein of interest:

- For Cdc20-3HA, Cdc15-3HA, Pol12 and Cdc14-GFP: 7,5% gel, 80 minutes at 190 V
- For Clb2, Clb2ΔN-13Myc and Mob1-GFP and Dbf2-GFP: 7,5% gel, 60 minutes at 180 V
- For Pgk1 and Tub1: 10% gel, 50 minutes at 180V
- For Sic1: 12% 70 min at 180V

In cases where we needed to resolve phosphorylation shifts with a much more refined resolution, we cast SDS-PAGE Phos-tag gels, adding 5 µM Phos-tag (Waco-RAFER, 300-93523) and 25 µM $MnCl_2$ to the resolving gel mix. Both the casting of

the gel and the running of the electrophoresis were performed in low light levels to minimise Phos-tag degradation. Phos-tag gels were run at constant 160V until the marker immediately below the protein of interest was at the bottom of the gel. Phos-tag stock was prepared at 5 mM in 3% (v/v) MeOH and stored at 4ºC away from the light.

2.4.3. Western Blot

Once proteins were adequately distributed throughout the SDS-PAGE gel, proteins were transferred onto nitrocellulose membranes (Amersham, 10600001) by semi-dry electrotransfer (TE 77W, Amersham Biosciences). The semi-dry transfer was set up at constant Amperage, at 60A for each gel transfer for at least 50 minutes. The gel and membrane were sandwiched using equal amounts of Whatman paper slices (VWR Life Science, WHA3030917) of the same size, soaked in transfer buffer. The nitrocellulose membrane was pre-soaked in distilled water as well. The transfer buffer used was a modified version of the classic Towbin buffer (50mM Tris-Glycine pH 9,1, 0,0373% (w/v) SDS, 20% (v/v) methanol).

When transferring Phos-tag gels, gels were pre-incubated 3 times for 10 minutes in transfer buffer supplemented with 1 mM EDTA, rinsed once in transfer buffer without EDTA and a final 10 minutes in transfer buffer without EDTA. This facilitated the release of phosphoproteins from the Phos-tag before transferring to the nitrocellulose membrane.

Transferred membranes were stained with Ponceau S (0.2% (w/v) Ponceau S, Sigma-Adlrich, P3504, 3% (v/v) trichloroacetic acid) to visualise the most prevalent proteins and check the efficiency of the transfer. Stained membranes were scanned for reference and/or loading control. The Ponceau S stain was removed by washing the membranes with TBS-T buffer (100 mM Tris-HCl pH 7.4, 150 mM NaCl, 0.1% (v/v) Tween-20), usually 3 times for 5 minutes each, or as many washes as needed to remove the staining. All incubations and washes were performed on a rocking table.

Next, the membranes were incubated in TBS-T supplemented with 5% powder skim milk for 30 minutes at room temperature (RT) to block the nonspecific binding of the

antibodies to the membrane. The membranes were then incubated with the primary antibody for the appropriate time, generally 1 hour at RT or overnight at 4ºC. Antibodies used were:

- Anti-Myc 9E10 (Roche, 11667149001), mouse monoclonal. Diluted 1:2000 in TBS-T 5% milk
- Anti-HA 3F10 (Roche, 1867423), rat monoclonal. Diluted 1:2000 in TBS-T 5% milk
- Anti-Clb2 (Santacruz, Y-180 sc-9071), rabbit polyclonal. 1:2000 in TBS-T 5% milk
- Anti-Sic1 (Santacruz, FL274 sc50441), rabbit polyclonal. 1:1000 in TBS-T 5% milk
- Anti-DNApol α primase B subunit or Anti-Pol12 (Ascites from Foiani et al 1995[247], 6D2), mouse monoclonal. Diluted 1:2000 in TBS-T 1% milk
- Anti-Pgk1 (Abcam, ab113687), mouse monoclonal. Diluted 1:10.000 in TBS-T 5% milk
- Anti-GFP (Invitrogen, 3E6), mouse monoclonal. Diluted 1:500 in TBS-T 5% milk

After the incubation with the primary antibody, the membranes were washed 3 times with TBS-T, 5 minutes each. Then, the membranes were incubated with horse-radish peroxidase (HRP) coupled secondary antibodies for the appropriate time, usually 30 minutes at room temperature. The secondary antibodies used were:

- Anti-Mouse (Millipore, AP200P), goat polyclonal. Diluted 1:20.000 in TBS-T 5% milk
- Anti-Rat (Santa Cruz, sc2006), goat polyclonal. Diluted 1:10.000 in TBS-T 5% milk
- Anti-Rabbit (DAKO, P0448), goat polyclonal. Diluted 1:2000 in TBS-T 5% milk

After incubation with the secondary antibody, the membrane was washed again 3 times with TBS-T, 5 minutes each, and incubated with Immobilon Western Chemiluminescent HRP Substrate for 3 minutes at RT. Membranes were then immediately exposed to sensitive photographic film (Medical X-Ray film blue, AGFA) for the appropriate time. Finally, exposed films were developed using a (Curix 60, AGFA).

2.5. Cell biology experiments

2.5.1. Cell density and budding index determination of yeast cultures

The cell density of a given culture was determined by counting cells in a light microscope using a *Neubauer* chamber. A small sample of the culture was diluted in chilled deionised water (1/10, 1/20 or 1/50 dilution depending on the density of the cell culture) and the dilution was sonicated for 8 seconds at 50W to separate cells. Around 8 µl of the sonicated dilution were dispensed in the chamber and the cells in all 25 squares in a *Neubauer* chamber were counted. Depending on the shape of the cells, we could distinguish between G1/S (unbudded cells and early budded cells), G2 (small to medium budded cells) and mitotic cells (dumbbell-shaped cells).

2.5.2. Cell cycle metaphase arrest experiment

A fresh colony of the strain of interest was inoculated in a 100 ml flask containing 20 ml of Synthetic Complete Media lacking methionine with either 2% glucose or 2% raffinose as a carbon source (SCD-Met or SCRaff-Met respectively). Cells were incubated overnight at 30ºC in an incubator with orbital shaking at 200 RPM. The next morning, cell density was counted using a Neubauer chamber (2.5.1.) and diluted to $5x10^6$ cells/ml in the appropriate volume of media and left incubating until exponentially growing cells reached $1x10^7$ cells/ml. Cell culture was then supplemented with 4mM methionine to arrest the expression of the *CDC20* gene under the methionine-repressible *MET3* promoter (2.1.3). Cells in glucose needed around 2 hours to consistently synchronise to metaphase, while cells in raffinose needed between 3 hours and 3 hours and 30 minutes.

Once >90% of the cells were in dumbbell shape, cells were released from the arrest by washing 3 times with pre-warmed SC-Met media, to finally release the culture in the appropriate media, also pre-warmed at the desired temperature (usually 30ºC). Aliquots were taken at the desired intervals during the desired extension of time.

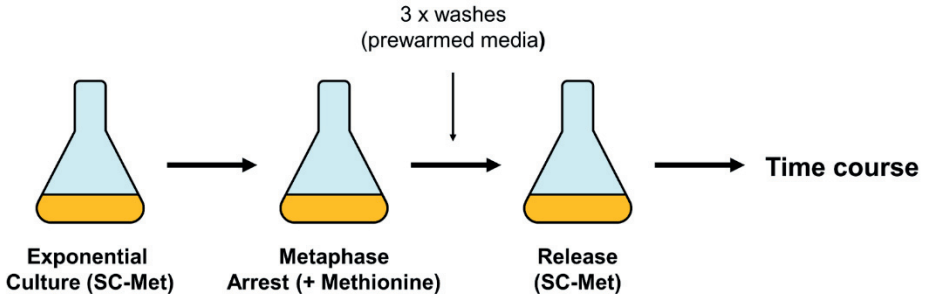

Figure 2.3. Steps of Time Course experiment with MET3-CDC20 synchronisation.

2.5.3. Time Course experiments with inducible protein over-expression in metaphase arrested cells

Two methods were followed to conditionally express the protein of interest in metaphase-arrested cells.

In strains carrying the *ADGEV* gene, cells growing in Synthetic Complete Media lacking methionine with 2% glucose (SCD-Met) were processed as described in 2.5.3. until metaphase synchronisation is achieved. Then, β-estradiol was added to 36 μM for 30 minutes. After *GAL1* promoter induction, methionine was washed out from the media as previously described and cells were resuspended in SCD-Met supplemented with β-estradiol.

In strains lacking the *ADGEV* gene, cells growing in Synthetic Complete Media lacking methionine with 2% raffinose (SCRaff-Met) were processed as described in 2.5.3. until metaphase synchronisation is achieved. Then, cells were spun down and resuspended in Synthetic Complete Media with 4 mM methionine supplemented with 2% Galactose (SCGal+Met). After 45 minutes incubation to allow for proper *GAL1* induction, methionine was washed out from the media as previously described and cells were resuspended in SCGal-Met.

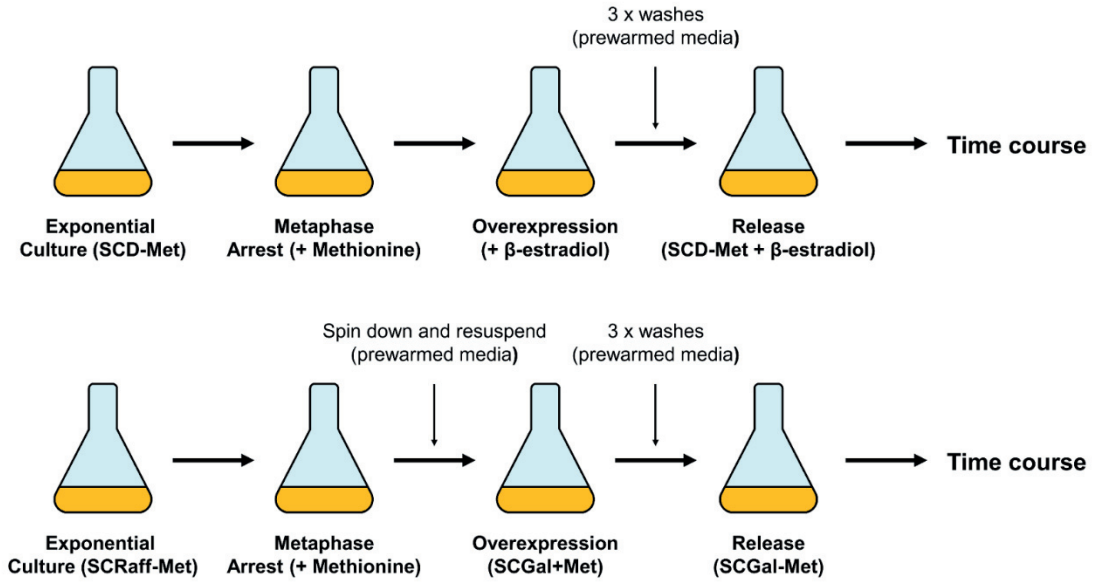

Figure 2.4. Steps of Time Course experiment for protein overexpression.

2.6. Microscopy experiments

2.6.1. Cell culture preparation for live cell imaging to monitor fixed timepoints

To monitor cells in a specific timepoint during an experiment, a 1 ml aliquot of the culture at the desired timepoint is spun down in a 1.5 ml Eppendorf tube and most of the media is discarded by decantation, resuspending the cells in the remaining 100 µl of media. A drop of 3-4 µl of the preparation is pipetted in a regular microscope slide and covered using a regular coverslip, carefully pushing the coverslip to fix cells into position without crushing them. The slide is then installed in the microscope for cell imaging. Each slide was processed within 10 minutes after slide preparation and at least 100 cells were counted for each timepoint.

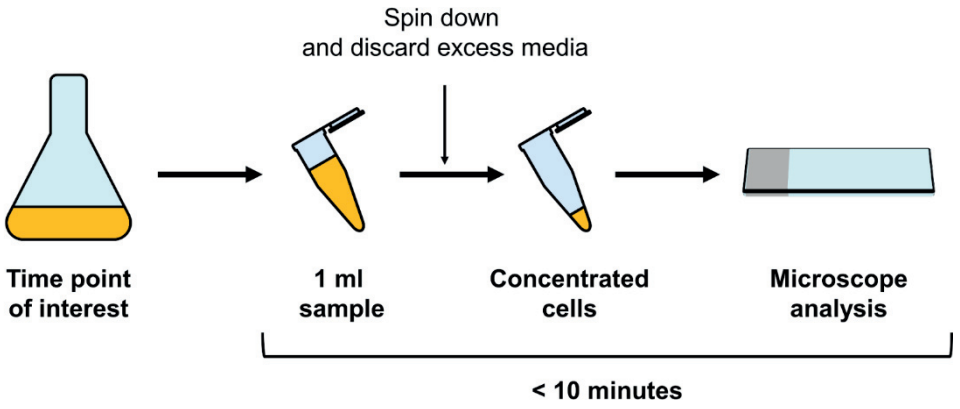

Figure 2.5. Steps for live cell imaging of specific timepoints.

2.6.2. Cell culture preparation for live cell imaging for single cell timelapse experiments

To monitor single cells released under certain conditions during an experiment for longer periods, an aliquot of the culture of interest was diluted to $2x10^6$ cells/ml in the appropriate pre-warmed media and sonicated for 4 seconds at 50W to allow for individual cell separation. 250 µl of the preparation were pipetted in a well of an uncoated µ-Slide 8 Well Ibidi slide. The slide is then installed in the microscope for cell imaging. Within 5 to 10 minutes after the slide preparation, most of the cells were deposited at the bottom ready to be monitored with the microscope. Since the cells are still in their media, they can grow as in regular liquid cultures for several hours. This allows for precise monitoring of tagged proteins during the cell cycle.

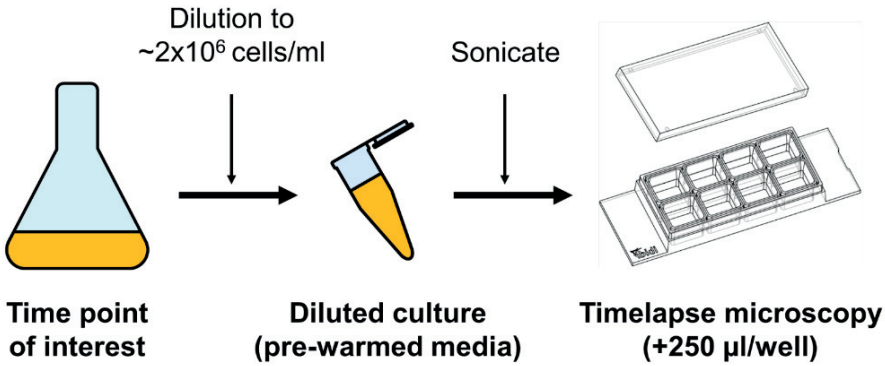

Figure 2.6. Steps for life-cell imaging using ibidi slides.

In cases in which cells were required to remain immobilised in the same position for long periods, the wells in the Ibidi slide were pre-coated with a 5 mg/ml solution of the lectin Concanavalin A (Con A, Sigma-Adlrich, L7647), adapting a protocol from Sanchez-Diaz et al. 2008[248]. Con A is a lectin from *Canavalia ensiformis* that shows specific affinity for molecules containing α-D-mannopyranosyl and α-D-glucopyranosyl, present in the *S. cerevisiae* cell wall. When covered with Con A, cells firmly get immobilised to the slide without compromising their viability or growth.

120 µl of the stock solution of Con A was added to each well, which is enough to cover the surface, and the slide was incubated for 10 minutes at room temperature. The solution was then discarded, and the wells were vigorously washed with distilled water, pipetting up and down to remove any excess of Con A. After carefully removing the water used for washing, the ibidi slide was left drying under a hood for at least 1 hour. After this, pre-coated Con A ibidi slides were used as mentioned previously. Con A stock solution was prepared with deionised water and stored at -80ºC.

2.6.3. Live cell imaging conditions for fluorescent microscopy

Several microscope devices were used during the course of this thesis. All of them were used to monitor strains that integrated proteins tagged with fluorescent proteins at their C-terminus. The fluorescent proteins used were: Yeast Enhanced Green Fluorescent Protein (GFP), monomeric cherry (mCherry) and Cyan Fluorescent Protein (CFP) from the pYM collection[242].

For observation of SPO20-GFP and Myo1-mCherry, the Leica TCS SP5 confocal microscope (*Servei de Microscòpia,* UAB) was used. Stacks of at least 11 µm with a step size of 0,34 µm were taken using the PL APO 63x/1.4-0.6 oil immersion objective. We used the Argon laser 488 nm for SPO20-GFP and the He-Ne 561 nm laser for Myo1-mCherry.

For observation of some experiments with Mob1-GFP, Hof1-GFP and Chs2-GFP, the Nikon Eclipse Ti semi-confocal microscope (*Departamento de Ciencias Básicas,* UIC) was used. The fields were focused around the bud neck of the cells using the Perfect Focus System and a single step-size image of the field was captured using

the 63x oil immersion objective. Green signal was detected using the GFP capture pre-set, with 2 seconds exposure for each field. To allow for optimal cell growth under the microscope, the microscope included a thermal chamber that was pre-heated at 30ºC at least 45 minutes before the start of the experiment.

For observation of Mob1-GFP, the Leica Thunder DMI8 microscope (Molecular Imaging Platform, IBMB-CSIC) was used as well. Stacks of 9 µm with a step size of 0.5 µm were captured using the HCX PL APO 40x oil objective. The SEDAT filter set with the standard pre-configuration for eGFP detection was set up. Brightfield images were taken alongside the GFP stacks. The microscope included a thermal chamber that was pre-heated at 30ºC 50 minutes before the start of the experiment.

For Mob1-GFP, Dbf2-GFP, Cdc15-GFP and Cdc14-GFP, the Zeiss Spinning Disc microscope (Dundee Imaging Facility, Dundee University) was used. Stacks of 6 µm width with a step size of 0.5 µm were taken using the 100X objective. For the visualisation of GFP, the 488 laser was used at 40% intensity, with an exposure time of 100 ms. Brightfield images were taken alongside the GFP stacks. For reliable focus throughout the experiment, the Definitive Focus 2 module was set up at the middle of the division site of the cells. The microscope included a thermal chamber that was pre-heated at 30ºC at least 30 minutes before the start of the experiment.

2.6.4. Cell culture preparation for fixed cell imaging using DAPI

To monitor nuclear DNA in cells at particular timepoints, we checked fixed cells stained with 4′,6-diamidino-2-phenylindole (DAPI, Thermofisher Scientific, 62248) using fluorescent microscopy.

To prepare the samples for DAPI staining, around $1x10^7$ cells in the desired timepoint were harvested into an Eppendorf tube, chilled on ice and sonicated for 7 seconds at 50W to allow for individual cell separation. Cells were then centrifuged at 3000g for 30 seconds at 4ºC and the media was completely removed. Pellet is resuspended in pre-chilled -20ºC methanol and stored in the -20ºC freezer for at least 6 minutes to fix and permeabilize the cells. After this, samples were centrifuged at 3000g for 30 seconds again, methanol was removed and cells were resuspended in pre-chilled -20ºC acetone. Finally, samples were stored at -20ºC until needed.

To prepare the samples for microscopy, 10 µl of the cells in acetone were dispensed throughout the middle of a regular slide, which evaporates immediately, and 5 µl of DAPI (0,1 µg/ml DAPI; 50% Glycerol; 0,5 x PBS) are added on top and distributed using a coverslip. The slides are then ready to install in the microscope for image acquisition.

We used an Olympus Fluoview 1000 with a UPlansApo 60x objective to visualise the nuclear DNA in the slides. To visualise stained nuclei, we used the 405-diode laser. Image acquisition was performed at different exposition times and at least 100 cells were counted for each condition.

2.6.5. Microscopy image processing using Fiji

To process the different microscope files generated with the different microscopes, we used the ImageJ distribution Fiji (https://imagej.net/software/fiji/) and the Bio-Formats plugin included in the software.

All images for a particular experiment were enhanced to the same Minimal and Maximum intensity values that allowed for background removal without compromising any signal. For timelapses with several fields, each one with a particular step size, a Z-projection of the stack for maximum intensity was performed, discarding the steps that were out of focus. For figure presentation, representative cells were isolated in 12 by 12 µm squares.

2.6.6. Evaluation of the Cdc14 subcellular localisation using Fiji image analysis

Timelapse images were obtained with a Zeiss Spinning Disc microscope as described in 2.6.3. All images were taken at the same resolution (pixels/micron).

Individual cells were randomly selected within a field. A Maximum Intensity Z-projection of the stack was then performed. The cell area was manually selected using the polygon selection tool, outlining the whole cell**.** Measurements used the same selection area, moving and rotating the selection when needed. The image

analysis software Fiji detects individual pixels and reads the respective brightness in the colour channel of interest.

For each cell, on every timepoint during the experiment, the Area, Mean Gray, Standard Deviation, and Min & max grey values were measured (Analyze → Set measurements to select the 4 variables, then Analyze → Measure at each timepoint). Measurements for each cell were then copied to an excel spreadsheet for analysis.

From these data, we estimated the subcellular localisation of Cdc14-GFP adapting the protocol by Neurohr and Mendoza, 2017[249]. The Coefficient of Variance of green intensity (CV), i.e. the ratio between the Standard Deviation and the Mean Gray Intensity, was determined for each cell at each timepoint:

CV = Standard Deviation / Mean Gray

For analysis, the timepoint immediately before the release of Cdc14 from the nucleolus to the nucleus was considered time 0. To normalise the CV curves, the average of the 3 previous timepoints was calculated to generate a baseline. The normalised data was termed CV_{Cdc14}.

CV_{Cdc14} = CV / Average (CV_{-3}, CV_{-2}, CV_{-1})

The normalised coefficient of variance (CV_{Cdc14}) allows distinguishing the three possible Cdc14-GFP subcellular distributions, as depicted in figure 20. The Cdc14 nucleolar localisation implies the highest coefficient of variation in the cell image, due to a bright localised signal surrounded by large low brightness surroundings (CV_{Cdc14} > 0,8). The nuclear localisation signal implies dilution and extension of the signal, hence decreasing the coefficient of variation in the cell image (CV_{Cdc14} between 0.4 to 0.6). Finally, when Cdc14 may translocate to the cytosol, the signal reaches the maximum dilution and extension, distributing with maximum homogeneity all over the cell, hence implying the lowest coefficient of variation (CV_{Cdc14} <0.4).

The CV_{Cdc14} curves of all the selected cells were then averaged and plotted in a graph for analysis, including the standard deviation bar.

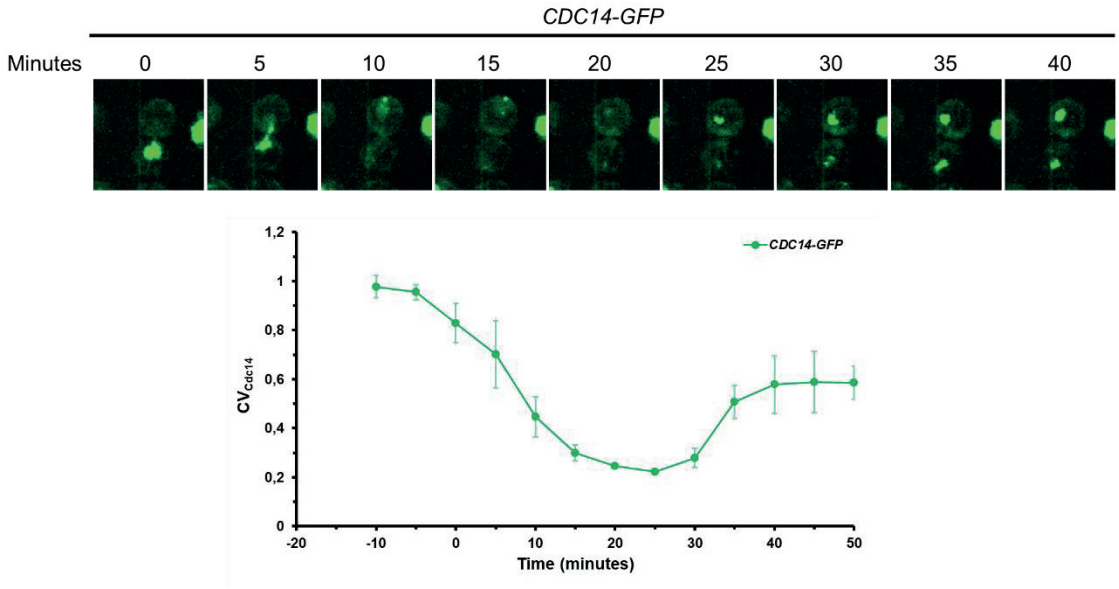

Figure 2.7. Cdc14 intensity quantification A culture of strain YAZ57 (*CDC14-GFP MET3-CDC20 GAL1-Clb2ΔN)* was grown to mid-exponential phase in SCRaff-Met and monitored by Spinning Disc Fluorescence Microscopy. Timelapse images correspond to a representative cell used for quantification (n = 3). The graph depicts the mean CV_{Cdc14} values and their standard deviation at the given timepoints.

2.7. Strains used in this thesis

Strain name	Relevant genotype	Origin
cdc7-4	*W303-1a MATa cdc7-4*	Bousset and Diffley, 1998
YCCL135	*W303-1a MATa bar1Δ mob1-7A-GFP:hph-NT1 mob1Δ dbf2-7A dbf2Δ GAL1-clb2ΔN-13MYC:HIS3 MET3-3HA-CDC20:LEU2*	This thesis
YCCL174	*W303-1a MATa bar1Δ MET3-CDC20-LEU2 ADGEV:URA3 GAL1-clb2∆N-13MYC:TRP1 HOF1-GFP:hphNT1*	This thesis
YAZ40	*W303-1a MATa bar1Δ GAL1-clb2ΔN-AID-9MYC:natNT2:TRP1 ADH1-OsTIR1-9Myc:URA3*	This thesis
YAZ86	*W303-1a MATa bar1Δ MET3-CDC20-LEU2 ADGEV:URA3 GAL1-clb2∆N-13myc:TRP1 MOB1-GFP:hphNT1*	This thesis
YAZ63	*W303-1a MATa bar1-del CDC14-GFP:hphNT1 HTB2-mCherry:HIS3 ADGEV:NAT1 Met3-cdc20:LEU2 GAL1-clb2∆N-13MYC:TRP1*	This thesis
YAZ91	*W303-1a MATa bar1Δ MET3-CDC20-LEU2 ADGEV:URA3 GAL1-clb2∆N-13myc:TRP1 MOB1-GFP:hphNT1 SPC42-mCHERRY:natNT2*	This thesis
YAZ133	*W303-1 MATa bar1Δ GAL1-clb2∆N-13MYC:HIS3 MET3-3HA-CDC20:LEU2 ADGEV:URA3 HOF1-GFP:hphNT1*	This thesis

YAZ137	*W303-1 MATa bar1Δ GAL1-clb2ΔN-13MYC:HIS3 MET3-3HA-CDC20:LEU2 ADGEV:URA3 CHS2-GFP:hphNT1*	This thesis
YAZ227	*W303-1a MATa bar1Δ mob1-7A-GFP:HIS3 mob1Δ dbf2-7A dbf2Δ cdc15-7A-3HA:LEU2 cdc15Δ::natNT1 GAL1-clb2ΔN-13MYC:ADE2 TRP1:MET3-CDC20*	This thesis
YAZ236	*W303-1a MATa bar1Δ MET3-CDC20-LEU2 ADGEV:Ura3 PGAL1-Clb2delN-13myc:Trp1 bar1Δ Dbf2-GFP:His3MX6*	This thesis
YAZ254	*W303-1a MATa bar1Δ mob1-7A mob1Δ dbf2-7A dbf2Δ cdc15-7A-3HA:LEU2 cdc15Δ::natNT2 GAL1-clb2ΔN-13MYC:ADE2 MET3-CDC20:TRP1 CDC14-GFP:HIS3MX6*	This thesis
YAZ265	*W303-1a MATa bar1Δ MET3-CDC20:TRP1 GAL1-clb2ΔN-13MYC:ADE2 mob1-7A-GFP:HIS3MX6 mob1Δ dbf2-7A dbf2Δ cdc15-7A-3HA:LEU2 cdc15Δ::natNT2 Iqg1-14A:URA3 iqg1Δ:hphNT1*	This thesis
YAZ267	*W303-1a MATa bar1Δ MET3-CDC20-LEU2 ADGEV:URA3 Gal1-clb2ΔN-13MYC:TRP1 CDC15-GFP:HIS3MX6*	This thesis
YAZ269	*W303-1a MATa bar1Δ MET3-CDC20:TRP1 GAL1-clb2ΔN-13MYC:ADE2 mob1-7A mob1Δ dbf2-7A dbf2Δ cdc15-7A-GFP:HIS3MX6:LEU2 cdc15Δ::natNT2*	This thesis
YAZ271	*W303-1a MATa bar1Δ MET3-CDC20:TRP1 GAL1-clb2ΔN-13MYC:ADE2 mob1-7A mob1Δ dbf2-7A-GFP:HIS3MX6 dbf2Δ cdc15-7A-3HA:LEU2 cdc15Δ::natNT2*	This thesis
YPR178	*W303-1a MATa bar1Δ MYO1-mCHERRY:hphNT1 GFP-spo20(51-91):HIS3 MET3-3HA-CDC20:LEU2 ADGEV:URA3*	Our lab
YPR205	*W303-1a MATa MYO1-mCHERRY:hphNT1 GFP-spo20(51-91):HIS3 MET3-3HA-CDC20:LEU2 ADGEV:URA3 GAL1-clb2ΔN-13myc:TRP1 bar1Δ*	Our lab

YPR225	*W303-1a MATa MET3-3HA-CDC20:LEU2 ADGEV:URA3 CHS2-GFP:HIS3 bar1Δ*	Our lab
YPR302	*W303-1a MATa MET3-3HA-CDC20:LEU2 GAL1-clb2ΔN-13myc:TRP1 ADGEV:URA3 IQG1-6HA*	Our lab
YPR331	*W303-1a MATa GAL1-clb2ΔN-13myc:TRP1 ADGEV:URA3 SPC42-mCHERRY:nat1NT2 MET3-3HA-CDC20:LEU2 MOB1-GFP:HIS3 bar1Δ*	Our lab

2.8. Constructs used in this thesis

Plasmid name	Description	Origin
P204	*pRS304-nud1-7A-3HA*	Marisa Segal[251]
P211	*pRS306-nud1-7A-CFP*	Marisa Segal[251]
pAZ7	*pRS402-GAL1-Clb2ΔN-13Myc*	This thesis, derived from pKL126[252]
pAZ8	*pRS403- GAL1-Clb2ΔN-13Myc*	This thesis, derived from pKL126[252]
pAZ13	*pRS304-GFP-spo20(51-91)*	This thesis, derived from Nakanishi et al. 2004[253]
pAZ14	*pRS402-mob1-7A*	This thesis
pAZ18	*pRS404-cdc15-7A*	This thesis
pAZ25	*pRS406-iqg1-14A*	This thesis, derived from Naylor and Morgan, 2014
pDM56	*pRS305-cdc15-7A*	Jaspersen and Morgan, 2000
pGC255	*pRS405-ADH1-OsTIR1-9Myc*	Gloria Palou, Quintana lab
pGC256	*pRS406-ADH1-OsTIR1-9Myc*	Gloria Palou, Quintana lab
pKL126	*pMHT-GAL-clb2Δ1-120-1Myc-9His-URA3*	Karim Labib [252]
pMet3-Cdc20	*pRS305-pMET3-3HA-CDC20*	Ethel Queralt [129]
pMM195	*Pgen360 ADGEV-URA3*	Francesc Posas [255]
pPR 1	*pRS306-mob1-7A*	Ping Ren, Quintana lab

pPR 4	*pRS306-dbf2-7A*	Ping Ren, Quintana lab
pPR 7	*pRS306-GAL1-Clb2ΔN-13Myc*	Ping Ren, Quintana lab, derived from pKL126[252]
pPR 19	*pRS304-GAL1-Clb2ΔN-13Myc*	Ping Ren, Quintana lab, derived from pKL126[252]
YIP22	*pRS304-pMET3-3HA-CDC20*	Ethel Queralt[129]

2.9. Primers used in this thesis

Name	**Sequence (5'-3')**	**Strains/ Construct**
9831 DBF2 Clone BamHI F	CGCGGATCCGGGCTCTTCTACATACTTG	YAZ 233, 254, 265, 269, 271, YCCL 135
9832 DBF2 Clone XhoI R	CGGCTCGAGCGAATGCAAGACAAGAATT	YAZ 233, 254, 265, 269, 271, YCCL 135
9833 DBF2 T493A F	CAATGATCCCGCCTTTTGCACCCCAACTAGACAGC	YAZ 233, 254, 265, 269, 271, YCCL 135
9852 CDC15 S2 oligo R	GTATTATTTCTCTATATATGTATGTATGCACATGCAATTCCTACAATCGATGAATTCGAGCTCG	YAZ 267
9853 CDC15 S3 oligo F	GATAAAAGTGACGGCTTTTCCGTCCCCATTACAACATTTCAAACACGTACGCTGCAGGTCGAC	YAZ 267, 269
oCCL 112 Gibson pRS marker F	CTGGCTTAACTATGCGGCATCAGAGCAGATTG	pAZ 13, 18
oCCL 113 Gibson pRS marker R	GTTCACGTAGTGGGCCATCGCCCTGATAGAC	pAZ 13, 18
oCCL 114 Gibson pRS F	GTCTATCAGGGCGATGGCCCACTACGTGAAC	pAZ 13, 18

oCCL 115 Gibson pRS R	CAATCTGCTCTGATGCCGCATAGTTAAGCCA G	pAZ 13, 18
oCCL 124 Cdc15 S1	CACACATAAGCACTACCCATTTTCCTGGTAA GACTATACCATGAACAGTATGGCCGATA-CGTACGCTGCAGGTCGAC	YAZ 227, 233, 236 254, 265, 267 269 271
oCCL 126 Nud1 S2	CATTTACTAATTACATACATTTTTAGTACTGC GTACGGGTATAGTTATGGGGATCGATGAATT CGAGCTCG	YAZ 233
oCCL 127 DBF2 S3	GGCATCTTATTCAACGGACTGGAACACTCAG ACCCCTTTTCAACCTTTTACCGTACGCTGCA GGTCGAC	YAZ 236
oCCL 128 dbf2-7A S2	GGGTACCGGGCCCCCCCTCGAGCGAATGCA AGACAAGAATTCATTTTTACGATCGATGAATT CGAGCTCG	YAZ 271
oCCL 129 DBF2 WT S2	GTTAAAGCTAATTATATCGCGGCGAATGCAA GACAAGAATTCATTTTTACGATCGATGAATTC GAGCTCG	YAZ 271
oCCL 130 Nud1 WT S1	GGTGAAAAAATTGCCGACTAGGTTGAATAGT AAAAGCATACCGAAATGCGTACGCTGCAGGT CGAC	YAZ 233
oCCL 131 Nud1 del check F	ATTGAGTCGTTGTAGGTAACG	YAZ 233
oCCL 132 Nud1 del check R	CTGCGTACGGGTATAGTTATG	YAZ 233
oCCL 133 Nud1 Seq-114	CGATGCACAACAGATAATGA	YAZ 233
oCCL 134 Nud1 Seq540	CGCTGAGAAGGTCTCATCGT	YAZ 233
oCCL 135 Nud1 SeqRe1598	TAATGAACAATGTGCGCTCG	YAZ 233
oCCL 2 Gal-CLB2ΔN-13myc- NotI-REV	CAGGGCGGCCGCTACCCTGTTATCCCTAGC GG	pAZ 7, 8
oCCL 25 Seq-chk-iqg1(14A)-1-FRW	GAAAATAAGAAAGTAGTTGG	YAZ 265
oCCL 30 Seq-chk-iqg1(14A)-6-FRW	GATTGACTCTTTAAGGGCCA	YAZ 265
oCCL 48 S3-CLB2ΔN	GGGCTTTAAAGGTTAGAAAAAACGGCTATGA TATAATGACCTTGCATGAACGTACGCTGCAG GTCGAC	YAZ 38

oCCL 67 cdc14-S2 (2480)	TAAGTTTTTTTATTATATGATATATATATATATAT AAAAATGAAATAAATTAATCGATGAATTCGAG CTCG	YAZ 63, YAZ 254
oCCL 68 cdc14-S3 (2481)	CTACAAGCGCCGCCGGTGGTATAAGAAAAAT AAGTGGCTCCATCAAGAAACGTACGCTGCAG GTCGAC	YAZ 63, YAZ 254
oCCL 73 S2 mob1-7A-GFP	CACTAAAGGGAACAAAAGCTGGGTACCGGG CCCCCCCTCGAGCAATACTAATCGATGAATT CGAGCTCG	YCCL 135, YAZ 227, 233, 265
oCCL 74 S3-mob1-GFP	TGATTTTGGTCCGCTGTTAGAATTAGTGATG GAGTTGAGGGATAGGCGTACGCTGCAGGTC GAC	YAZ 86, 92, 227, 233, 265, YCCL 135, YPR 331
oCCL 77 S2-MOB1(wt)-GFP	CATGCATGGAAGAATACAACCTACAAGCAGA CTTATATAAATATACAATACTAATCGATGAAT TCGAGCTCG	YAZ 86, 92, YPR 331
oCCL 93 Chs2-S2	AGAAAAAAGAGGGAATGACGAGAAATTAGCT GAAAAATACTGGCATTAATCGATGAATTCGA GCTCG	YAZ 129, 137
oCCL 94 Chs2-S3	GAAGTCTCTAAATTAGACTTACCAAATGTTTT CCACAAAAAGGGCCGTACGCTGCAGGTCGA C	YAZ 129, 137
oCCL 95 Hof1 S2	CTTTTTTTCTTTTATCAGAAAACTAGTAAAATT GATATACATCGAGATCAATCGATGAATTCGA GCTCG	YAZ 133, YCCL 174
oCCL 96 Hof1 S3	GGATTAATTCCCTATAATTTCATTCAGCTACT GCATCAAGGTCTTCGTACGCTGCAGGTCGA C	YAZ 133, YCCL 174
oCCL20 Iqg1(14A)-REV	CCATTTAAACAAATGATGATTGCC	YAZ 265
oCCL27 Seq-chk-iqg1(14A)-3-FRW	CGAATATACCGGTGGAAGAA	YAZ 265
oCCL33 Seq-chk-iqg1(14A)-9-REV	GTCATCACTAACGAGGAATCG	YAZ 265
oCCL80 Not1-pIqg1-Iqg1-FW (539-559)	ATACCGCGGCCGCGTATCGATTGCAAACAA GTGG	YAZ 265
oCCL81 Iqg1-XhoI-RV (5798-5819)	CTATCCTCGAGTTTCTTGGGCCTATTTGGTC G	YAZ 265
oFL 114 MOB1-T105A-F	TAACGGACTTTAACTATGCACCATCGCATCA GAAG	YAZ 233, 254, 265, 269, 271, YCCL 135

oFL 118 DBF2-S37A-F	GAACTCCATGGTTGGGGCTCCGGATTATATGGC	YAZ 233, 254, 265, 269, 271, YCCL 135
oFL 1189 DBF2-T413A-R	GATCCACTAAATGGTGCATAACCAACTAAACT	YAZ 233, 254, 265, 269, 271, YCCL 135
oFL 20 DBF2-T62A-F	GTTTCGATGGGCATGGGGCTCCTGGGGGCACTGGAC	YAZ 233, 254, 265, 269, 271, YCCL 135
oFL 24 DBF2S53A-F	GTATCAATGATGCACCTGCGCCGGTAAAACCATCC	YAZ 233, 254, 265, 269, 271, YCCL 135
oFL 25 DBF2-S83A-R	GGTGGAAGCTTCTTGGGAGCGTTCGAGACATCCATATC	YAZ 233, 254, 265, 269, 271, YCCL 135
oFL 31 Mob1clone-BamHI-F	CGC**GGATCC**GCTTATGGCACAAAAGTACAC	YAZ 233, 254, 265, 269, 271, YCCL 135
oFL 32 Mob1clon-Xho1-R	CCGCTCGAGCAATACTACCTATCCCTCAAC	YAZ 233, 254, 265, 269, 271, YCCL 135
oFL 34 MOB1-S10A-F	CCTTTTGAAAGCAGTCATATAGCTCCCGGCCAAACAATAAGATC	YAZ 233, 254, 265, 269, 271, YCCL 135
oFL 40 MOB1-S80A-F	CGACCATGGAAGGATGGCTCCCGTCCTCACTACG	YAZ 233, 254, 265, 269, 271, YCCL 135
oFL 41N MOB1-T85A-R	CGTGCCTCTTTGGCGCAGTGAGGACGGGAG*C*CATC	YAZ 233, 254, 265, 269, 271, YCCL 135
oFL 71 Mob1-check-F	CTTATGGCACAAAAGTACAC	YAZ 233, 254, 265, 269, 271, YCCL 135
oPing 13 Cdc15-del NAT1-R	CAGATGCGTTTTCAGTATTGGAAGGTTCACAATTCTATATATAGTGTTAATGTAATGCTGATCGATGAATTCGAGCTCG	YAZ 227, 265, 269, 271
oPing 175 Myo1-CHK-F	GTTTGGAGAGAGCAGTGGAAG	YPR 178, 205
oPing 176 Myo1-CHK-R	GAAGGATACGGGGTGAAAGAG	YPR 178, 205

oRP 70 Spc42 F	GCGTTGGCTCGTGTTACACA	YPR 331
oRP 71 Spc42 R	ACGTCTATTCGTAGGATTGG	YPR 331

3. Results

3.1. The experimental approach

To screen for the essential M-Cdk1 targets that inhibit cytokinesis, we devised the following experimental approach, based on previous reports showing that high M-Cdk1 activity blocks cytokinesis, as discussed in the introduction. We hypothesised that cells conditionally over-expressing *clb2ΔN*, a hyperstable mutant of the mitotic cyclin Clb2 lacking the D-box and KEN-boxes, should remain blocked after anaphase, unable to enter cytokinesis. However, if the set of critical targets through which M-Cdk1 blocks entry into mitotic exit were replaced by non-phosphorylatable alleles, cells should be able to undergo cytokinesis despite the presence of high M-Cdk1 activity (figure 3.1).

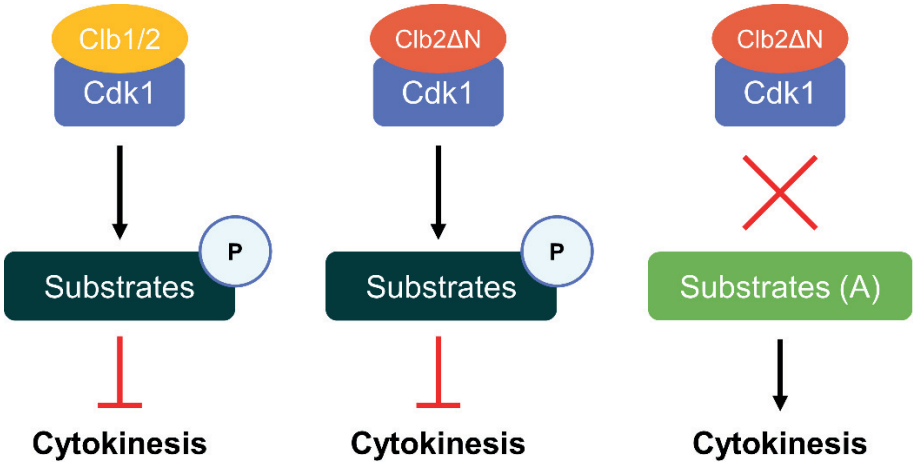

Figure 3.1. Bypassing the M-Cdk1 block of cytokinesis with non-phosphorylatable alleles of the set of critical targets. In a normal cell cycle (left), M-Cdk1 blocks cytokinesis until MEN activation shifts the balance of activities in favour of Cdc14. In our experimental approach (centre), overexpression of the hyperstable *clb2ΔN* allele blocks cytokinesis permanently. Cells carrying the corresponding non-phosphorylatable mutants of the set of critical M-Cdk1 targets (right) should be able to enter cytokinesis when hyperstable *clb2ΔN* is overexpressed.

We therefore created strains that integrated a galactose-inducible, ectopic copy of the hyper-stable *clb2ΔN* allele in different backgrounds.

We first went on to characterise our experimental system. That is, (1) to obtain experimental evidence indicating that cells arrest at a post-anaphase, pre-cytokinesis stage, (2) with M-Cdk1 kinase activity prevailing over Cdc14 phosphatase antagonistic activity, and (3) whether persistent high M-Cdk1 compromises the cells ability to undergo cytokinesis when the kinase control is abrogated.

3.1.1. Cells under high M-Cdk1 activity are unable to undergo cytokinesis and arrest in anaphase

We first explored the microscopical profile of cells arrested under high M-Cdk1. We used three different markers. First, cell morphology, as cells arrested in mitosis should all show a dumbbell. Second, we followed the actomyosin ring (AMR), which is present in mitosis until it contracts and disassembles in cytokinesis. Finally, cytokinesis was tracked using Spo20, a protein that coats the inner side of the plasma membrane.

Strains were created carrying the *GAL-clb2ΔN* mutant, the AMR component Myo1 tagged with mCherry, and a copy of *GFP-SPO20(51-91)* (see Materials and Methods). Also, to allow for quick over-expression of *GAL-clb2ΔN* using β-estradiol, we integrated the *ADGEV* construct. Finally, for metaphase synchronisation, the endogenous *CDC20* gene was put under the control of the methionine-repressible *MET3* promoter (*MET3-CDC20*).

For the experiment shown below, exponentially growing *MET3-CDC20 ADGEV GAL-clb2ΔN MYO1-mCherry GFP-SPO20* cells, and isogenic control cells lacking the *GAL-clb2ΔN* gene, were synchronised in metaphase by depleting Cdc20 with the addition of methionine to the media. β-estradiol was then added to induce the over-expression of Clb2ΔN. Finally, methionine was washed out from the media and cells were released in media lacking methionine but with β-estradiol, allowing for Cdc20 expression and progression through mitosis. Cells were inspected using confocal microscopy.

As shown in figure 3.2, control cells show membrane closure 30 minutes after metaphase arrest release, as evidenced by the GFP-Spo20 signal, indicating progression into cytokinesis. However, cells over-expressing Clb2ΔN were unable to close the plasma membrane at the bud neck for the 120 min of the experiment, indicating that they were unable to enter cytokinesis. Further supporting the above evidence, control cells show loss of Myo1-mCherry at the bud neck, whereas cells over-expressing Clb2ΔN were unable to contract the AMR.

Finally, in contrast to control cells, cells overexpressing Clb2ΔN remain dumbbell shaped and unable to divide for the whole duration of the experiment.

In all, over-expression of Clb2ΔN arrests cells in a dumbbell morphology, unable to enter cytokinesis.

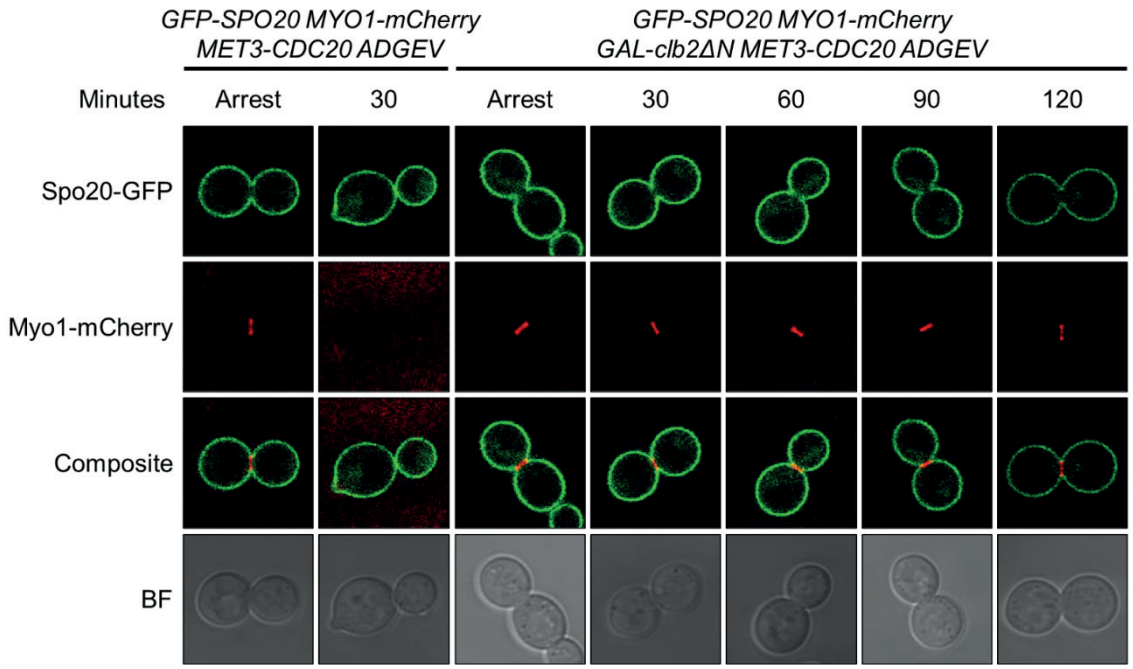

Figure 3.2. High M-Cdk1 activity bocks cell membrane ingression and AMR contraction. Confocal images of Strains YPR178 (*Myo1-mCherry GFP-SPO20 MET3-CDC20 ADGEV)* and YPR205 (*Myo1-mCherry GFP-SPO20 MET3-CDC20 ADGEV GAL1-clb2ΔN*) released from metaphase arrest over-expressing Clb2ΔN. *Arrest* timepoint refers to cells during metaphase arrest overexpressing Clb2ΔN. Each column depicts a representative cell stack from the given timepoint. Images were taken in a Leica TCS SP5. The figure is representative of 2 independent experiments.

We next wished to check whether the cells arrested by high M-Cdk1 had completed anaphase. Otherwise, the block of cell cycle progression might be caused by a defect resulting in the activation of either the SAC or the SPOC checkpoints (see Introduction 1.4.1 and 1.4.2).

We harvested a sample of cells from the previous experiment at the given timepoints, fixed them with -20ºC methanol/acetone, stained their DNA with DAPI, and checked their nuclei under fluorescence microscopy.

As shown in figure 3.3, both control cells and cells over-expressing Clb2ΔN were indeed arrested in metaphase, as shown by the presence of a single nucleus at the mother cell, near the bud neck. After release from the metaphase arrest, both control cells and cells under high M-Cdk1 activity can undergo anaphase, as shown by the presence of two fully separated nuclei at both ends of mother and daughter cells. In all, these results support that high M-Cdk1 activity efficiently blocks mitotic exit after anaphase completion in our experimental system, discarding that the block of cytokinesis is due to checkpoint activation.

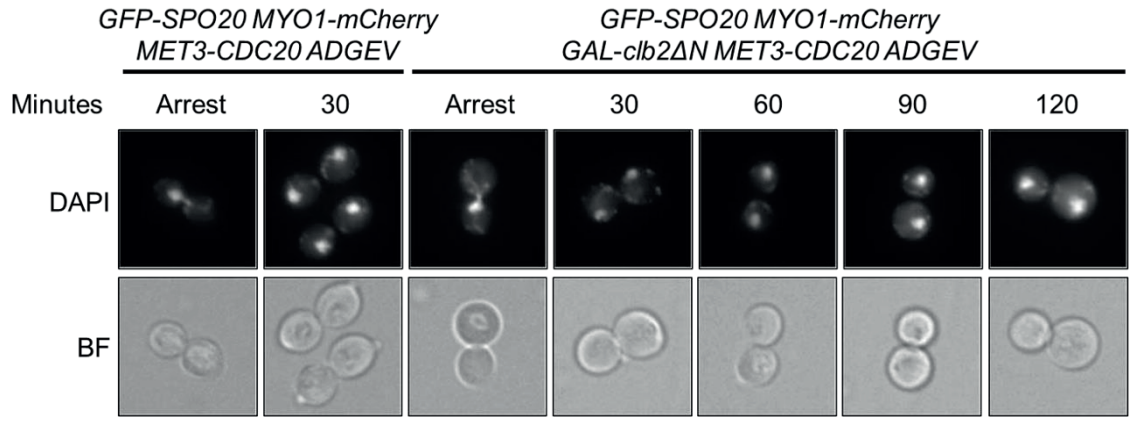

Figure 3.3. High M-Cdk1 arrested cells undergo full anaphase. DAPI images of Strains YPR178 (*Myo1-mCherry GFP-SPO20 MET3-CDC20 ADGEV)* and YPR205 (*Myo1-mCherry GFP-SPO20 MET3-CDC20 ADGEV GAL1-clb2ΔN*) released from metaphase arrest over-expressing Clb2ΔN. *Arrest* timepoint refers to cells during metaphase arrest overexpressing Clb2ΔN. Each column depicts a representative cell from the given timepoint. Images taken in an Olympus Fluoview 1000. The figure is representative of 2 independent experiments.

Together with Myo1, another element of the AMR recruited before the G2/M transition is the F-Bar protein Hof1. Hof1 is recruited to the bud-neck in G2/M and thus is not inhibited by M-Cdk1 activity. The Hof1 bud-neck signal contracts as cells enter cytokinesis (see Introduction 1.4.5). Thus, we decided to monitor Hof1 localisation under high M-Cdk1 as well.

Exponentially growing *MET3-CDC20 ADGEV GAL-clb2ΔN HOF1-GFP* cells, and isogenic control cells lacking *GAL-clb2ΔN,* were exposed to β-estradiol to allow for Clb2ΔN expression, and cells were monitored by timelapse fluorescence microscopy. We followed only small-budded cells, that have finished S-phase, to skip tracking cells where untimely M-Cdk1 activity would tamper with G1 thus affecting normal cell cycle progression.

As shown in figure 3.4, both WT and *GAL-clb2ΔN* successfully recruited Hof1 at the neck. However, whereas the AMR contracted normally in control cells, as visualised through the Hof1 signal at the bud-neck, Clb2ΔN blocked contraction. This result further supports that high M-Cdk1 activity is blocking mitotic exit in our experimental system.

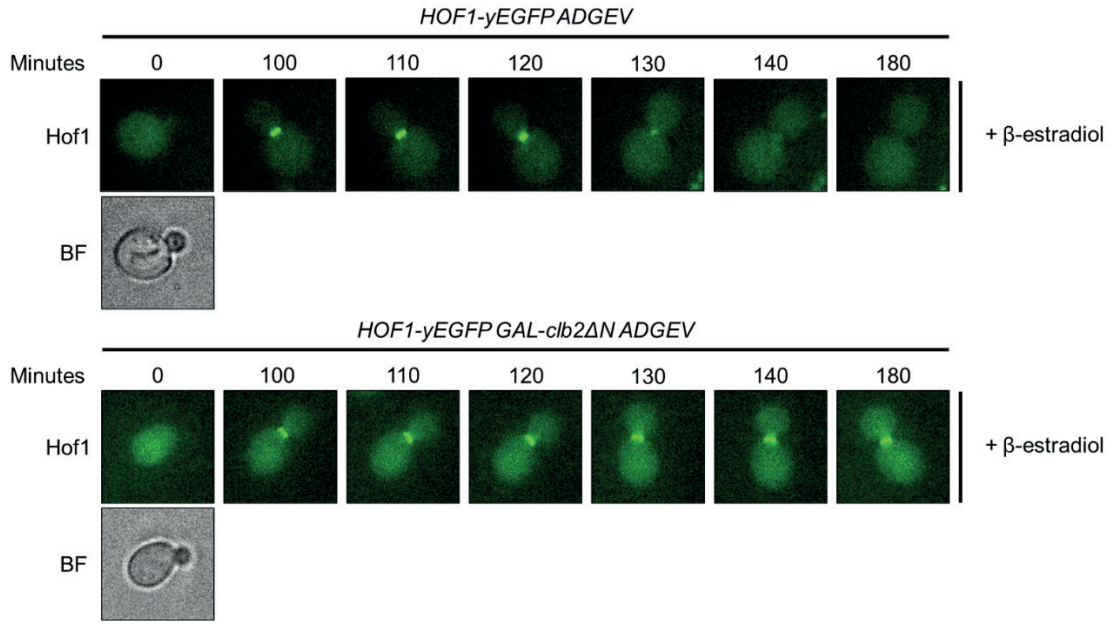

Figure 3.4. High M-Cdk1 activity blocks AMR contraction monitored by Hof1. Timelapse fluorescence microscopy images of representative cells of each strain. Cultures of strains CCL174 (*MET3-CDC20 ADGEV HOF1-GFP*) and YAZ133 (*MET3-CDC20 ADGEV GAL-clb2ΔN HOF1-GFP*) were grown to mid-exponential phase in SCD-Met media and monitored by timelapse fluorescence microscopy (Nikon Eclipse Ti) in the presence of β-estradiol. Images of the same fields were taken every 10 minutes. Time 0 represents the start of the video. A Brightfield image of the field was taken at the first timepoint. The figure is representative of 3 independent experiments.

3.1.2. M-Cdk1 activity prevails over Cdc14 activity

M-Cdk1 activity promotes entry to mitosis while inhibiting cytokinesis. Upon MEN activation, the balance of M-Cdk1 and Cdc14 activities is shifted towards the phosphatase, thus driving cells through cytokinesis (see 1.4).

To investigate the balance of M-Cdk1 and Cdc14 activities in our experimental system through two different markers. First, we monitored the balance of M-Cdk1 and Cdc14 activities of the B subunit of DNA polymerase α Pol12, a *bona fide* substrate of both M-Cdk1[56] and Cdc14[256].

Second, we chose to monitor APC^{Cdh1} activity, which is inhibited by M-Cdk1 and is activated in telophase by Cdc14. APC^{Cdh1} is responsible for the complete destruction

of mitotic cyclins at the exit of mitosis. The levels of endogenous mitotic cyclin Clb2 were used to evaluate APC^{Cdh1} activity (see section 1.4.2.2).

MET3-CDC20 GAL-clb2ΔN cells in complete synthetic media with 2% raffinose lacking methionine (SCRaff-Met) were arrested at metaphase by depletion of Cdc20. The culture was split in two and the media was changed to either fresh SCRaff+Met or Synthetic Media with 2% Galactose (SCGal+Met) to allow for Clb2ΔN overexpression. Methionine was washed out from the media and cells were allowed to finish the cell cycle. To synchronise dividing cells at G1, α-factor was added to both cultures 30 minutes after release. Samples were processed for western blotting of whole cell extracts, and for cell density and dumbbell index quantification for each timepoint.

As shown in figure 3.5-A, Pol12, a *bona fide* M-Cdk1 substrate (see 3.1.2 for details), becomes phosphorylated in metaphase-arrested cells, when M-Cdk1 activity is high, evidenced by the electrophoretic mobility shift in the band of the western blot. In control cells, Pol12 starts de-phosphorylating 60 minutes after release, being completely dephosphorylated by 120 minutes. In contrast, cells overexpressing Clb2ΔN have Pol12 fully phosphorylated during the whole time course, indicating that M-Cdk1 activity prevails over Cdc14 in our experimental system.

Whole-cell extracts were also probed for endogenous Clb2 as a marker of APC^{Cdh1} activation. As shown in figure 3.5-A, Clb2 starts decreasing 60 minutes after the metaphase arrest release, and completely disappears by 120 minutes upon release. In deep contrast, cells overexpressing Clb2ΔN show stable Clb2 levels, indicating that APC^{Cdh1} remains blocked due to M-Cdk1 activity prevailing over Cdc14 in our experimental system.

Finally, figure 3.5-B and C shows that control cells successfully finished the cycle after around 60 to 90 minutes after release. In contrast, cells induced with galactose stayed arrested in dumbbell shape and did not increase their density throughout the whole experiment, up to 3h after release.

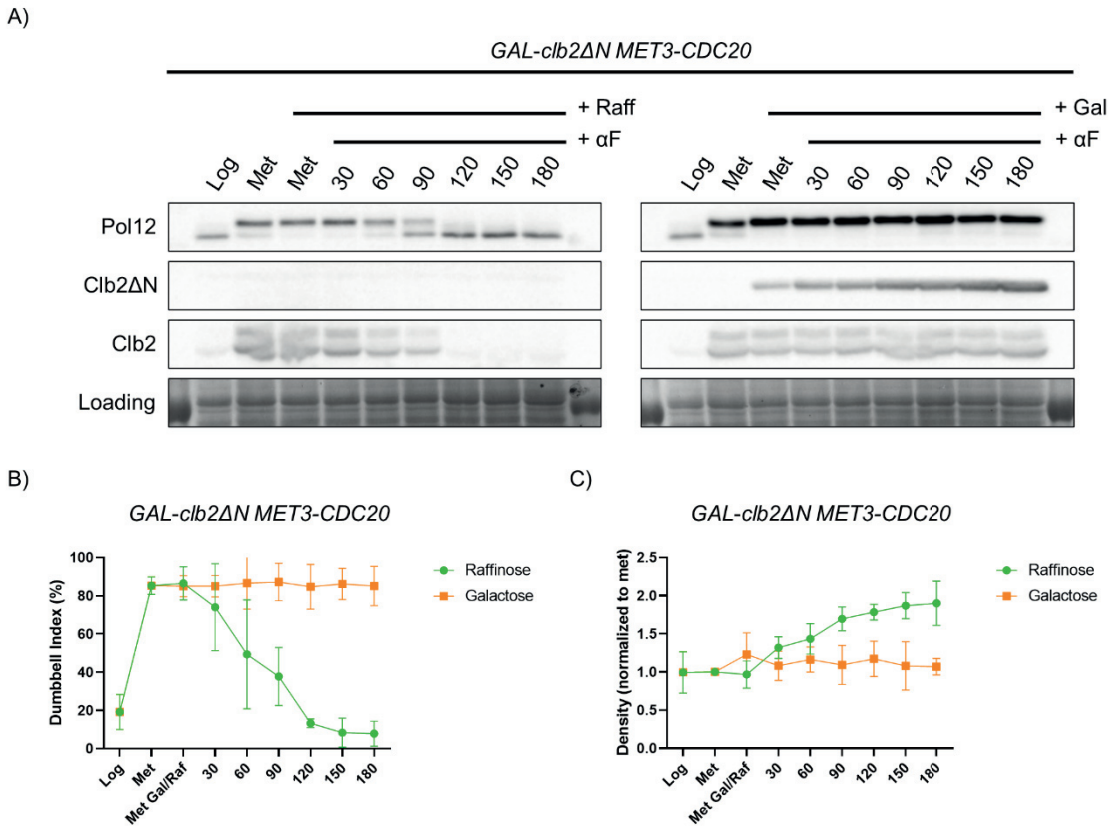

Figure 3.5. Over-expression of GAL-clb2ΔN prevails over Cdc14 and APC^{Cdh1} activities. A culture of YPR302 (*MET3-CDC20 GAL-clb2ΔN*) was grown on SCRaff-Met media and arrested by depletion of Cdc20. The culture was split and overexpression of *GAL-clb2ΔN* was induced in one culture using 2% galactose (SCGal+Met). Both cultures were then released from the metaphase either in raffinose (SCRaff-Met) or galactose (SCGal-Met). Cells were collected at the indicated times. (A) Immunoblot against Pol12 and Clb2 of whole cell extracts. Pol12 mobility shift was used to track phosphorylation. Clb2 immunoblot showed both endogenous Clb2 and Clb2ΔN protein levels. The Ponceau-S staining of the membrane is shown as a loading control. (B) and (C) show the mean dumbbell index and cell density of cells throughout the experiment, respectively. Cell density was normalised to the methionine arrest timepoint (Met) to allow for comparison between replicas. Error bars indicate standard deviation. The figure is representative of 3 independent experiments.

Another marker of the balance of M-Cdk1 and Cdc14 activities is the subcellular localisation of chitin synthase Chs2. Chs2 remains at the endoplasmic reticulum (ER) by direct phosphorylation of M-Cdk1. Upon dephosphorylation by Cdc14, Chs2 is relocated to the bud neck (see 1.4.5).

To analyse the subcellular localisation of Chs2 in cells overexpressing Clb2ΔN, exponentially growing *MET3-CDC20 ADGEV GAL-clb2ΔN CHS2-GFP* cells, and isogenic control cells lacking GAL-*clb2ΔN,* were exposed to β-estradiol, to allow for Clb2ΔN overexpression, and monitored by timelapse fluorescence microscopy. We followed only small-budded cells, that have finished S-phase, to skip tracking cells where untimely M-Cdk1 activity would tamper with G1 thus affecting normal cell cycle progression.

As seen in Figure 3.6, control cells in dumbbell shape transiently recruit Chs2 to the neck as expected (Oh et al. 2012). In contrast, cells overexpressing Clb2ΔN fail to accumulate Chs2 at the bud neck during the 3 hours timelapse, further supporting that M-Cdk1 activity prevails over Cdc14 in our experimental system

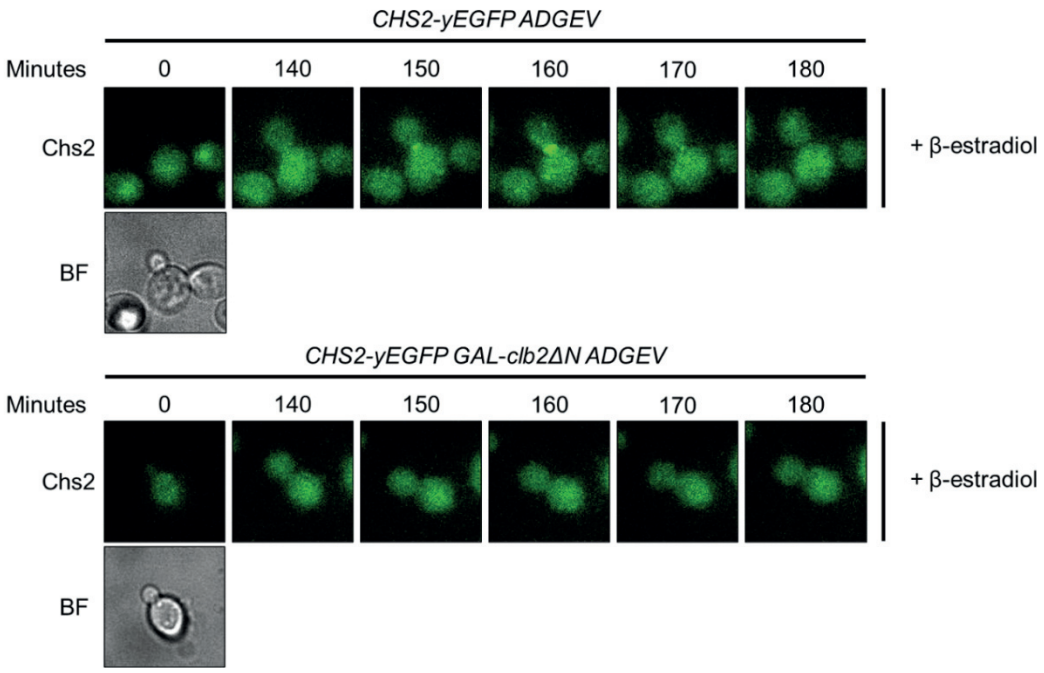

Figure 3.6. High M-Cdk1 activity blocks Chs2 recruitment to the division site. Timelapse fluorescence microscopy images of a representative cell of each strain. Cultures of strains YAZ129 (*MET3-CDC20 ADGEV CHS2-GFP*) and CCL182 (*MET3-CDC20 ADGEV GAL-clb2ΔN CHS2-GFP*) were grown to mid-exponential phase in SCD-Met media and monitored by timelapse fluorescence microscopy (Nikon Eclipse Ti) in the presence of β-estradiol. Images of the same fields were taken every 10 minutes. T = 0 represents the start of the video. A Brightfield image of the field was taken at the first timepoint. The figure is representative of 2 independent experiments.

3.1.3. Cells under persistent high M-Cdk1 remain competent to undergo cytokinesis when the kinase is terminated

Our experimental approach might have a limitation, if persistent high M-Cdk1 activity affected the cell's ability to undergo cytokinesis, e.g. by targeting a cytokinesis critical factor for destruction or disassembling a critical complex. In that case, replacing the critical M-Cdk1 targets with non-phosphorylatable mutants would result in a false negative result.

We generated a strain carrying the *GAL-clb2ΔN* cassette tagged with an auxin-inducible degron (AID) module at its C-terminus. To allow for the degradation of Clb2ΔN-AID by the addition of Auxin, we integrated OsTIR1 under the control of the housekeeping *ADH1* promoter.

3.1.3.1. Destruction of Clb2ΔN with a regulatable degron rescues the cells ability to grow in galactose

Exponentially growing wild-type, *GAL-clb2ΔN* and *GAL-clb2ΔN-AID* cells were grown in YPD to allow for Clb2ΔN expression. Then, serial dilutions of each culture were performed, and cells were plated in either YPD or YPGal plates, each with IAA or DMSO.

As shown in figure 3.7 control cells were able to grow in all conditions, as expected, and *GAL-clb2ΔN* cells were unable to grow as much as control cells in YPGal plates.

Significantly, the growth defect is rescued in *GAL-clb2ΔN-AID* cells, as it can form colonies in YPGal supplemented with IAA. The reason that cells grow at a slower path than wild-type cells is likely due to the continuous expression of *GAL-clb2ΔN-AID* and the limiting concentration of IAA in the plates to avoid long-term toxicity. These conditions may keep low levels of Clb2ΔN in the cells rather than complete destruction.

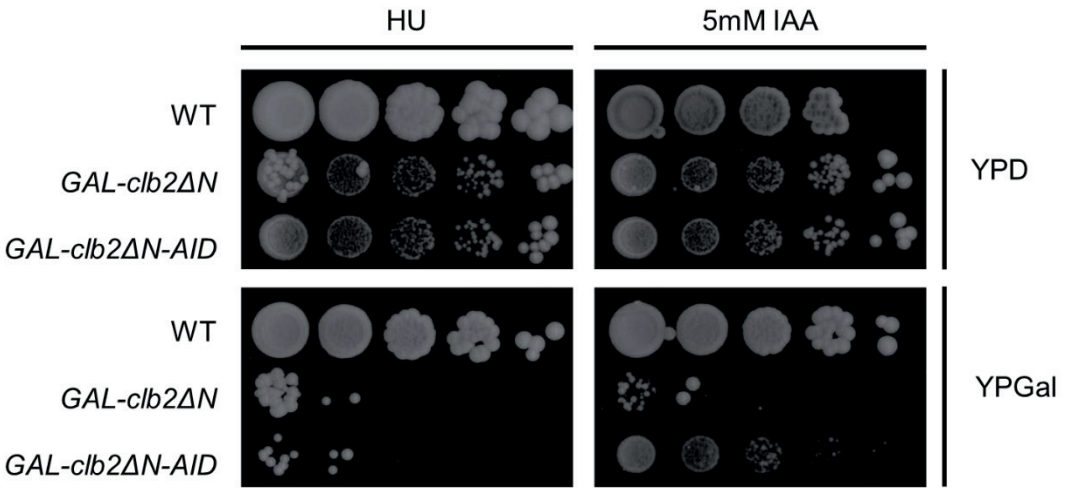

Figure 3.7. Destruction of Clb2ΔN rescues cells' ability to grow on galactose. Spot assay of a culture of strain YAZ40 (*GAL-clb2ΔN-AID ADH1-OsTIR1*). Cells were plated in YPD and YPGal plates, either supplemented with 5mM IAA or DMSO. The figure is representative of 2 independent experiments.

3.1.3.2. Cells over-expressing Clb2ΔN are able to undergo cytokinesis after M-Cdk1 activity is terminated

To explore the reversibility of our experimental system more finely, we carried out a cell cycle experiment in liquid culture, which allows for more efficient AID activation to ensure the complete destruction of Clb2ΔN.

GAL-*clb2*ΔN ADH1-OsTIR1 cells grown in YPRaff were synchronised in G1 with α-factor, released and arrested again at G2/M by the addition of Nocodazole to the media. After synchronisation, Clb2ΔN overexpression was induced by the addition of 2% galactose for 45 minutes. Next, the culture was split, Nocodazole was washed away from the media, and cells were released in YPRaff supplemented with either Auxin or the same volume of DMSO. Samples were taken at given timepoints for western blot analysis and cells were counted for budding index and cell density.

As shown in figure 28-A, control cells overexpressing Clb2ΔN supplemented with DMSO stayed arrested in dumbbell shape and were not able to divide. In contrast, cells exposed to IAA started dividing around 60 minutes after the release of the G2/M arrest, and most of them divided 90 minutes after release, as evidenced by the low

peak in the budding index (figure 28-B). In concordance, the budding index remains constant in control cells, whereas it decreases in cells exposed to IAA (figure 28-B, 90 minutes timepoint). IAA-treated cells are also able to re-bud (figure 28-B, 120 min timepoint), indicative of cells being able to start a new cycle.

The timing of division of the cells treated with IAA correlates with the disappearance of Clb2ΔN, 30 minutes after exposure to IAA, and the disappearance of endogenous Clb2 by min 60 (figure 28-C). In control cells, both Clb2ΔN and endogenous Clb2 levels remain constant as expected.

In summary, our results indicate that exposure to continued, high M-Cdk1 activity does not compromise the ability of cells to undergo cytokinesis, further validating our experimental system.

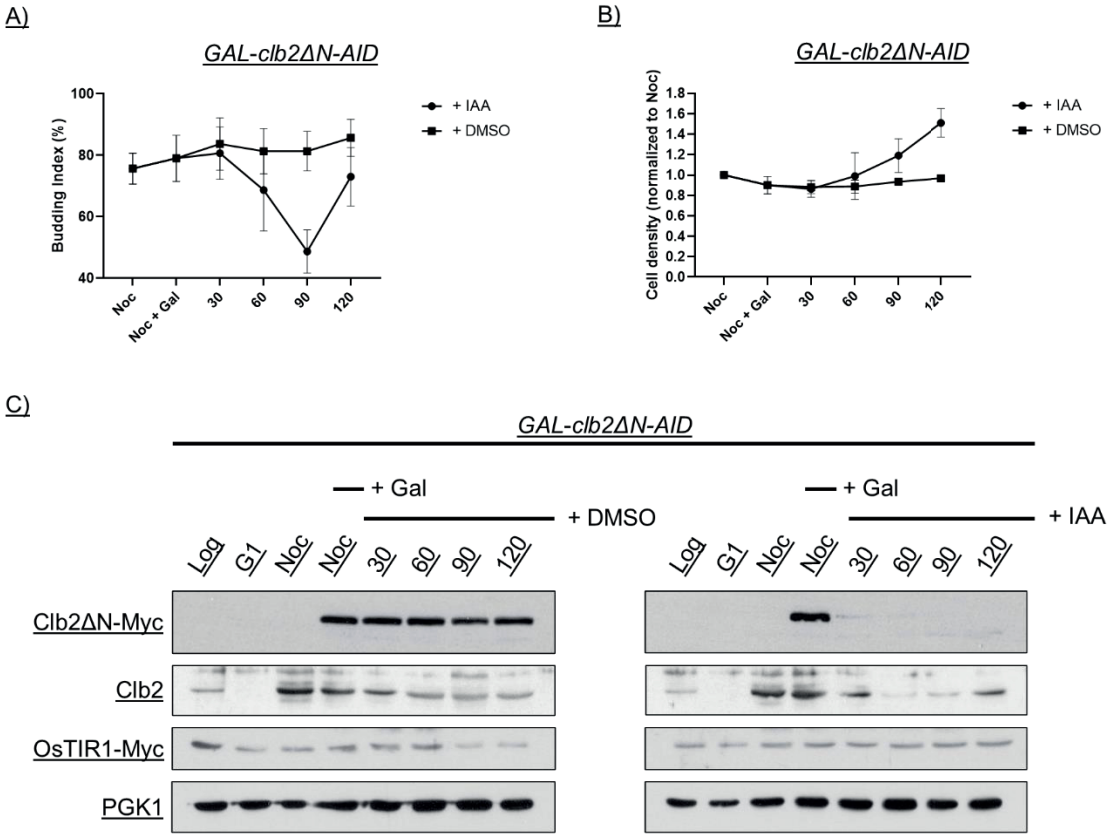

Figure 3.8. Destruction of Clb2ΔN allows cells to divide. A culture of strain YAZ40 (*GAL-clb2ΔN-AID ADH1-OsTIR1-9Myc*) was grown on SCRaff-Met media and arrested by the addition of nocodazole. Overexpression of *GAL-clb2ΔN* was induced using 2% galactose (SCGal+Met) for 45 minutes. The culture was split in two and released in YPRaff supplemented either with 5 mM IAA or DMSO. Both cultures were then released from the arrest. Cells were collected at the indicated times. (A) and (B) show the mean budding index and cell density of cells throughout the experiment, respectively. Cell density was normalised to the methionine arrest timepoint (Met) to allow for comparison between replicas. Error bars indicate standard deviation. (C) Immunoblot against Clb2, Myc tag and Pgk1 of whole cell extracts. Clb2 immunoblot showed both endogenous Clb2 and Clb2ΔN protein levels. The Myc tag monitors OsTIR1 expression. Pgk1 was used as a loading control. The figure is representative of 3 independent experiments.

3.2. Exploration of potential M-Cdk1 targets in the control of cytokinesis (I): The MEN kinases

The Mitotic Exit Network (MEN) is the upstream-most pathway essential for cytokinesis. Two of its constituents, namely Cdc15 and Mob1, have been described to be inhibited by M-Cdk1 activity[184,254]. In addition, in a global analysis for Cdk1 substrates, Dbf2 was found to be phosphorylated at at least three sites[257], although no reports have been published on its possible biological significance.

Dbf2-Mob1 activation is essential for full Cdc14 release, the phosphatase that counteracts M-Cdk1 to trigger cytokinesis[132,258]. In addition, Dbf2-Mob1 may also play a direct role in the site of cell division, as it localises at the bud neck at the time of AMR contraction[187,215] and has been shown to phosphorylate Chs2, essential for cytokinesis[178,183,196]. Furthermore, Mob1 has been shown to be an M-Cdk1 substrate[259]. All this makes the Mob1-Dbf2 kinase a compelling candidate as an M-Cdk1 target in the negative control of cytokinesis.

Because Dbf2 requires phosphorylation by the upstream MEN kinase Cdc15[174], and given that Cdc15 is also negatively regulated by M-Cdk1[254], we included Cdc15 in the M-Cdk1 bypass attempt.

We therefore hypothesised that cells carrying non-phosphorylatable alleles of Cdc15, Mob1, and Dbf2 might allow cytokinesis in the presence of sustained high M-Cdk1 activity.

As a preliminary work, we first explored the behaviour of the MEN constituents Mob1-Dbf2 and Cdc15, both in an unperturbed cell cycle and in the presence of high M-Cdk1 activity.

3.2.1. Mob1-Dbf2 localisation in an unperturbed cell cycle

We first assessed the known subcellular localisation behaviour of Mob1 and Dbf2 in an unperturbed cell cycle. We generated a strain carrying Mob1 tagged with GFP as well as SPB scaffolding protein Spc42 tagged with mCherry and monitored exponentially growing cells using confocal fluorescence microscopy.

As shown in figure 3.9, we were able to detect two distinct dots of Mob1 in dumbbell-shaped cells in anaphase, which colocalise with both the mother and daughter SPBs as previously described [149,187,260].

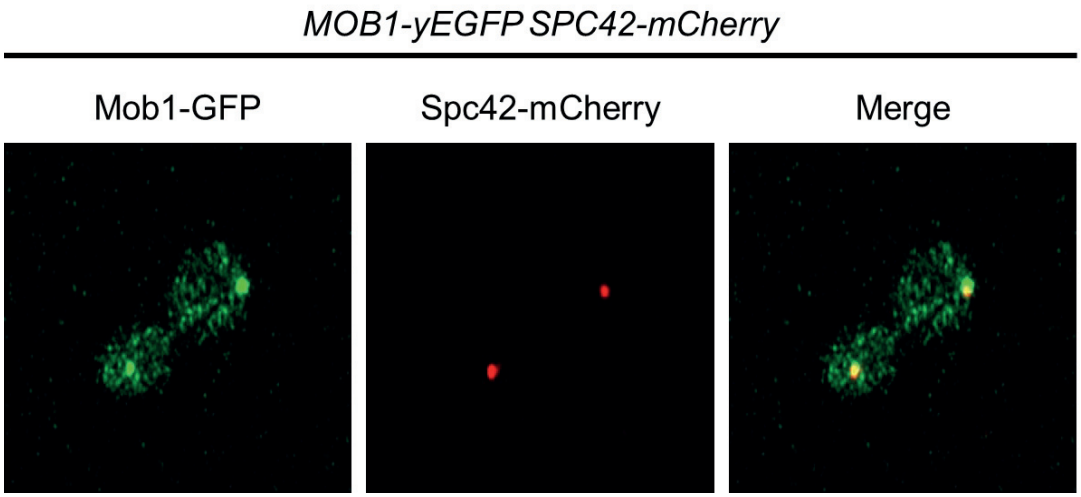

Figure 3.9. Co-localisation of Mob1 and Spc42 during anaphase. Representative image of *MOB1-GFP SPC42-mCherry* cells. A culture of YAZ91 *(MOB1-GFP SPC42-mCherry)* was brought to mid-exponential phase and images were taken using confocal microscopy.

To explore how Mob1 and Dbf2 behave during the whole cell cycle, strains were generated carrying either of the proteins tagged with GFP in an otherwise wild-type background. Protein location was monitored in exponential growing cells using timelapse fluorescence microscopy.

As shown in figure 3.10-A and B, during most of the cell cycle cells lack a Mob1-Dbf2 signal. In early anaphase, Mob1-Dbf2 is first recruited at the mSPB in around 75% of cells, whereas the signal appears at the dSPB as anaphase progresses, as previously described[171,261–263]. Such orderly localisation of Mob1-Dbf2 at the different SPBs is consistent in most cells observed, as depicted in figure 3.10-C.

After anaphase, but before Mob1-Dbf2 localises to the bud neck, Mob1-Dbf2 shows a localisation compatible with the nucleolus, as recently described[148]. In the two representative cells shown in the figure, the faint image, similar to the images reported in the cited work, can be observed at the -5 minute timepoint and figure 3.10-C. Soon after, a fraction of Mob1-Dbf2 is transiently relocated to the bud neck. After cytokinesis, Mob1-Dbf2 either stays briefly at one or both SPBs or just dilutes again. Around 20-25 minutes after Mob1-Dbf2 contraction at the bud neck, full cell separation can be observed in the brightfield channel, as evidenced in the 20 minute timepoint of the Mob1-GFP cell.

A) *MOB1-GFP*

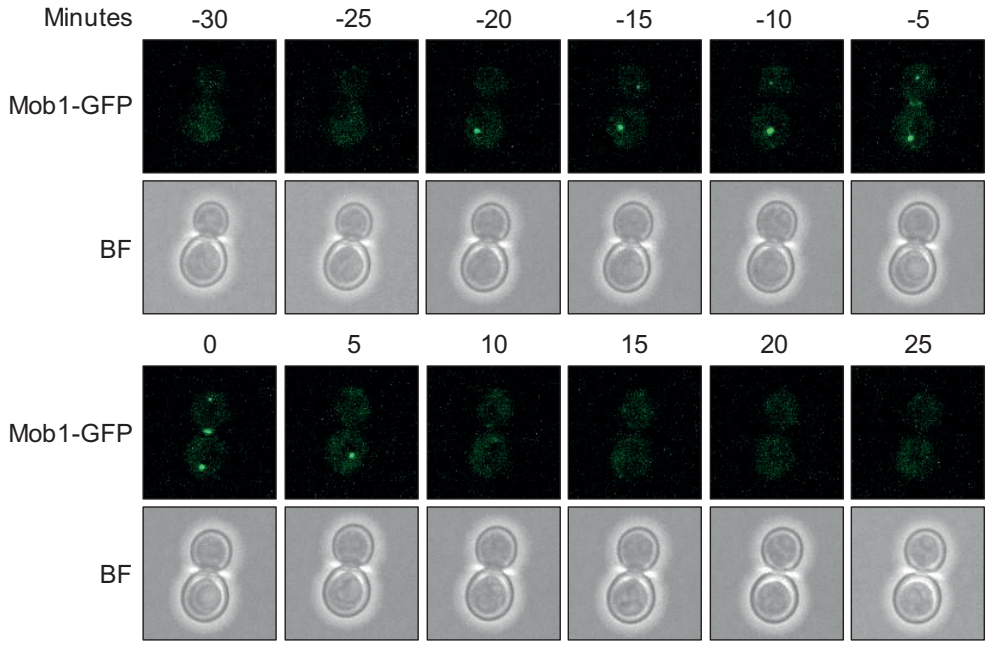

B) *DBF2-GFP*

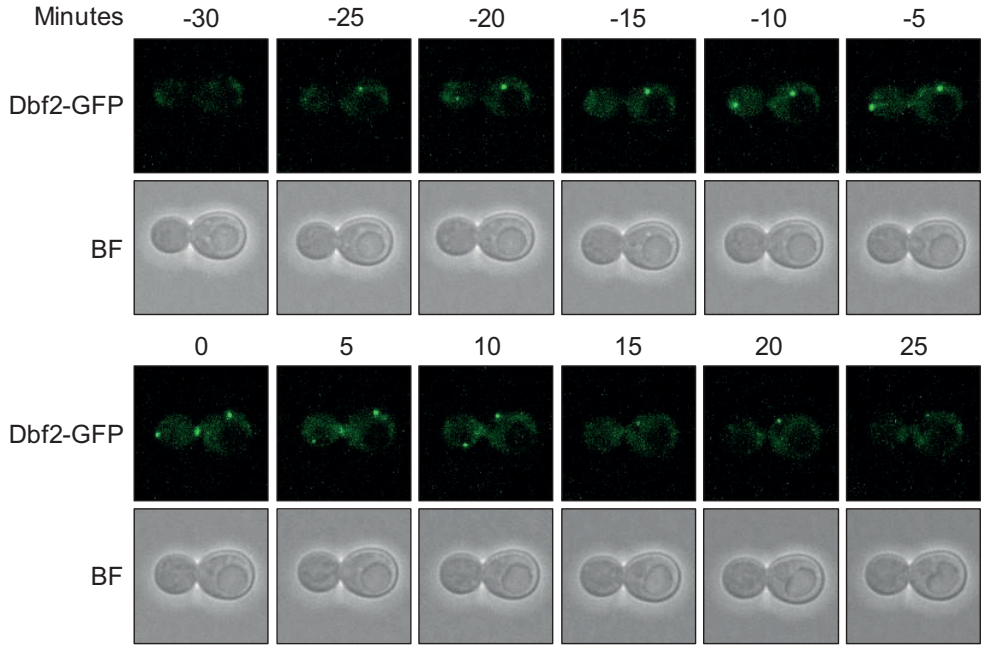

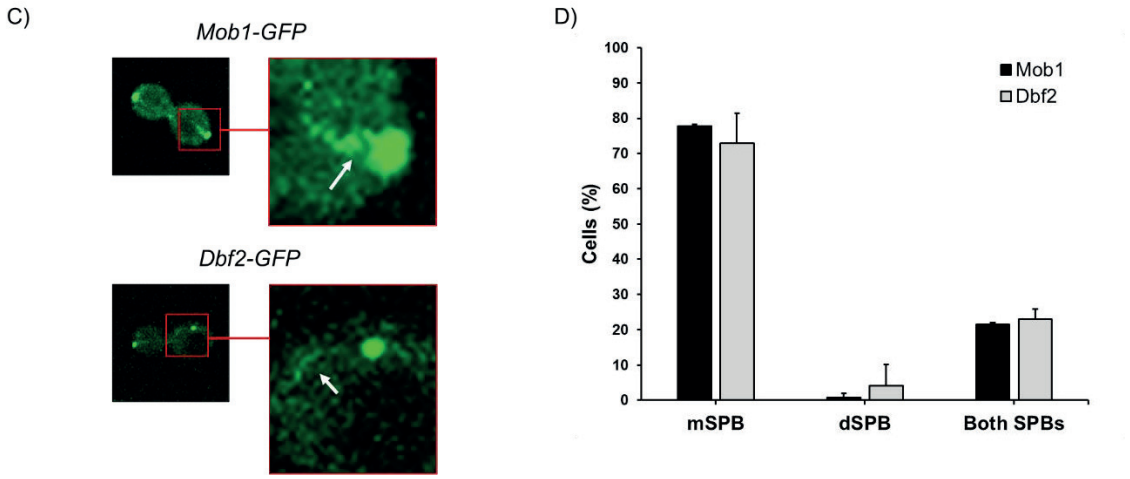

Figure 3.10. Mob1-Dbf2 behaviour in an unperturbed cell cycle. (A) and (B) show representative timelapses of strains YAZ86 (*MOB1-GFP MET3-CDC20 GAL-clb2ΔN*) and YAZC236 (*DBF2-GFP MET3-CDC20 GAL*-clb2ΔN) grown in SCD-Met media, respectively. Cells were monitored by Spinning Disc fluorescence microscopy (Zeiss). Images stacks of 6 µm width with a step size of 0.5 µm each were taken every 5 minutes. Time 0 represents the timepoint at which Mob1-Dbf2 displayed the brightest signal at the division site. (C) Representative cells showing the presence of both Mob1-GFP and Dbf2-GFP compatible with the nucleolus during anaphase. (D) Preferential localisation of Mob1-Dbf2 during an unperturbed cell cycle. The graph shows the first subcellular localisation at which Mob1-Dbf2 showed during the cell cycle, either mother SPB (mSPB), daughter SPB (dSPB), or at both, in the same timepoint. Error bars indicate standard deviation. The figure is representative of 2 independent experiments for each strain. At least 30 cells were randomly selected and monitored for each strain and repeat.

In all, the above observations confirm that we are able to reproduce the previously described behaviour of Dbf2-Mob1 throughout an unperturbed M phase. Such behaviour will serve us as a reference for subsequent studies in cells under high M-Cdk1, both with the wild-type proteins and with non-phosphorylatable mutants in an attempt to bypass M-Cdk1 control on cytokinesis.

3.2.2. Cdc15 localisation during an unperturbed cell cycle

Nud1 phosphorylation by Cdc15 is required for Mob1-Dbf2 recruitment to the SPBs[264]. Cdc15 has been previously described to localise first preferentially to the SPB that is pulled to the daughter, and later to both SPBs[154,184].

To visualise the subcellular localisation of Cdc15, we generated strains carrying Cdc15 tagged with GFP in an otherwise wild-type strain. We monitored Cdc15 in exponentially growing cells using timelapse fluorescence microscopy.

We first noticed that the Cdc15 signal was visibly fainter, and bleached more quickly, than the Mob1 and the Dbf2 signals, limiting the quality of the analysis. With the attainable resolution, the localisation pattern of Cdc15 appears to be different from that of Mob1-Dbf2. As shown in figure 3.11-A, Cdc15 is already present as a bright dot, compatible with an SPB, near the bud neck in small-budded G2. However, in the timelapse series, the Cdc15 SPB localisation consistently disappears transiently in most cells before anaphase (figure 31-C, -20 and -15 minutes timepoints). At these early times it is not possible to assign the signal either to the mSPB or the dSPB. The early presence of Cdc15 at one SPB in small-budded cells does not result in the recruitment of Mob1, e.g. when the cells in the experiment in figure 3.10 are analysed at earlier timepoints in the timelapse series.

Later, when cells enter anaphase, Cdc15 is first seen either at the mSPB or at both SPBs in around 75% of the cells. Likewise, Cdc15 is first seen either at the dSPB or at both SPBs in a similar percentage of cells (figure 3.11-B). Cdc15 is required at the SPBs for Mob1-Dbf2 to be recruited [173]. The percentage of cells with a Cdc15 signal at the mSPB is compatible with the 75% of cells with Mob1-Dbf2 at the mSPB in early anaphase (figure 3.10). However, the presence of Cdc15 at the dSPB in around 75% of the cells does not result in a similar percentage of cells loading Mob1 at the dSPB early in anaphase, indicating that a negative control might be preventing the recruitment.

As anaphase progresses, Cdc15 is eventually present at both SPBs in all cells.

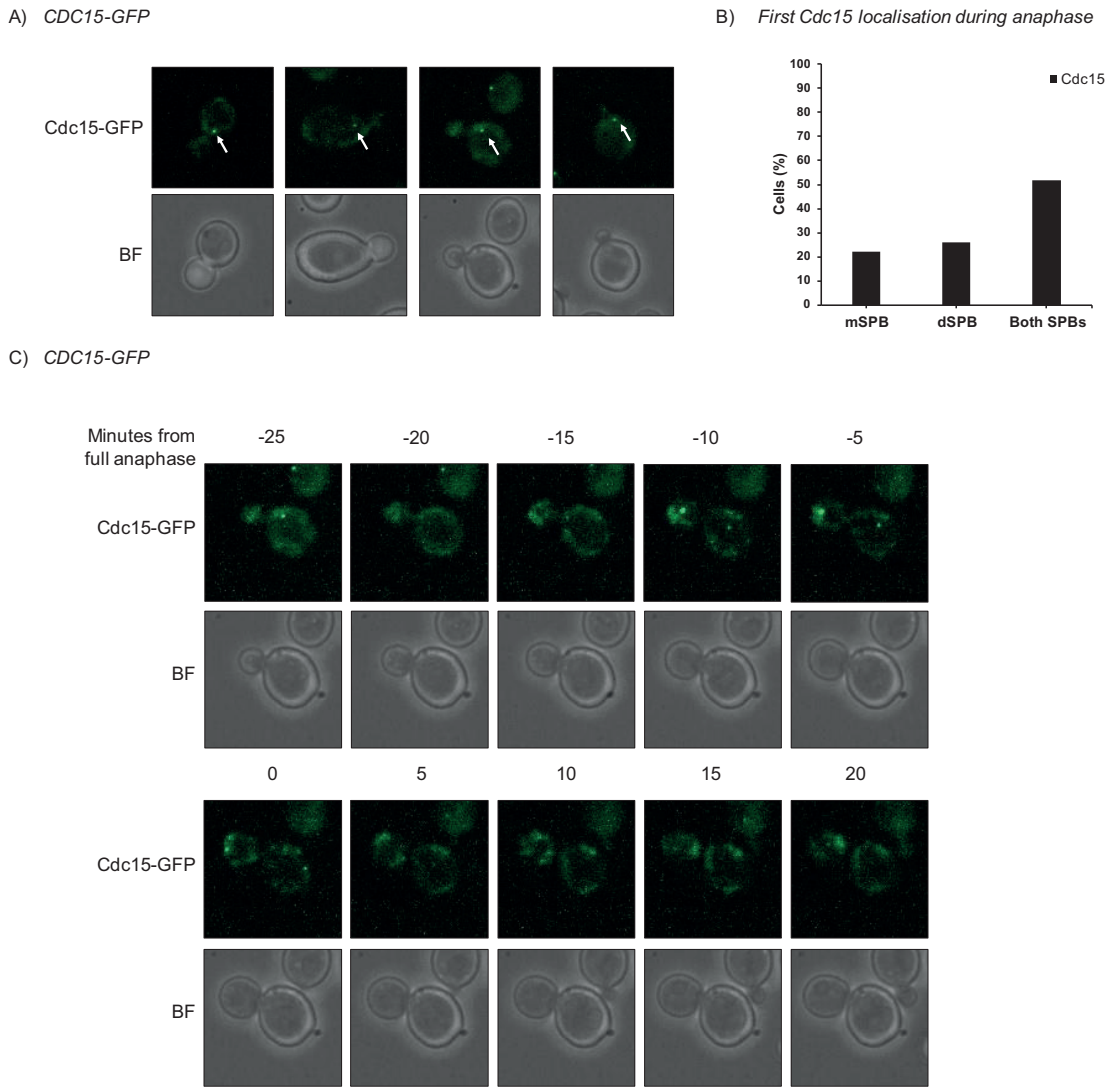

Figure 3.11. Subcellular localisation of Cdc15 during an unperturbed cell cycle. A culture of strain YAZ267 *(CDC15-GFP)* was brought to mid-exponential phase in SCD-Met media and monitored by Spinning Disc fluorescence microscopy (Zeiss). Images stacks of 6 µm width with a step size of 0.5 µm each were taken every 5 minutes. (A) 4 representative small-budded cells showing Cdc15 at one SPB. (B) Preferential localisation of Cdc15 during an unperturbed cell cycle. The graph shows the first subcellular localisation at which Cdc15 showed during the cell cycle, either mother SPB (mSPB), daughter SPB (dSPB) or at both in the same timepoint (n = 27). (C) Timelapse of a representative cell. T=0 represents the timepoint at which Cdc15 signals were at maximum distance, indicating complete anaphase.

3.2.3. Sustained high M-Cdk1 activity inhibits Dbf2 re-localisation to the nucleolus and to the site of cell division

M-Cdk1 has been proposed to inhibit Dbf2-Mob1 activity via Mob1 phosphorylation[184]. In fact, both Dbf2 and Mob1 contain multiple Cdk1 consensus phosphorylation sites. In addition, Mob1-Dbf2 must be recruited at the SPBs to be activated by the Cdc15 kinase[174], which is also inhibited by M-Cdk1[184]. We, therefore, wished to study whether sustained high M-Cdk1 activity affects Mob1-Dbf2 localisation at the SPBs.

MET3-CDC20 GAL-clb2ΔN DBF2-GFP exponentially growing cells were grown in Synthetic Media with 2% Raffinose lacking methionine (SCRaff-Met) to exponential phase. Cells were then arrested at metaphase by depletion of Cdc20. Media was next changed to SCGal+Met to allow for Clb2ΔN overexpression. Finally, Methionine was washed out from the media and cells were allowed to resume cell cycle progression in the continued presence of Galactose (SCGal-Met).

Dbf2-GFP was monitored by timelapse fluorescence microscopy. As shown in figure 3.12-A, Dbf2 is already present at both SPBs in cells in early anaphase under M-Cdk1 released from metaphase arrest. Therefore, the M-Cdk1 inhibition of Mob1-Cdk1 does not affect the SPB localisation.

However, in contrast to the behaviour in an unperturbed cell cycle, Dbf2 did not re-localise to the nucleolus nor to the division site for the duration of the whole experiment. Expectably, cells under high M-Cdk1 were not able to divide, as evidenced by the brightfield images.

In all, our results show that, while high M-Cdk1 activity does not inhibit Dbf2 localisation at the SPBs, the kinase is unable to further re-localise at the subcellular compartments where it is required to trigger a mitotic exit.

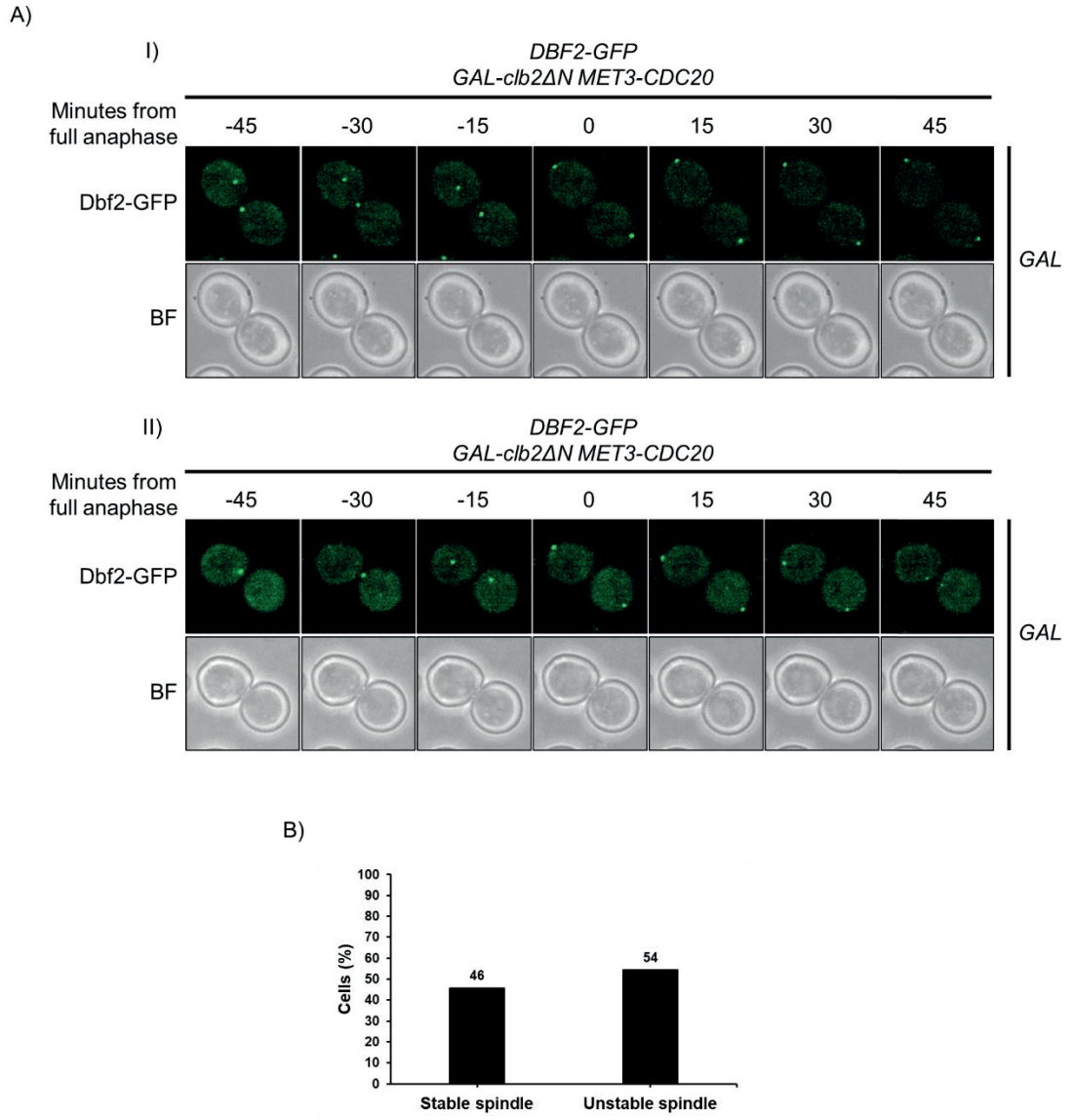

Figure 3.12. Localisation of Dbf2 during the high M-Cdk1 activity arrest. (A) Representative timelapse of strain YAZC236 (*DBF2-GFP MET3-CDC20 GAL*-clb2ΔN). Cells were released from metaphase arrest under continuous *GAL-clb2*ΔN overexpression and monitored by Spinning Disc fluorescence microscopy (Zeiss). Images stacks of 6 µm width with a step size of 0.5 µm each were taken every 5 minutes. Time 0 represents the timepoint of the maximum distance between the Dbf2 signals, indicating complete anaphase. (I) A representative cell displaying a persistent anaphase. (II) A representative cell displaying an unstable spindle. (B) Percentage of cells that showed stable or unstable spindles during the arrest (n = 86).

One observation called our attention concerning the stability of the spindle during the M-Cdk1 arrest. Two distinct patterns can be observed. Around half of the cells displayed a stable late anaphase spindle, with both Dbf2 signals at the SPBs fully separated (figure 3.12-A, cell I). However, the remaining half of the cells did not maintain the SPBs separation at longer arrest times under high M-Cdk1 activity, as evidenced by the presence of one or both Dbf2 foci moving around in the cell (figure 3.12-A, cell II). The observation is consistently observed in all the experiments involving sustained M-Cdk1 activity, and is compatible with previous reports that dephosphorylation of M-Cdk1 substrates by Cdc14 promotes spindle stability during elongation[265,266].

3.3. Characterisation of strains carrying non-phosphorylatable alleles of the MEN kinases

3.3.1. The triple MEN bypass is viable and grows with the same doubling time as wild-type cells

We showed above that sustained high M-Cdk1 activity keeps Mob1-Dbf2 locked at the SPBs, unable to re-localise to the critical subcellular compartments where it is required to trigger mitotic exit, namely the nucleolus, where it targets Cdc14 for full release and the site of cell division (see section 1.4.4.2 for details).

We therefore wished to explore whether cells carrying non-phosphorylatable alleles of Mob1 and Dbf2 might abrogate the M-Cdk1 inhibition. Because Cdc15 is required to activate Mob1-Dbf2 at the SPBs and, given that Cdc15 also contains multiple putative Cdk1 phosphorylation sites, we also used a non-phosphorylatable allele of Cdc15[254]. Each of the three proteins has 7 putative Cdk1 phosphorylation sequences, including the full S/T-P-x-K/R and partial S/T-P Cdk1 consensus sequences. We generated strains carrying all putative M-Cdk1 sites mutated to alanine (termed *mob1(A) dbf2(A) cdc15(A)* from here on). Once the non-phosphorylatable alleles were integrated under their own promoter, the wild-type genes were deleted to avoid a dominant negative effect.

Before doing any experiments we first tested the *cdc15(A) mob1(A) dbf2(A)* strain in comparison with wild-type cells, to rule out cell cycle defects that might alter subsequent experiments.

We first checked the doubling time and the cell cycle distribution of the mutant strain. As shown in figure 3.13-A and B, no significant differences in doubling time are seen in the triple mutant with respect to the wild-type strain in the two sources of carbon tested in synthetic complete medium. Also, the budding indexes, and more significantly the dumbbell indexes, are undistinguishable between the two strains, ruling out a synthetic interaction resulting in a hypomorphic defect in mitosis. Finally, no apparent sign of unfitness was evident based on visual inspection of the cells, as can be appreciated in the several ensuing figures.

We also tested the strain for thermosensitivity to check whether the multiple mutations in the three essential (Cdc15, Mob1) or critical (Dbf2) kinases resulted in a significant structural alteration. *cdc15(A) mob1(A) dbf2(A)* cells, and isogenic wild-type cells, were grown in SCD-Met plates for 48 hours at 30ºC and 72 hours at 37ºC. As a positive control for thermosensitivity, a strain carrying a thermosensitive allele for the Dbf4-dependent kinase catalytic subunit (*cdc7-4*) was included. Such strain is unable to grow at 37ºC.

As shown in figure 3.13-C, both *cdc15(A) mob1(A) dbf2(A)* cells grew equally as wild-type cells at 37ºC, ruling out major conformational alterations in the proteins.

In all, the above pieces of evidence argue against the possibility that the 21 mutations in the three proteins result in a hypomorphic phenotype that might mask the cell's ability to abrogate the M-Cdk1 inhibition of cytokinesis.

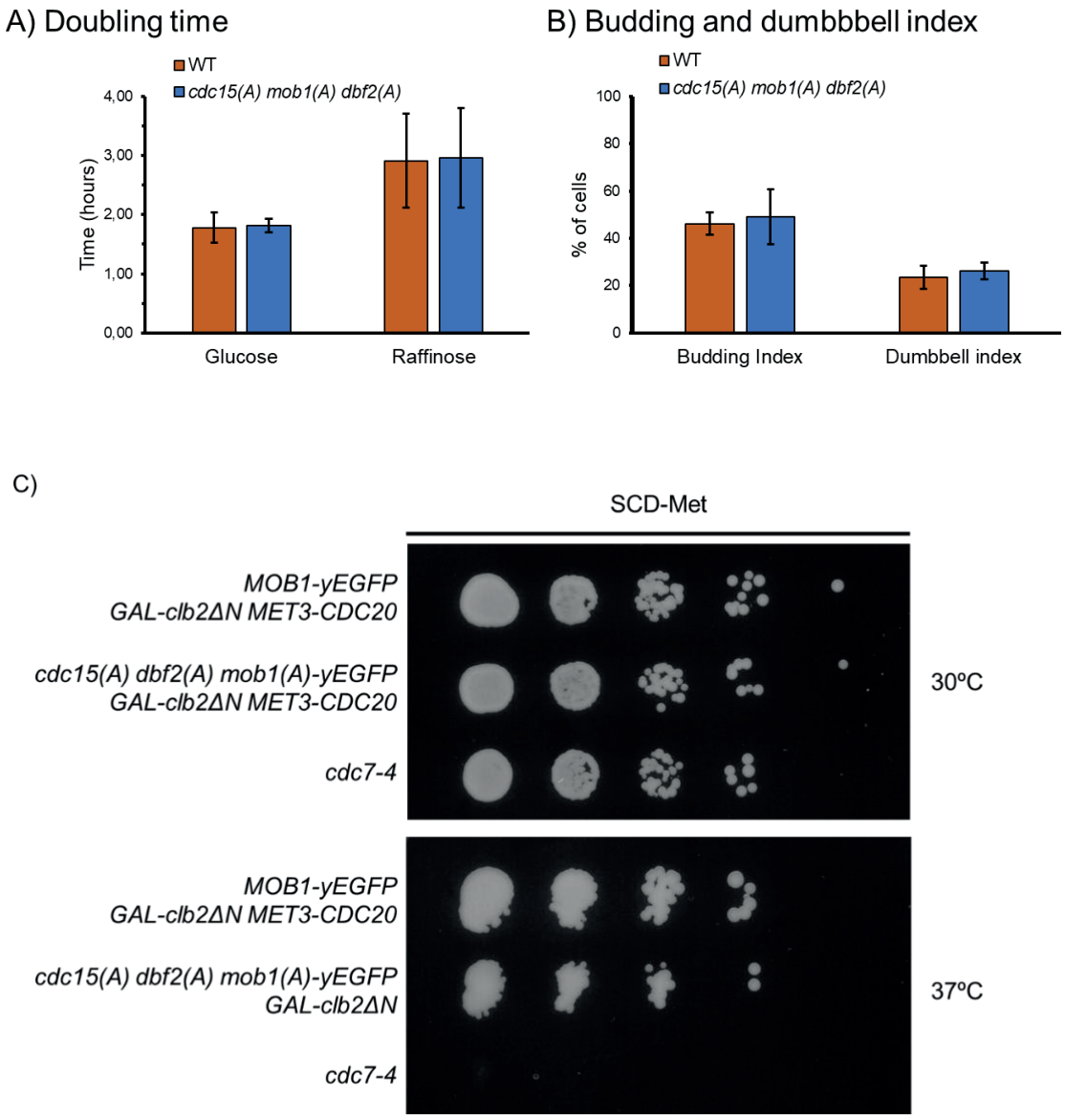

Figure 3.13. Cells carrying the non-phosphorylatable alleles of the MEN kinases grow as wild-type cells. (A) Cultures of strains YAZ86 (*MOB1-GFP MET3-CDC20 GAL-clb2ΔN*) and YAZ227 (*cdc15(A) mob1(A) dbf2(A) MET3-CDC20 GAL-clb2ΔN)* were brought to mid-exponential cells monitored for their doubling time under SCD-Met and SCRaff-Met media by light microscopy. The figure represents the mean of 4 independent experiments. (B) Mean Budding and Dumbbell indexes of (A) experiments. Error bars indicate standard deviation. (C) Spot assay of YAZ86, YAZ227, and *cdc7-4* cells. Cells were grown in SCD-Met at either 30ºC or 37ºC for 72 hours. The figure is representative of 2 independent experiments.

3.4. MEN regulation in the triple bypass cells in an unperturbed mitosis

In the search for the minimal set of M-Cdk1 targets that prevent premature entry into cytokinesis, we chose to explore the MEN kinases Cdc15 and Mob1-Dbf2 (see section 3.2). We hypothesised that cells carrying non-phosphorylatable alleles of Cdc15, Mob1, and Dbf2 might abrogate the M-Cdk1 control and allow cytokinesis in the presence of sustained high M-Cdk1 activity.

We first explored differences in MEN regulation in the triple bypass strain vs wild-type cells in an unperturbed mitosis.

3.4.1. The triple MEN bypass *cdc15(A) mob1(A) dbf2(A)* recruits *mob1(A)* earlier at the SPBs and the signal persists for longer in an unperturbed cell cycle

We next explored how the subcellular localisation of the non-phosphorylatable proteins compares to the wild-type counterparts. Strains were generated carrying either Mob1 or Dbf2 tagged with GFP. Protein subcellular localisation was monitored in exponentially growing cells using timelapse fluorescence microscopy.

Thus, exponentially growing *cdc15(A) mob1(A)-GFP dbf2(A)* cells, and isogenic control cells carrying the wild-type genes, were tracked by timelapse fluorescence microscopy for 3h. As shown in figure 3.14-A, presenting timelapses of representative cells, control cells recruit Mob1 at the SPBs only in anaphase (see also figure 3.10), and the signal persists until around 10-15 minutes after the time of cytokinesis, as determined by the contraction and disappearance of the Mob1 signal from the site of cell division. In contrast, *cdc15(A) mob1(A)-GFP dbf2(A)* cells display Mob1(A) at both SPBs nearly simultaneously and before anaphase onset, according to the position of the two SPBs in the mother body. At this time, the M-Cdk1 activity peaks.

Moreover, Mob1 persists at both SPBs for longer, well beyond the end of cytokinesis, as determined by the contraction and disappearance of the Mob1 signal at the site of cell division.

To better quantify the above observations, we measured the time that Mob1 remained at each SPB before and after the completion of anaphase, as judged by the maximum distance between SPBs. As shown in figure 3.14-B, *cdc15(A) mob1(A)-GFP dbf2(A)* cells recruit Mob1(A) at the SPBs an average of 20 minutes earlier than wild-type cells. In addition, in contrast to what is seen in wild-type cells (see also figure 3.10), the signal appears simultaneously at the two SPBs.

The time that Mob1 and Mob1(A) remain at the bud neck in each strain shows no significant differences. However, after the bud neck localisation is lost, Mob1(A) remains at the SPBs for an average extra 50 minutes in *cdc15(A) mob1(A)-GFP dbf2(A)* cells after anaphase is completed.

Pre-anaphase SPB localisation was detected in Dbf2(A)-GFP as well, coincident with the behaviour of Mob1(A)-GFP. However, the signal is too weak and labile for an objective quantification.

In all, the above experiments show an alteration in the subcellular localisation dynamics of Mob1-Dbf2 in cells carrying non-phosphorylatable alleles of the three MEN kinases. Mob1-Dbf2 localises to the SPBs for around 65 extra minutes than the wild-type proteins. Such observation suggests that M-Cdk1 plays a direct role in limiting the window of time that the kinases remain at the SPBs, where activation of the MEN pathway occurs.

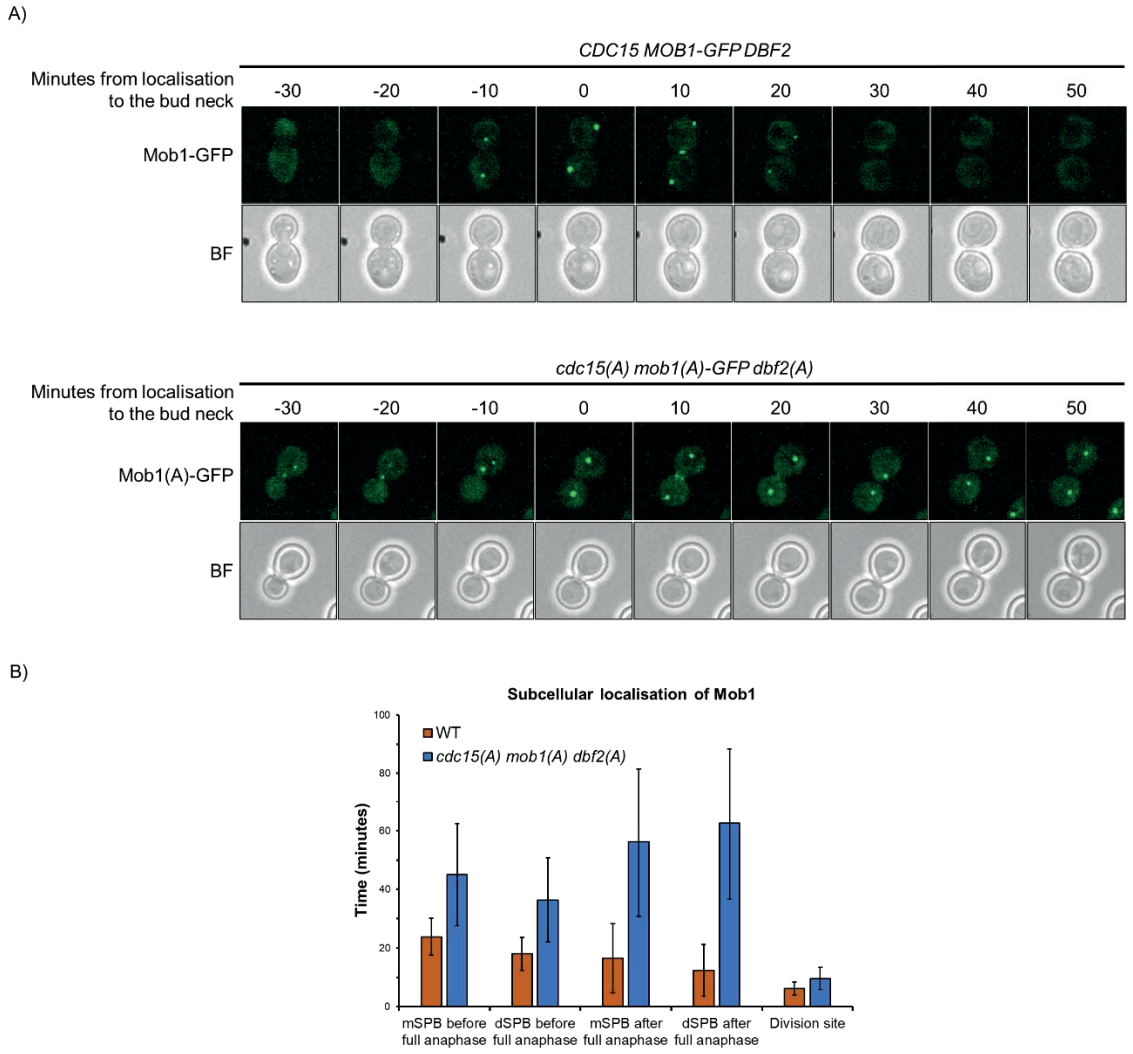

Figure 3.14. The triple MEN bypass prematurely recruits Mob1 at the SPBs and the localisation persists after anaphase in an unperturbed mitosis. Cultures of strains YAZ86 (*MOB1-GFP*), YAZ227 *(cdc15(A) mob1(A) dbf2(A))* and YCCL135 *(mob1(A) dbf2(A))* were grown to mid-exponential phase in SCRaff-Met and monitored by Spinning Disc fluorescence microscopy (Zeiss). Images stacks of 6 µm width with a step size of 0.5 µm each were taken every 5 minutes. (A) Representative cells of strains YAZ86 and YAZ227. Time 0 represents the timepoint of the maximum distance between the Mob1 signals, indicating complete anaphase. (B) Subcellular localisation of Mob1 in YAZ86 (n = 32) and YAZ227 (n = 27) cells. Bars indicate the amount of time Mob1 was present at each localisation before and after anaphase. Error bars indicate standard deviation.

3.4.2. The triple MEN bypass *cdc15(A) mob1(A) dbf2(A)* recruits *cdc15(A)* earlier at the SPBs and the signal persists for longer in an unperturbed cell cycle

Cdc15 is required for the loading of Mob1-Dbf2 at the SPBs. The phosphorylation of the spindle pole body scaffold protein Nud1 by Cdc15 creates a landing pad for Mob1-Dbf2[173]. We therefore asked whether the observed early and persistent recruitment of Mob1(A) (figure 3.14) also occurs with the *cdc15(A)* allele.

A culture of *cdc15(A)-GFP mob1(A) dbf2(A)* cells was grown to mid-exponential phase in SCD-Met and monitored using Spinning Disc fluorescence microscopy (Zeiss).

As shown in figure 3.15, Cdc15(A) shows an SPB localisation already in late S/G2 phase, based on the size of the bud. In addition, the signal is not transient as in wild-type cells (figure 3.11), where the SPB localisation is lost with a timing compatible with the completion of anaphase. Cdc15(A) is also detected at the second SPB before anaphase (see figure 3.15A, min 25), whereas in wild-type Cdc15 is only loaded at the second SPB during mid-anaphase (figure 3.11).

Besides of the early recruitment, Cdc15(A) dramatically lingers at the SPBs for a much longer time than Cdc15 in wild-type cells, where Cdc15 leaves the SPBs immediately after anaphase is completed (compare figure 3.11 and 3.15). In the triple non-phosphorylatable strain, the Cdc15(A) signal at the SPBs remains present in cells that are already separated by independent cell walls (figure 3.15, minute 75) and in the subsequent G1 phase (rebudding cell at minute 85).

The early recruitment and extended permanence of *cdc15(A)* at the SPBs in the triple bypass strain provides a base for the premature localisation of *mob1(A)* seen in figure 3.14. These observations further support the notion that M-Cdk1 activity plays an active role in the regulation of the recruitment of the MEN kinases at the SPBs. However, the permanence of the kinases beyond mitotic exit (Mob1) or anaphase (Cdc15) is difficult to reconcile with the switch to Cdc14 prevailing conditions, and requires further investigation (see discussion).

Figure 3.15(B) shows timelapse frames of 4 representative *cdc15(A)-GFP mob1(A) dbf2(A)* cells in mid-exponential cultures. The signal is present in newly divided G1

cells but disappears later when the same cells are small-budded. The morphology is compatible with the time of SPB duplication in S phase[267].

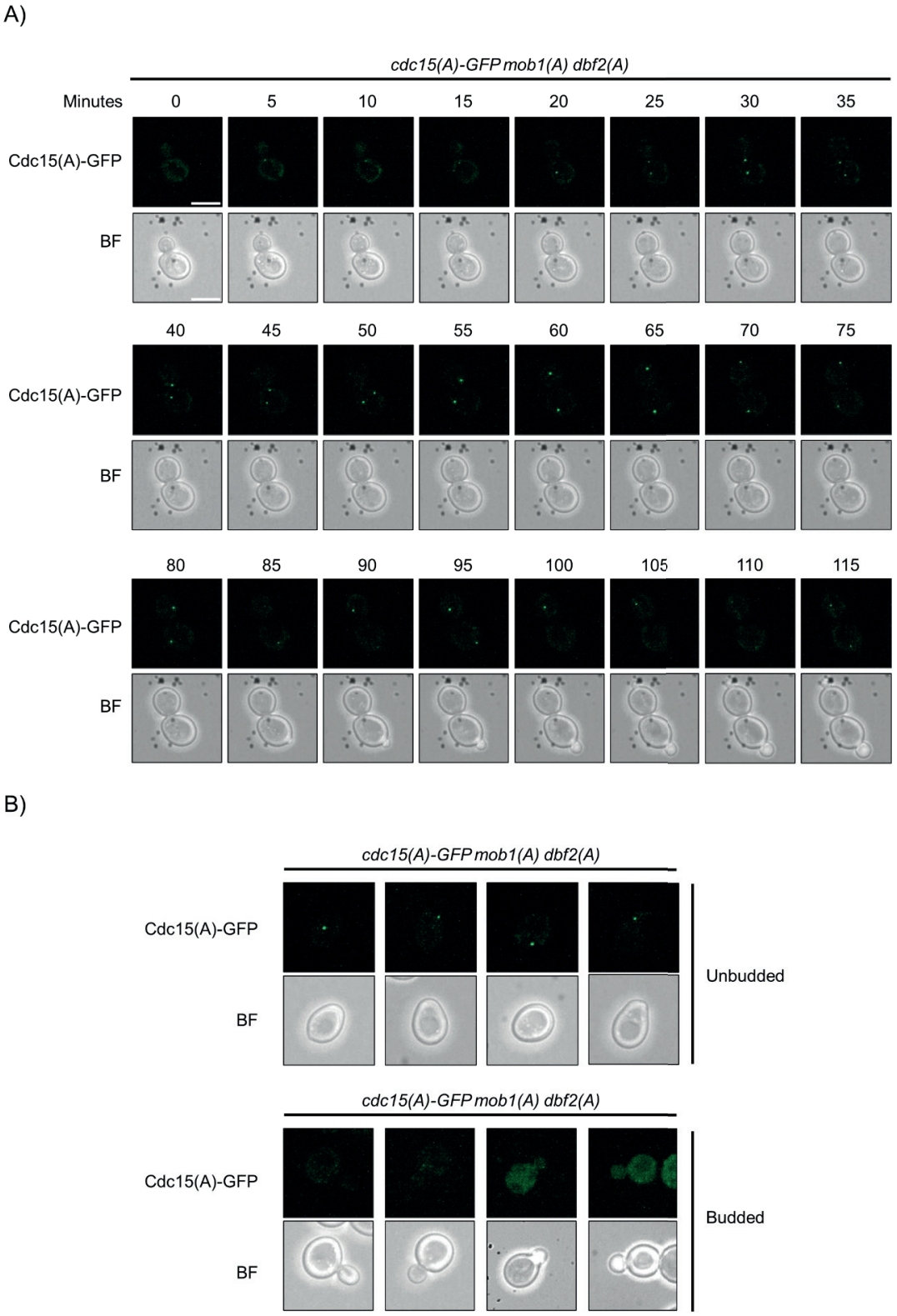

Figure 3.15. The triple MEN bypass prematurely recruits Cdc15 to both SPBs in an unperturbed cell cycle. A culture of YAZC269 (*cdc15(A)-GFP mob1(A) dbf2(A)*) was grown

to mid-exponential phase in SCD-Met and monitored using Spinning Disc fluorescence microscopy (Zeiss). Images stacks of 6 µm width with a step size of 0.5 µm each were taken every 5 minutes. Time 0 represents the start of the timelapse. (A) Timelapse of a representative cell undergoing anaphase. (B) Representative unbudded and small-budded cells. The figure is representative of 2 independent experiments.

3.5. MEN regulation in the triple bypass cells under sustained high M-Cdk1 activity

In the search for the minimal set of M-Cdk1 targets that prevent premature entry into cytokinesis, we chose to explore the MEN kinases Cdc15 and Mob1-Dbf2 (see section 3.2). We hypothesised that cells carrying non-phosphorylatable alleles of Cdc15, Mob1, and Dbf2 might abrogate the M-Cdk1 control and allow cytokinesis in the presence of sustained high M-Cdk1 activity.

3.5.1. The triple bypass strain does not divide in the presence of sustained high M-Cdk1 activity

A testable prediction derived from the above hypothesis is that cells carrying the triple bypass might abrogate the M-Cdk1 inhibition of the Mob1-Dbf2 release. In that event, cells might divide in the presence of high M-Cdk1 activity

To test the hypothesis, *cdc15(A) mob1(A)-GFP dbf2(A) MET3-CDC20 ADGEV GAL-clb2ΔN* cells, and their isogenic control strain carrying the wild-type alleles, were grown in Synthetic Media with 2% Raffinose lacking methionine (SCRaff-Met). The cultures were allowed to grow to mid-exponential phase and then cells were arrested at metaphase by depletion of Cdc20. Media was then changed to SCGal+Met to allow for Clb2ΔN overexpression. Methionine was washed out from the media to allow the cells to resume cell cycle progression. Samples were taken at different timepoints, and the cell density and the dumbbell index were counted. Cells from the same timepoints were harvested and processed for western blotting to control for correct over-expression of *clb2ΔN.*

As shown in figure 3.16-A, *clb2ΔN* was efficiently expressed in both strains.

The continued presence of endogenous Clb2 indicates that mitotic exit was blocked, as APC^{Cdh1} was not activated. In addition, same as the control strain, the bypass strain was unable to divide as the control strain for the 3 h duration of the experiment, as indicated by the block in cell density and the stability of the budding index (figure 3.16-B).

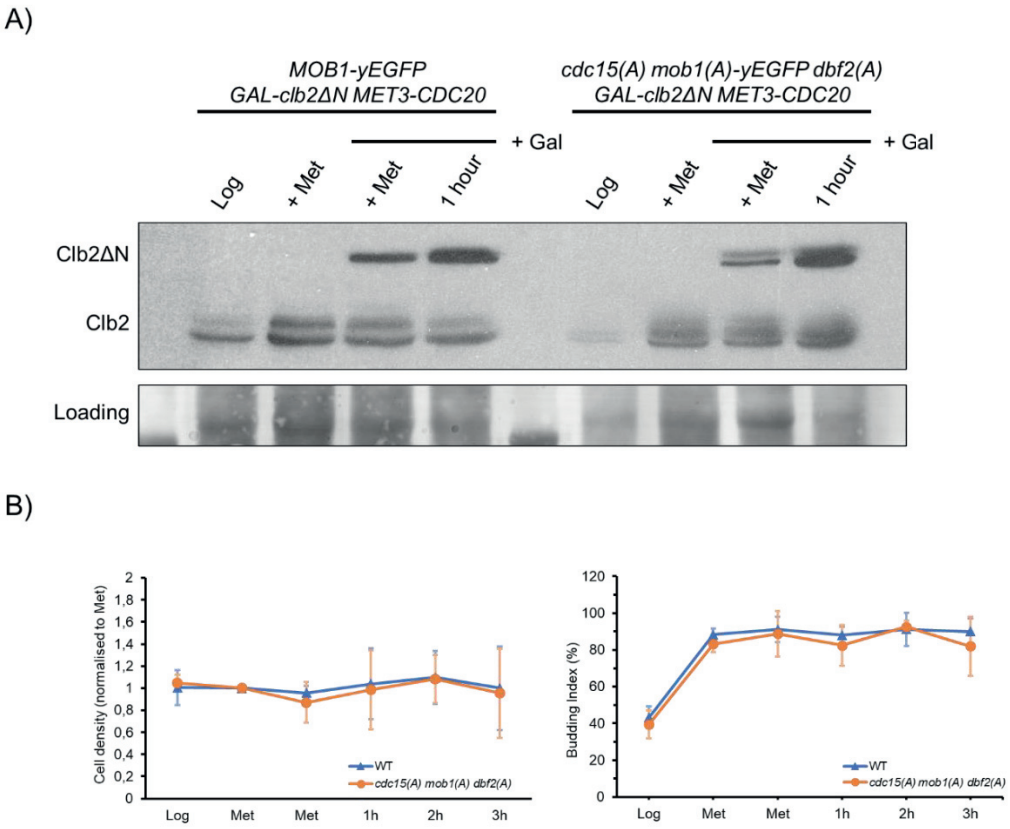

Figure 3.16. The triple bypass strain does not divide in the presence of sustained high M-Cdk1 activity. Cultures of strains YAZ86 (*MOB1-GFP MET3-CDC20 GAL*-clb2ΔN) and YAZ227 (*cdc15(A) mob1(A)-GFP dbf2(A) MET3-CDC20 GAL-clb2ΔN)* were released from metaphase arrest in the presence of galactose. Samples were taken at the indicated timepoints. (A) Immunoblot against Clb2 on whole cell extracts, showing both endogenous Clb2 and Clb2ΔN protein levels. The Ponceau-S staining of the membrane is shown as a loading control. (B) Mean cell density and mean budding index at the indicated timepoints of the experiment. To allow for comparison between experiments, density is normalised to the metaphase arrest timepoint (Met). The results are the mean and the standard deviation from two independent experiments. In each experiment, a minimum of 75 cells were counted for each strain and timepoint.

3.5.2. Mob1-Dbf2 is not released from the SPBs in the triple bypass strain in the presence of sustained high M-Cdk1 activity

The above observation that the strain carrying non-phosphorylatable alleles of Cdc15, Mob1, and Dbf2 was unable to abrogate the negative control of M-Cdk1, led us to explore the point of control. In wild-type cells, sustained high M-Cdk1 keeps Mob1-Dbf2 locked at the SPBs, unable to translocate to the nucleolus and to the bud-neck to trigger mitotic exit (see section 3.2.3).

The subcellular localisation of Mob1-GFP in cells from the experiment above (section 3.5.1) was monitored using timelapse fluorescence microscopy on individual cells.

As shown in figure 3.17-A, upon release from the metaphase arrest, both strains can undergo anaphase normally, as monitored by SPB elongation. However, at later times, the MEN kinase Mob1 remains locked at the SPBs in both strains for the whole duration of the experiment. This observation indicates that the presence of the non-phosphorylatable alleles *cdc15(A), mob1(A) and dbf2(A)* is not enough to allow the recruitment of Mob1 to the site of cell division, in contrast to the normal behaviour in wild-type cells undergoing an unperturbed mitosis (figure 3.10). The results indicate that M-Cdk1 is still able to keep the MEN pathway inhibited in the bypass strain, suggesting the existence of at least one more critical substrate downregulated by M-Cdk1 to keep mitotic exit blocked.

Despite that the bypass strain does not abrogate the M-Cdk1 inhibition of MEN activation, a significant difference is visible with respect to the early recruitment to the SPBs. In the bypass strain, Mob1(A) localises to both SPBs immediately upon release from metaphase in 70% of the cells. In comparison, in the wild-type control, 56% of the cells show no presence of Mob1 at either SPB at that time, and the Mob1 signal appears at the dSPB only in anaphase, as determined by migration of the SPBs.

The observed differences between the bypass and the control strains under high M-Cdk1 activity go in the same direction as those observed between the two strains in an unperturbed mitosis (figures 3.10 and 3.14), indicating that the Cdc15(A) Mob1(A) Dbf2(A) mutants are able to bypass a direct M-Cdk1 restriction of Mob1-Dbf2 localisation at the SPBs.

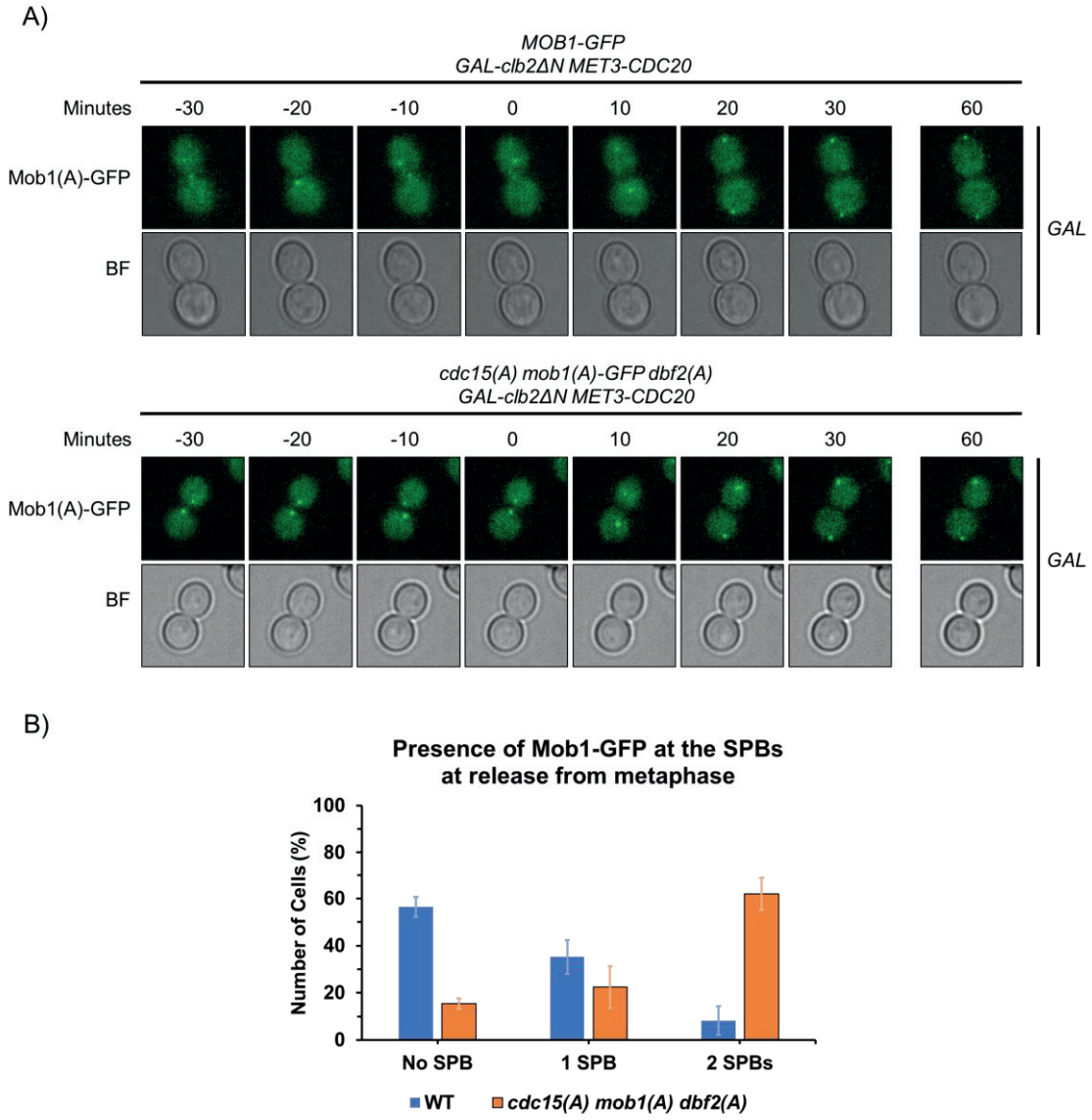

Figure 3.17. Localisation of Mob1 in the triple MEN bypass in the presence of sustained high M-Cdk1 activity arrest. Cultures of strains YAZ86 (*MOB1-GFP MET3-CDC20 GAL-*clb2ΔN) and YAZ227 (*cdc15(A) mob1(A)-GFP dbf2(A) MET3-CDC20 GAL-clb2ΔN)* were released from metaphase arrest in the presence of galactose and monitored by timelapse fluorescence microscopy using a Leica Thunder DMI8 microscope. Stacks of 9 µm with a step size of 0.5 µm were taken every 10 minutes. (A) Timelapse immunofluorescence microscopy images of a representative cell of each strain. Time 0 represents the timepoint immediately before anaphase onset. (B) Localisation of Mob1-GFP at the SPBs at the start of the timelapse video on each strain. Bars indicate the mean percentage of cells of 3 independent experiments (control cells N=98, N=21, N=64; bypass cells N=109, N=21, N=25). Error bars indicate standard deviation. The figure is representative of 3 independent experiments.

3.5.3. Exploration of the role of Nud1 as a putative M-Cdk1-controlled anchor for Mob1-Dbf2

The lack of recruitment of Mob1-Dbf2 at the nucleolus and at the bud neck in the triple bypass cells under high M-Cdk1 is compatible with the existence of one or more additional substrates through which M-Cdk1 keeps cytokinesis inhibited. One possible scenario is the existence of an anchoring protein at the SPB, substrate of M-Cdk1, that keeps Mob1-Dbf2 locked for as long as the anchor remains phosphorylated by M-Cdk1.

Among the known SPB components, we chose Nud1 based on three considerations, First, it plays a scaffolding role at the SPB[258]. Second, it physically recruits Mob1-Dbf2 at the SPB[173]. Third, it contains seven Cdk1 phosphorylation sequences, five of which have been confirmed to be *bona fide* Cdk1 phosphorylation sites[264]. We therefore hypothesised that Nud1 might not only recruit Mob1-Dbf2 to the SPBs to enable MEN activation, but also keep the kinase locked for as long as Nud1 remains phosphorylated by M-Cdk1. In a normal cell cycle, the FEAR-driven accumulation of Cdc14 at the SPBs might be responsible for the unlock.

A testable prediction derived from the above hypothesis is that cells carrying a non-phosphorylatable allele of Nud1, together with the non-phosphorylatable Cdc15, Mob1 and Dbf2 alleles, might be able to release Mob1-Dbf2 in the presence of sustained high M-Cdk1 activity. To test this hypothesis, we generated a strain carrying non-phosphorylatable alleles of Cdc15, Mob1, Dbf2 and Nud1, under their own promoters, and the wild-type open reading frames deleted.

Therefore, to test the hypothesis, *cdc15(A) mob1(A)-GFP dbf2(A) nud1(A) GAL-clb2ΔN MET-CDC20* cells, and their isogenic control carrying the wild-type *NUD1* gene, were grown in SCRaff-Met to mid-exponential phase and synchronised in metaphase by the depletion of Cdc20. Clb2ΔN overexpression was induced with galactose and methionine was washed out from the media. Cells were released from metaphase arrest in SCGal-Met media and monitored by fluorescence microscopy.

As shown in figure 3.18., both control cells and cells carrying the *nud1(A)* allele underwent anaphase normally, as visualised by the separation of the Mob1 SPB signals. Mob1 remained locked at the SPBs after anaphase also in the *cdc15(A) mob1(A) dbf2(A) nud1(A) bypass strain*. No re-localisation to the site of cell division

was visible in the bypass strain beyond the shown time, for the whole duration of the experiment, 3 h after metaphase release.

Therefore, including a non-phosphorylatable allele of Nud1 in the triple bypass background does not result in the release of Mob1-Dbf2 from the SPBs under high M-Cdk1 activity.

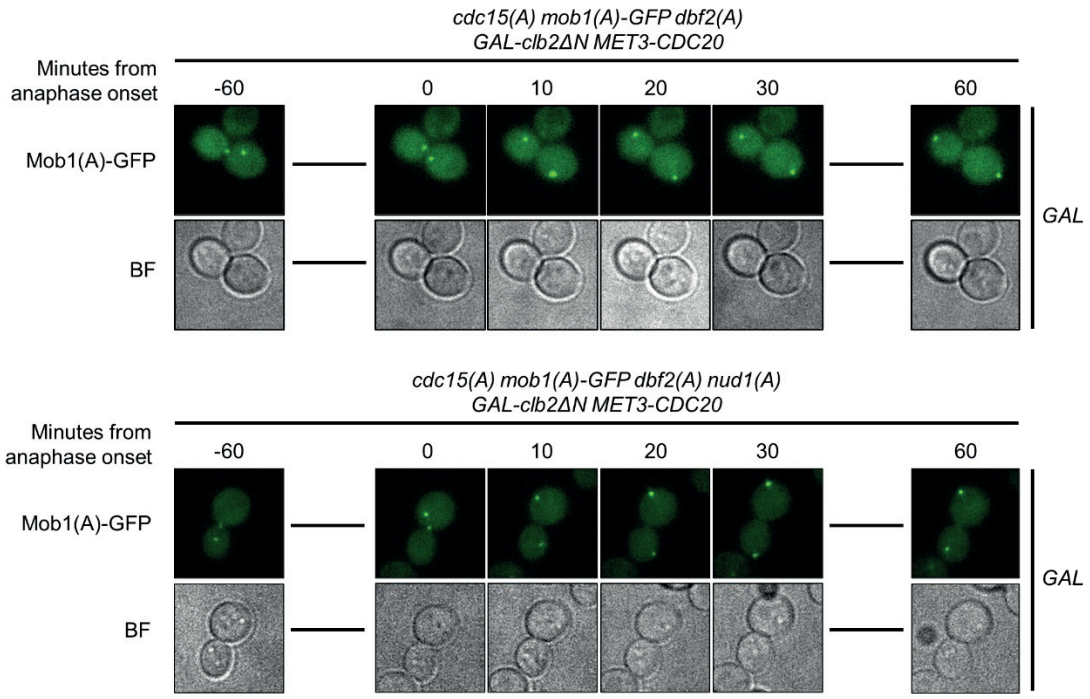

Figure 3.18. Localisation of Mob1 in the MEN-Nud1 bypass in the presence of sustained high M-Cdk1 activity. Timelapse immunofluorescence microscopy images of a representative cell of each strain YAZ227 (*cdc15(A) mob1(A)-GFP dbf2(A) MET3-CDC20 GAL-clb2ΔN)* and YAZ233 (*cdc15(A) mob1(A)-GFP dbf2(A) nud1(A) MET3-CDC20 GAL-clb2ΔN)* were released from metaphase arrest in the presence of galactose and monitored by timelapse fluorescence microscopy using a Nikon Eclipse Ti. Images of the same fields were taken every 10 minutes for a total of 3 h from the metaphase release. Samples were taken for immunoblot assay at the indicated timepoints. Time 0 represents the timepoint immediately before anaphase onset. The figure is representative of 3 independent experiments.

3.5.4. Exploration of the role of Iqg1 as a putative M-Cdk1-controlled landing pad for Mob1-Dbf2 at the site of cell division

The lack of recruitment of Mob1-Dbf2 at the nucleolus and at the bud neck in the triple bypass cells under high M-Cdk1 is compatible with the existence of one or more additional substrates through which M-Cdk1 keeps cytokinesis inhibited. In addition to the SPB lock hypothesis explored in section 3.5.3, an alternative scenario would be that M-Cdk1 targets proteins are required for the recruitment of active Mob1-Dbf2 at the nucleolus and at the bud-neck.

Because we visualise the faint Mob1 nucleolar localisation only with the Zeiss Spinning Disc fluorescence microscope in Dundee (see for instance figure 30), but not with our usual Nikon Eclipse Ti fluorescence microscope (see section 2.6.3 for details), we chose to focus on the more prominent signal at the site of cell division. If the strategy with the bud-neck localisation worked, it would further encourage the identification of a recruiting protein at the nucleolus under the control of M-Cdk1.

Thus, we shortlisted candidates that met the following requirements: (1) They are located at the bud-neck, either at the septin ring or at the Ingression Promotion Complex (IPC); (2) they are either essential proteins or proteins whose loss of function resulted in a delayed or a defective cytokinesis; (3) they are known to be phosphorylated by Cdk1, and whenever the information was available, *bona fide* Cdc14 substrates. These conditions resulted in the identification of a strong candidate, the IPC protein Iqg1.

A testable prediction derived from the above hypothesis is that cells carrying a non-phosphorylatable allele of Iqg1, together with the non-phosphorylatable Cdc15(A), Mob1(A), and Dbf2(A) alleles, should be able to localise Mob1-Dbf2 at the site of cell division by the end of anaphase, despite the presence of sustained high M-Cdk1 activity.

Therefore, to test the hypothesis, we used an Iqg1(A) allele where the 14 serine and threonine residues in consensus CDK phosphorylation sequences had been replaced by alanine[177]. A strain was generated carrying non-phosphorylatable alleles of *cdc15(A), mob1(A), dbf2(A) and iqg1(A)*, under their own promoters, and the wild-type open reading frames deleted.

Strain *cdc15(A) mob1(A)-GFP dbf2(A) iqg1(A) GAL-clb2ΔN MET-CDC20*, and its isogenic control carrying wild-type *IQG1*, were grown in SCRaff-Met to mid-exponential phase and synchronised in metaphase by the depletion of Cdc20. Clb2ΔN overexpression was induced with galactose and methionine was washed out from the media. Cells were released from metaphase arrest in SCGal-Met media and monitored using fluorescence microscopy using a Zeiss Spinning Disc microscope.

As shown in figure 3.19-A, both control cells and cells carrying the *iqg1(A)* allele underwent anaphase normally, as visualised by the separation of the Mob1 SPB signals. Both strains over-expressed *clb2ΔN*, as shown in figure 38-C, and in both cases M-Cdk1 activity prevailed over Cdc14 activity, as monitored in the Pol12 western blot (see 3.1.2 for details). Both strains were blocked unable to divide, as evidenced by the continuously high dumbbell index and the maintained cell density of the cultures shown in figure 3.19-B, and also by the constant levels of endogenous Clb2 (figure 3.19-C).

As shown in figure 3.19-A, Mob1 remained locked at the SPBs after anaphase also in the *cdc15(A) mob1(A) dbf2(A) iqg1(A) bypass strain*. No re-localisation to the site of cell division was visible in the bypass strain beyond the shown time, for the whole duration of the experiment, 3 h after metaphase release.

Therefore, including a non-phosphorylatable allele of Iqg1 in the triple bypass strain does not result in the localisation of Mob1-Dbf2 at the site of cell division under high M-Cdk1 activity.

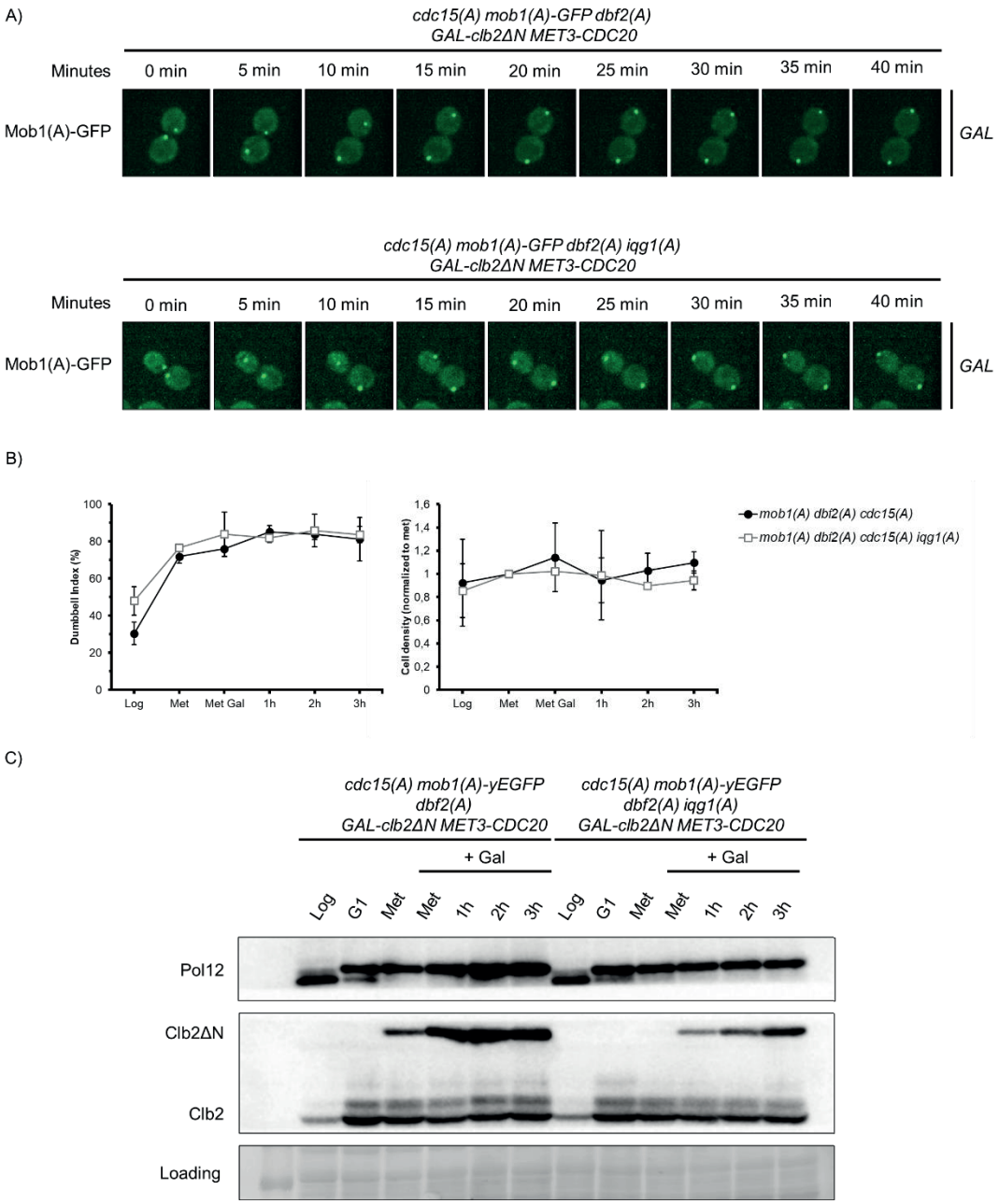

Figure 3.19. Localisation of Mob1 in the MEN iqg1 bypass in the presence of sustained high M-Cdk1 activity arrest. Cultures of strains YAZ227 (*cdc15(A) mob1(A)-GFP dbf2(A) MET3-CDC20 GAL-clb2ΔN)* and YAZ265 (*cdc15(A) mob1(A)-GFP dbf2(A) iqg1(A) MET3-CDC20 GAL-clb2ΔN)* were released from metaphase arrest under continuous *GAL-clb2*ΔN overexpression and monitored by timelapse fluorescence microscopy using a Zeiss Spinning Disc microscope. Samples were taken for immunoblot assay at the given timepoints. (A) Timelapse immunofluorescence microscopy images of a representative cell of each strain. Image stacks of 6 µm width with a step size of 0.5 µm each were taken every 5 minutes, for a total of 3 h from the metaphase release. Time 0 represents the timepoint immediately before anaphase onset. (B) Mean Dumbbell Index and Density at the given timepoints throughout the experiment. To allow for comparison between experiments, Density is

normalised to the metaphase arrest timepoint (Met). The error bar indicates the standard deviation. (C) Immunoblot against Pol12 and Clb2 of whole cell extracts, showing Pol12 and both endogenous Clb2 and Clb2ΔN protein levels. The Ponceau-S staining of the membrane is shown as a loading control. The figure is representative of 3 independent experiments.

3.5.5. Subcellular localisation of Cdc14 in the triple bypass strain under sustained high M-Cdk1 activity

In wild-type cells undergoing a normal cell cycle, upon activation of the MEN pathway, a fraction of Mob1-Dbf2 translocates to the nucleolus to promote the release of Cdc14 to the cytosol, required for mitotic exit (see 1.4.4.2). In contrast, wild-type cells under sustained high M-Cdk1 activity arrest after anaphase, unable to release Cdc14 to the cytosol[89,170]. We therefore asked whether cells carrying non-phosphorylatable alleles of Cdc15, Mob1, and Dbf2, can promote the release of Cdc14 to the cytosol in the presence of sustained high M-Cdk1 activity.

The exploration was worth undertaking despite the previous observations showing that bypass strain is unable to enter cytokinesis in the presence of sustained high M-Cdk1 activity. We rationalised that in our e experimental setting, MEN might abrogate the M-Cdk1 inhibition and activate, releasing Cdc14 to the cytosol, and yet the high M-Cdk1 activity compared to normal levels might prevail and continue preventing cytokinesis by keeping one or more downstream targets inhibited.

To explore the subcellular localisation of Cdc14 under high M-Cdk1, we GFP-tagged Cdc14 in the triple bypass background and in an isogenic control strain. Both strains were grown in SCRaff-Met to mid-exponential phase, and then synchronised in metaphase by the depletion of Cdc20. The culture was split in two and the media was changed to either fresh SCRaff+Met or SCGal+Met to allow for Clb2ΔN overexpression. Methionine was washed out from the media and cells were allowed to progress through the cell cycle. We then monitored Cdc14 using spinning disc fluorescence microscopy.

3.5.5.1. Behaviour of the bypass strain in an unperturbed mitosis

Figure 3.20-A shows timelapse images of representative cells at each of the four experimental settings. The changes in subcellular localisation of Cdc14 in wild-type cells in an unperturbed mitosis match previous reports, with a nuclear release in anaphase, with accumulation of Cdc14 at the dSPB, and a subsequent MEN-driven release to the cytosol[141,169,249,268].

In bypass cells, the kinetics of nucleolar to nuclear release, the accumulation of Cdc14 at the dSPB, and the time of cytosolic release are coincident with those observed in wild-type cells. However, the time that Cdc14 remains released from the nucleolus before being re-sequestered in the triple bypass cells is dramatically reduced to around 10 minutes, in deep contrast to the canonical 25 min seen in the wild-type control cells. Such a reduction of time does not result in a defective mitotic exit, as the bypass strain is fit and divides with the same doubling time as wild-type cells (figure 3.20-D and section 3.3.1).

Despite the shorter release time of Cdc14, the bypass cells take the same time to divide as the control cells, as monitored by the morphology in the bright field images. Figure 3.20-B shows the continuation times for the timelapses shown in figure 3.20-A for the bypass and the control strains under normal mitotic M-Cdk1 levels. When cells finish cytokinesis, they remain bound by the shared wall septa until the primary septum is hydrolysed (see section 1.4.5.3). Despite the two descendant cells usually remain in close contact, the individualisation of the cell walls is normally visible in the bright field. As shown in figure 3.20-B, the bypass cells are fully separated by individualised cell walls by timepoints 40-45 min, that is 30-35 min after the Cdc14 cytosolic release. The wild-type control cells are fully separated by individualised cell walls by timepoint 55 min, which is 40 min upon the start of the Cdc14 release to the cytosol. Whereas we do not know whether the shorter mitotic exit time is significant, the reduction is hardly compatible with a compromised mitotic exit.

Next, to objectively quantify the visual observations, the subcellular localisation of Cdc14 was evaluated by measuring the coefficient of variation (CV_{Cdc14}) of the GFP signal in randomly selected individual cells throughout the cell cycle (see 2.6.6. for details). As shown in figure 3.20-C, the results support the visual conclusions. Wild-type cells released from metaphase arrest into raffinose start lowering their CV_{Cdc14}

value as Cdc14 is released from the nucleolus to the nucleoplasm. In all cells, the timing of this event was coincident with the expected time of the onset of anaphase, as evidenced by the localization of Cdc14 at separated SPBs (figure 39-A). By the time of anaphase completion, the CV_{Cdc14} value further decreases until it reaches a low peak of around 0.25, in which the Cdc14 signal is indistinguishable from the background by the naked eye and Cdc14 localises also to the cytosol. Soon after, with a timing compatible with the destruction of mitotic cyclins by APC^{Cdh1} at the mitotic exit (see section 1.4.2.2), Cdc14 is re-sequestered at both mother and daughter nucleoli. Of note, upon nucleolar re-sequestration, the CV_{Cdc14} value reproducibly averages to around half the original intensity. The pattern is coincident with the one shown by Neurohr and Mendoza, 2017. This occurs despite Cdc14 levels are not cell-cycle regulated and remain constant[269,270].

In summary, the above analyses show that the presence of non-phosphorylatable alleles of the MEN kinases results in a faster switch in the biochemical control of mitotic exit. The period during which MEN is active is dramatically reduced. However, this does not result in an inefficient mitotic exit.

3.5.5.2. Behaviour of the bypass strain in the presence of sustained high M-Cdk1 activity

The subcellular localisation of Cdc14 was also analysed in cells under sustained high M-Cdk1 activity. As shown in figure 3.20-D, both bypass cells and wild-type control cells are equally unable to divide as expected (see 3.1.2). Under these conditions, Cdc14 undergoes nuclear release but not cytosolic release, and the phosphatase does not return to the nucleolus for the duration of the experiment in any of the two strains (timelapse images in figure 3.20-A). The quantification in figure 39-D supports the visual observations: although Cdc14 is released from the nucleolus in both strains, the CV_{Cdc14} values never go below 0.4, suggesting a lack of cytosolic release. The CV_{Cdc14} values remain flat for the duration of the experiment -except for the slow downward drift resulting from the bleaching of the GFP fluorophore by laser exposure.

The observations are compatible with the high M-Cdk1 activity blocking the MEN-driven release of Cdc14 to the cytosol, and hence mitotic exit. Therefore, despite the

bypass strain showing a deregulated behaviour under normal levels of M-Cdk1 activity, it is not enough for cells to override the high levels of M-Cdk1 activity generated by the over-expression of Clb2ΔN.

Of note, the prevailing high M-Cdk1 activity (see section 3.1.12) does not suppress the accumulation of Cdc14 at the dSPB.

A)

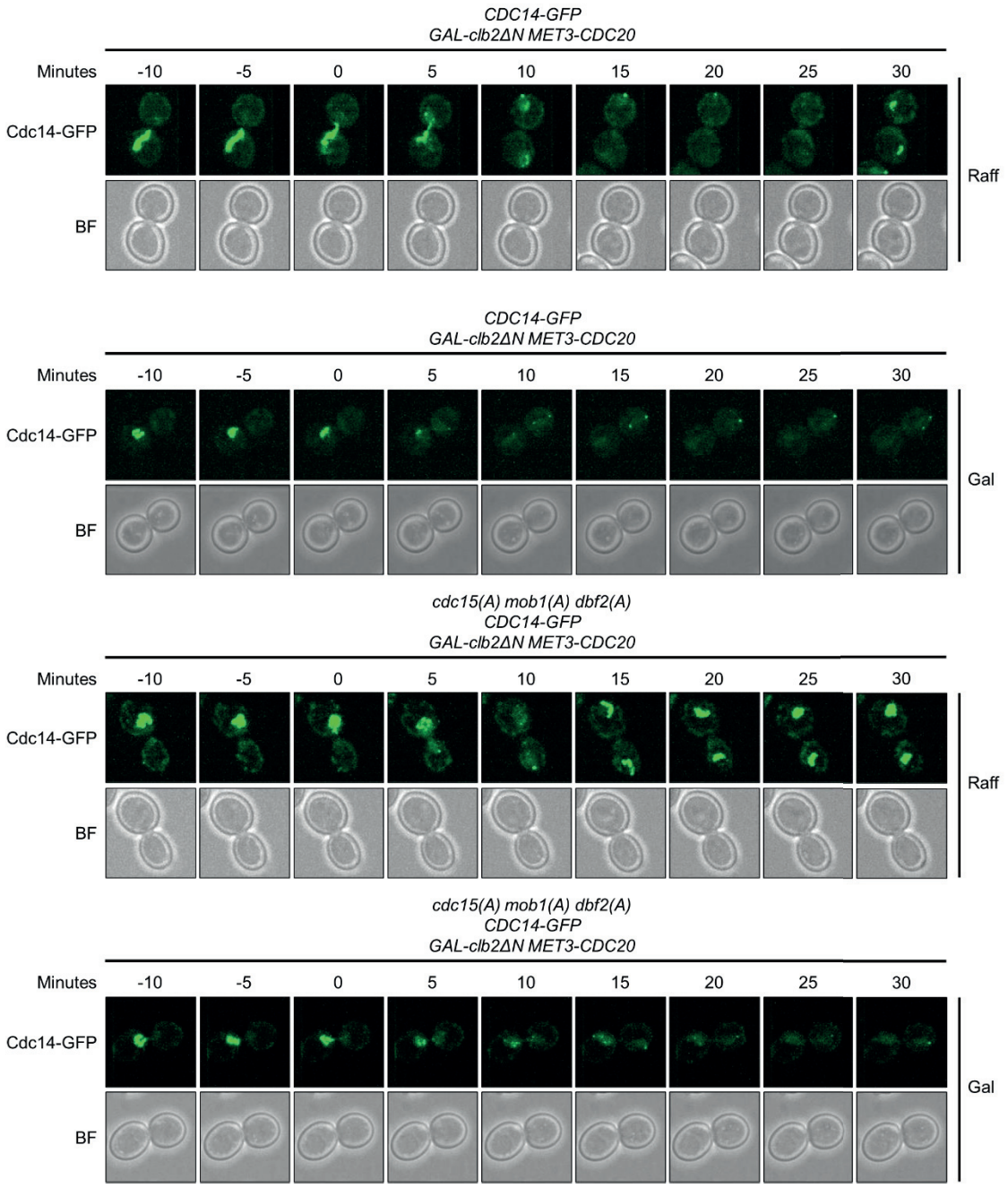

B)

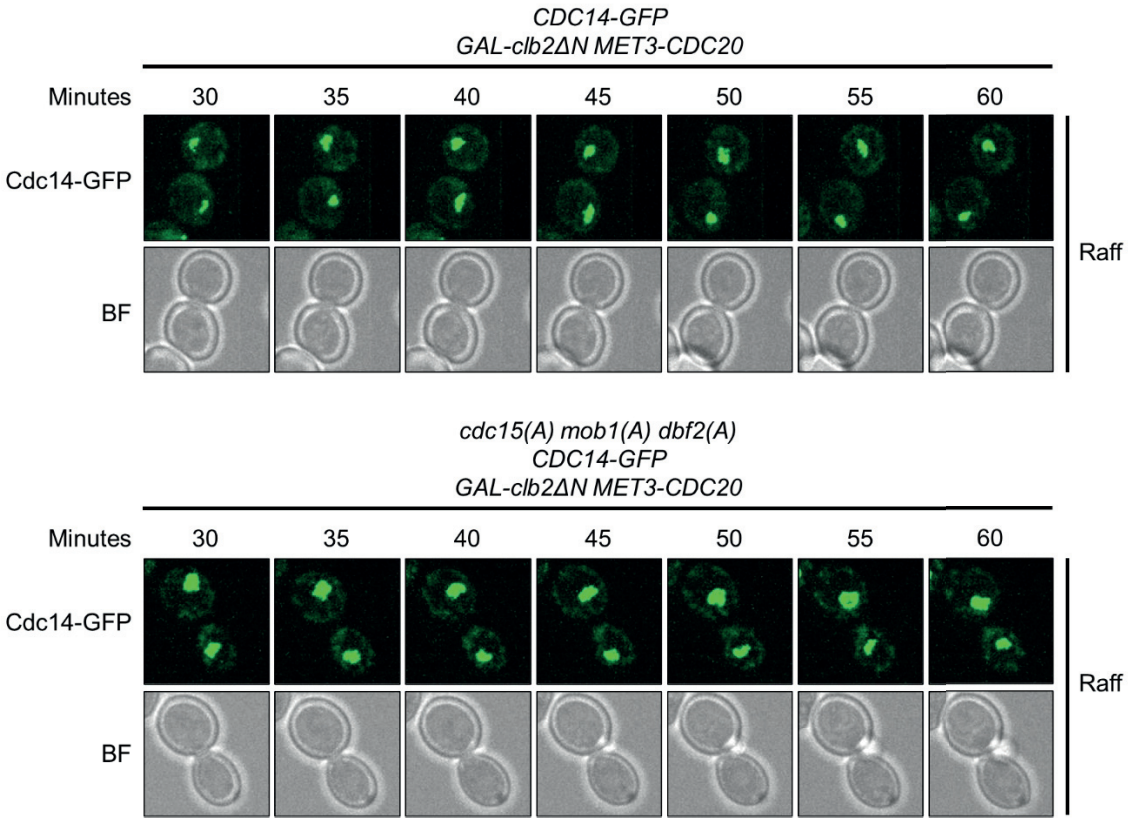
CDC14-GFP
GAL-clb2ΔN MET3-CDC20
Minutes
30
35
40
45
50
55
60
Cdc14-GFP
BF
Raff
cdc15(A) mob1(A) dbf2(A)
CDC14-GFP
GAL-clb2ΔN MET3-CDC20
Minutes
30
35
40
45
50
55
60
Cdc14-GFP
BF
Raff

C)

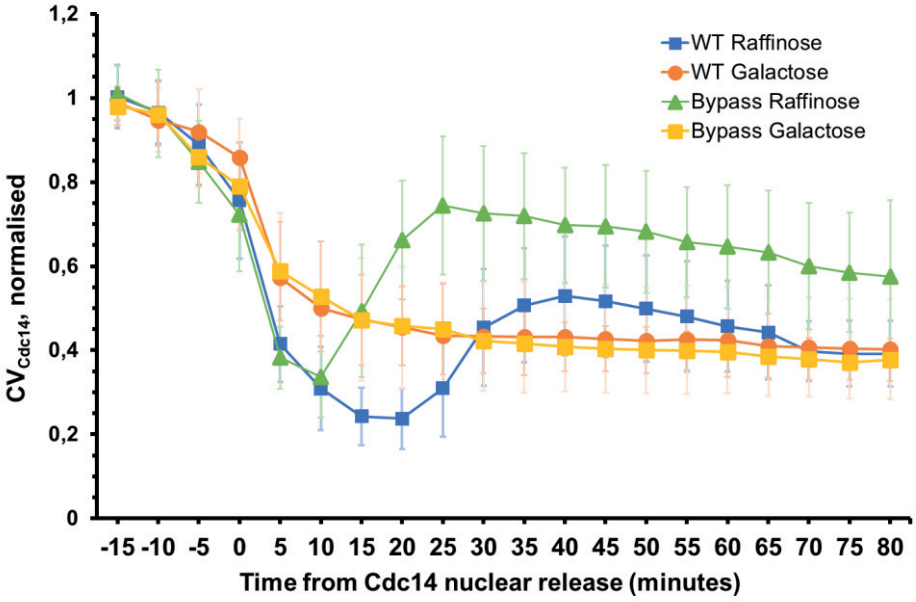
WT Raffinose
WT Galactose
Bypass Raffinose
Bypass Galactose
CV Cdc14, normalised
1,2
1
0,8
0,6
0,4
0,2
0
-15 -10 -5 0 5 10 15 20 25 30 35 40 45 50 55 60 65 70 75 80
Time from Cdc14 nuclear release (minutes)

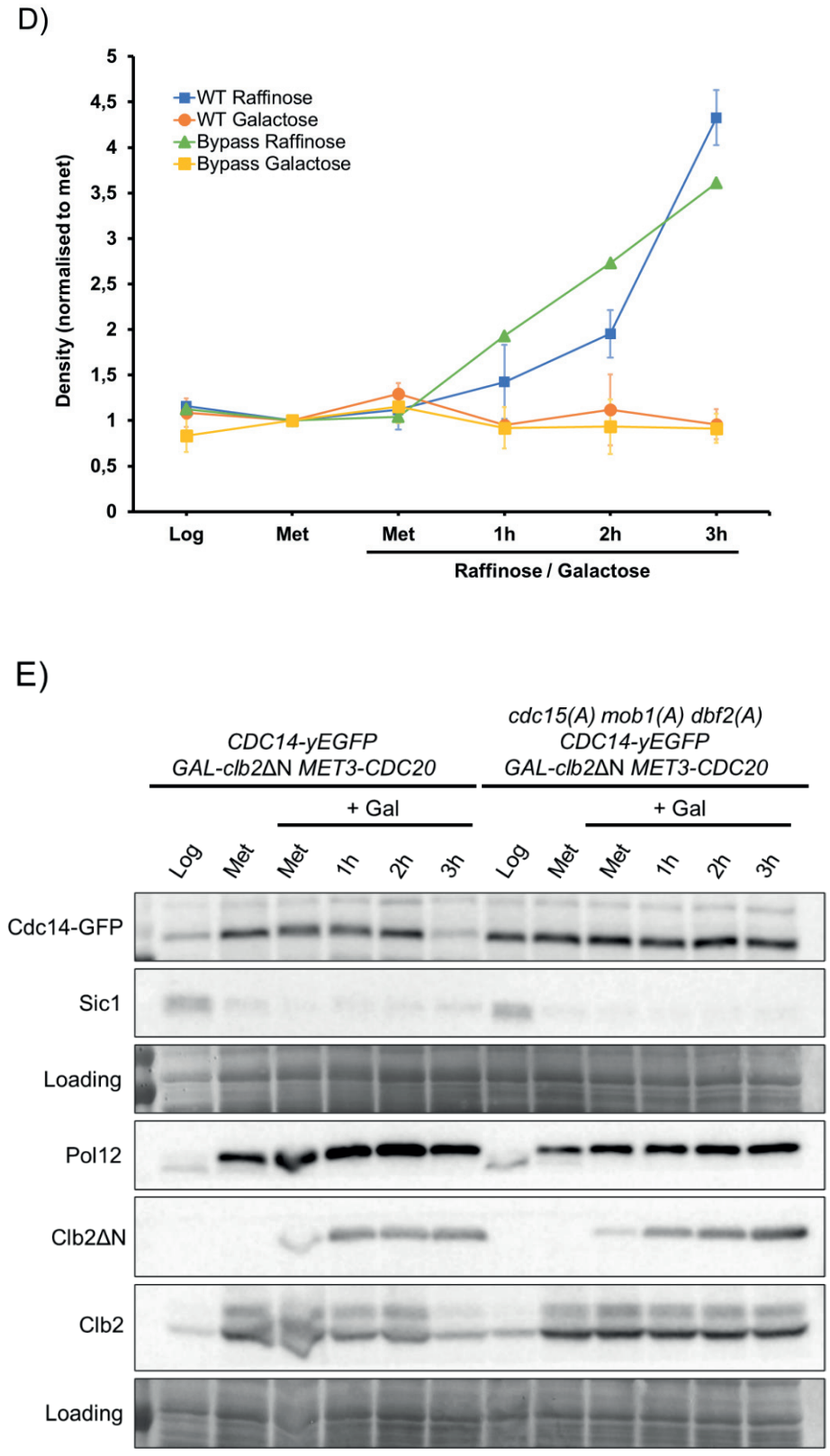

Figure 3.20. Localisation of Cdc14 in the triple MEN bypass in the presence of sustained high M-Cdk1 activity. Cultures of strains YAZ63 (*CDC14-GFP MET3-CDC20 GAL-clb2ΔN)* and YAZ254 (*cdc15(A) mob1(A) dbf2(A) CDC14-GFP MET3-CDC20 GAL-clb2ΔN)* were released from metaphase into raffinose (Raff) or galactose (Gal) containing

media. Cells were monitored by timelapse fluorescence microscopy using a Zeiss Spinning Disc microscope. Samples were taken for immunoblot assay at the indicated timepoints. (A) Timelapse immunofluorescence microscopy images of a representative cell of each strain. Image stacks of 6 µm width with a step size of 0.5 µm each were taken every 5 minutes, for a total of 3 h from the metaphase release. Time 0 represents the timepoint immediately before Cdc14 is released from the nucleolus to the nucleus. (B) Continuation of timelapses from (A) cells released in Raffinose. The first timepoint (30 minutes) corresponds to the last timepoint in the (A) series). (C) Quantification of the subcellular localisation of Cdc14 (see section 2.6.6). At least 30 cells (WT Raffinose 45 cells, WT Galactose 32 cells, Bypass Raffinose 43 cells, Bypass GAL 30 cells) were selected and quantified for each condition. The figure is representative of 3 independent experiments, except for the bypass strain in raffinose, which was performed only once. (D) The cell density of the cultures at the indicated timepoints, normalised to the density at the time of metaphase arrest (Met). The error bars in (C) and (D) are standard deviations. (E) Immunoblot against Pol12, Clb2 and Sic1 on whole cell extracts. The anti-Clb2 antibody recognises both endogenous Clb2 and Clb2ΔN. The Ponceau-S staining of the membrane is shown as a loading control.

3.5.6. Exploration of Cdc15(A) signalling under sustained high M-Cdk1

We showed that in cells carrying the Cdc15(A) Dbf2(A) Mob1(A) alleles, the three proteins localise at the SPBs, the site of MEN activation, under sustained high M-Cdk1 (section 3.5.2). The recruitment of Mob1-Dbf2 from the SPBs requires the phosphorylation of the scaffold protein Nud1 by active Cdc15, which is therefore happening (see section 1.4.4.2).

However, Mob1-Dbf2 is not released from the SPBs (section 3.5.2), an essential event to trigger mitotic exit (section 3.5.5). The release requires the phosphorylation of Dbf2 by Cdc15 (see section 1.4.4.2).

Because the Cdc15(A) mutant cannot be phosphorylated by Cdk1, we explored different alternative mechanisms to try and explain how the Cdc15(A) can phosphorylate Nud1 but not activate Dbf2 in the presence of sustained M-Cdk1 activity.

3.5.6.1. Cdc15(A) remains at the SPBs under sustained high M-Cdk1

One possible scenario would be that high M-Cdk1 activity targets an SPB substrate, such as Nud1, that results in the removal of Cdc15 / Cdc15(A) *after* the recruitment of Mob1-Dbf2, which thus cannot be activated. We therefore wished to investigate the dynamics of Cdc15 / Cdc15(A) localisation under these conditions.

Strain *cdc15(A)-GFP mob1(A) dbf2(A) GAL-clb2ΔN MET-CDC20*, and its isogenic control carrying wild-type were grown in SCRaff-Met to mid-exponential phase and synchronised in metaphase by the depletion of Cdc20. The culture media was changed SCGal+Met to allow for *clb2ΔN* overexpression. Methionine was washed out from the media and cells were allowed to resume progression through mitosis in SCGal-Met media. The subcellular localisation of Cdc15-GFP was investigated using spinning disc fluorescence microscopy.

As shown in figure 3.21, both Cdc15(A) and wild-type Cdc15 remain stably present at the SPBs in the presence of sustained high M-Cdk1 activity, indicating that Cdc15 is not removed from the SPBs by M-Cdk1 dependent phosphorylation.

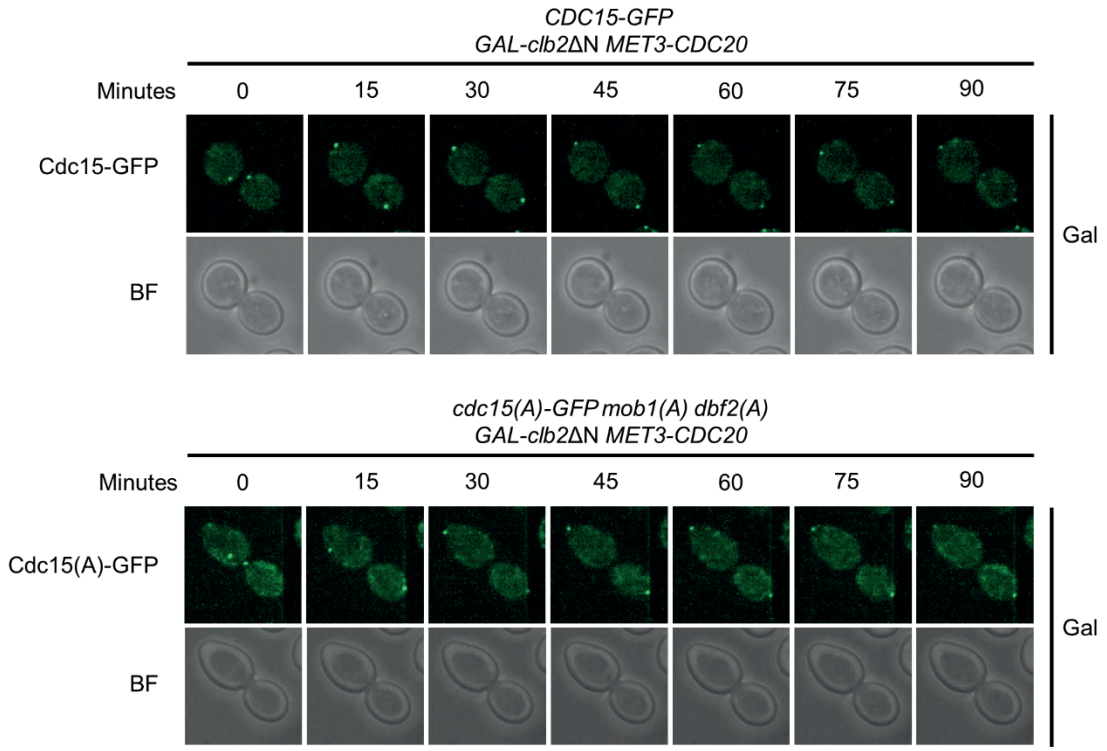

Figure 3.21. Subcellular localisation of Cdc15(A) during the high M-Cdk1 activity arrest. Timelapse immunofluorescence microscopy images of a representative cell of each strain. Cultures of strains YAZ267 (*CDC15-GFP MET3-CDC20 GAL-clb2ΔN)* and YAZ269 (*cdc15(A)-GFP mob1(A) dbf2(A) MET3-CDC20 GAL-clb2ΔN)* were released from metaphase arrest under continuous *GAL-clb2*ΔN overexpression and monitored by timelapse fluorescence microscopy. Image stacks of 6 µm width with a step size of 0.5 µm each were taken every 15 minutes. Time 0 represents the timepoint immediately before anaphase onset. The figure is representative of 2 independent experiments.

3.5.6.2. Cdc15(A) does not phosphorylate Dbf2 in the presence of sustained high M-Cdk1

A second scenario to explain the lack of Mob1-Dbf2 release from the SPBs in cells under sustained high M-Cdk1 activity, would be that M-Cdk1 targets a substrate upstream in the MEN pathway, such as Tem1 or Lte1, which results in the lack of Cdc15 activity towards Dbf2 -while sparing the activity towards Nud1.

We therefore asked whether Cdc15(A) was able to phosphorylate Dbf2(A) in the presence of sustained high M-Cdk1 activity. To assess Dbf2 / Dbf2(A) phosphorylation based on electrophoretic mobility, the triple bypass strain and the

corresponding wild-type isogenic control strain were grown in SCRaff-Met to mid-exponential phase, and then synchronised in metaphase by the depletion of Cdc20. The culture media were changed to fresh SCGal+Met to allow for *Clb2ΔN* overexpression. Methionine was then washed out and cells were allowed to resume mitosis in SCGal-Met media. Samples for western blot were collected at 1, 2 and 3 h upon the metaphase arrest release.

Whole-cell extracts were run on a Phos-tag electrophoresis gel and on a regular SDS-PAGE gel, and western-blotted with specific antibodies. As shown in figure 3.22, *clb2*ΔN was effectively expressed and resulted in the phosphorylation of the *bona fide* M-Cdk1 substrate Pol12.

The different mobility bands seen in Dbf2 from wild-type cells are absent in Dbf2(A) from bypass cells, compatible with lack of phosphorylation by Cdk1, and are therefore due to M-Cdk1. Interestingly, when cells are released from the metaphase arrest, the slowest mobility bands decrease in intensity, compatible with FEAR-released Cdc14 prevailing locally over M-Cdk1 at the SPBs. Such a scenario is compatible with the accumulation of Cdc14 at the SPBs seen in figure 3.20-A.

However, no change in mobility is detected upon release from the metaphase arrest, as would be expected in the case of phosphorylation by Cdc15 in the highly sensitive Phos-tag electrophoresis analysis.

This result therefore suggests that MEN is not active despite that the three proteins that make up the two MEN kinases, Cdc15 Mob1-Dbf2, cannot be inhibited by Cdk1 phosphorylation. The lack of Cdc15 activity on Dbf2 points to the existence of an additional substrate, upstream of Cdc15, under the negative control of M-Cdk1.

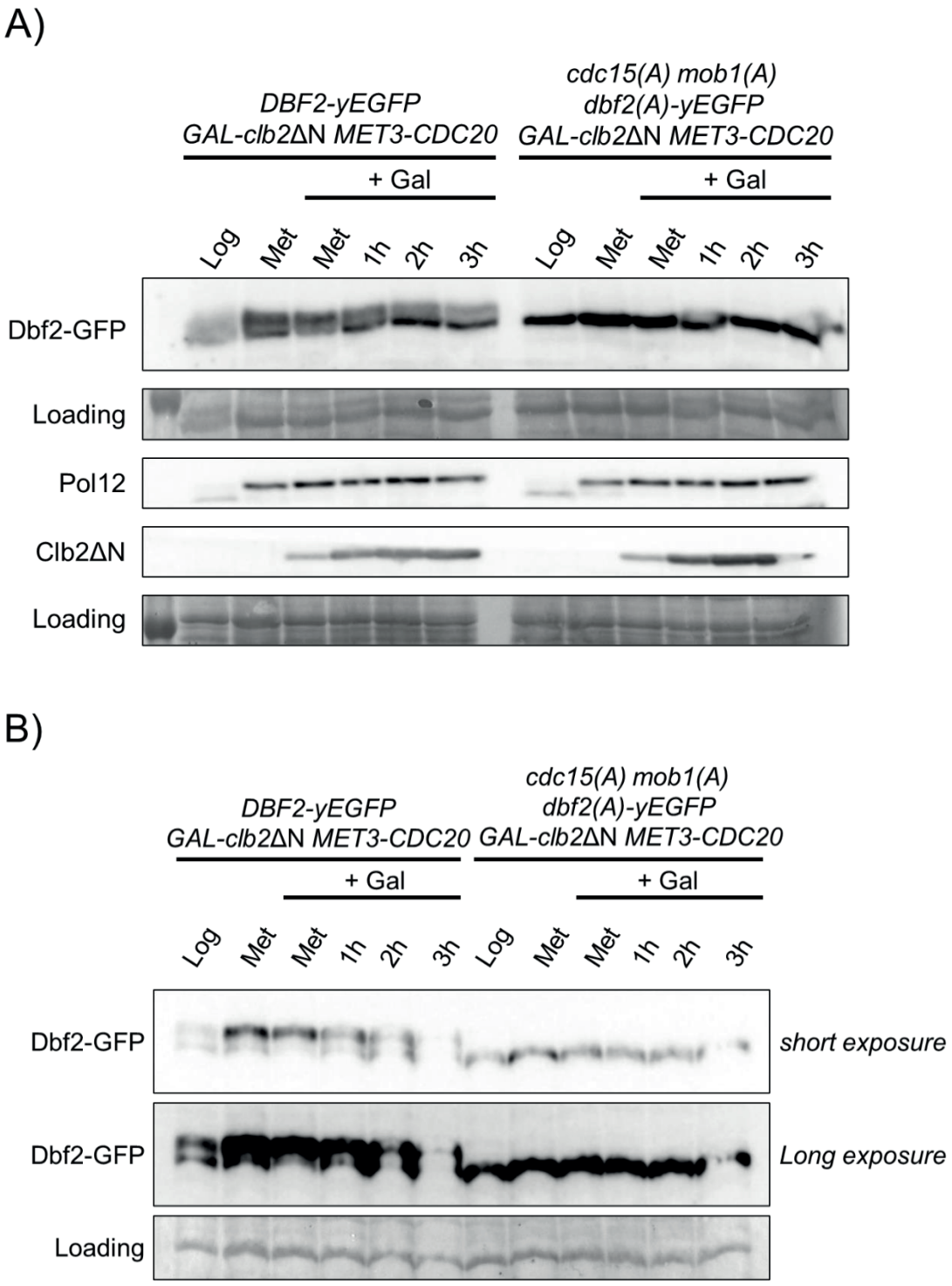

Figure 3.22. Dbf2(A) is not phosphorylated in bypass cells under sustained high M-Cdk1. Cultures of strains YAZ236 (*DBF2-GFP MET3-CDC20 GAL-clb2ΔN*) and YAZ271 (*cdc15(A) dbf2(A)-GFP mob1(A) MET3-CDC20 GAL-clb2ΔN*) released from metaphase arrest under continuous *GAL-clb2*ΔN overexpression. Cells were harvested at the indicated times for immunoblot analysis. (A) Immunoblot against GFP, Pol12 and Clb2 on whole cell extracts. GFP antibody recognises Dbf2-GFP,

while Clb2 recognises Clb2ΔN. (B) Immunoblot against GFP of a Phos-tag electrophoresis. Two exposure times are shown. The Ponceau-S staining of the membranes is shown as a loading control.

3.5.6.3. The Dbf2(A) signal at the SPBs decays with time in the sustained high M-Cdk1 arrest

Taking advantage of the Dbf2(A)-GFP strain, we investigated a third scenario. Even in the event of an effective bypass of M-Cdk1, Dbf2(A) might be artifactually lost from the site of activation, or not loaded at all, resulting in the lack of MEN activation. This could be the case, for instance, if one of the mechanisms of MEN inhibition by M-Cdk1 were to phosphorylate Mob1-Dbf2 to increase its affinity for the docking protein Nud1, thus locking the kinase at the SPBs. In that event, the non-phosphorylatable Mob1(A) Dbf2(A) proteins might be lost during the arrest under sustained high M-Cdk1 activity. We have shown that Mob1(A) remains stably localised to the SPBs under these conditions (see section 3.5.2). We therefore wished to investigate the behaviour of the Dbf2(A) mutant during the mitotic arrest due to sustained high M-Cdk1 activity.

Cells from the previous experiment (3.5.6.1), that is *cdc15(A) dbf2(A)-GFP mob1(A)* bypass cells and isogenic wild-type control cells. Upon release from metaphase synchronisation under continuous *GAL-clb2*ΔN overexpression, cells were analysed using timelapse fluorescence microscopy. As seen in figure 3.23, both wild-type and triple bypass cells display Dbf2 at the SPBs in cells arrested at the end of anaphase, as assessed by the separation of the SPBs. However, whereas the Dbf2 intensity of the signal remains stable in wild-type cells, the intensity of the Dbf2(A) signal decreases with time.

The Dbf2(A) mutant is not hypomorphic for mitotic exit, as the triple bypass strain divides with a normal doubling time and does not show a slower mitosis (see section 3.3.1), indicating that in a regular mitosis, the Mob1(A)-Dbf2(A) kinase assembles, activates and functions efficiently. In consequence, the progressive slow loss of Dbf2(A) from the SPBs during the arrest might reveal that one point of control through which M-Cdk1 blocks the premature activation of cytokinesis, might be locking Dbf2 at the SPBs by direct phosphorylation.

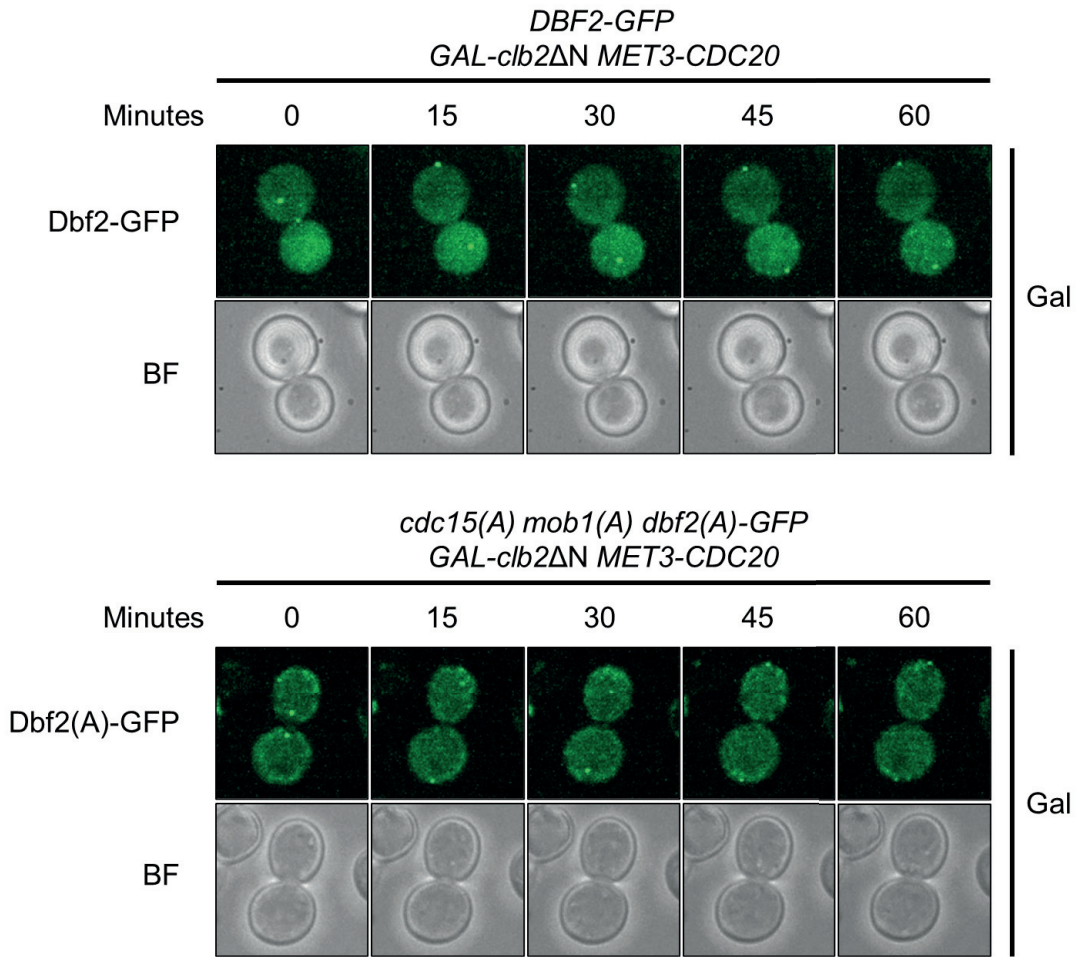

Figure 3.23. The Dbf2(A) signal, but not the wild-type Dbf2 signal, decays from the SPBs during the mitotic arrest under sustained high M-Cdk1. See details in figure 3.22. Dbf2 was monitored in individual cells by timelapse fluorescence microscopy using a Spinning Disc fluorescence microscope (Zeiss). Image stacks of 6 µm width with a step size of 0.5 µm each were taken every 15 minutes with a Spinning Disc fluorescence microscope (Zeiss). Time 0 represents the timepoint immediately before anaphase onset.

4. Discussion

4.1. The experimental approach

4.1.1. Inducible sustained high M-Cdk1 activity to block mitotic exit

We have created a robust experimental system to test the minimal set of M-Cdk1 substrates that block cytokinesis. Over-expression of the hyperstable *clb2ΔN* mutant results in sustained high M-Cdk1 activity that prevails over Cdc14 biochemically (figure 3.5), as assessed by the state of *bona fide* substrates shared by both M-Cdk1 and Cdc14, such as Pol12, or the stability of endogenous Clb2, whose destruction requires APC^{Cdh1} activity. Cdh1 is also a shared substrate of M-Cdk1 and Cdc14 and must be dephosphorylated by Cdc14 for activation.

As a result of *clb2ΔN* over-expression, cells block after anaphase completion (figure 3.3), unable to divide (figure 3.5), fail to recruit essential elements for cytokinesis to the site of division (figure 3.12 Dbf2, figure 3.17 Mob1, figure 3.6 Chs2), the lack of AMR contraction (figures 3.2 Myo1, 3.4 Hof1), and do not undergo membrane ingression (figure 3.2).

The testable prediction in this experimental approach is the following: A strain carrying non-phosphorylatable alleles for all the critical proteins targeted by M-Cdk1 to block mitotic exit, should override the *clb2ΔN* arrest, whereas isogenic wild-type cells under the same conditions cannot.

The high M-Cdk1 activity is safely induced in metaphase and does not affect the cells ability to undergo anaphase normally (section 3.1.1). Thus, contrary to other approaches requiring mutations, the SPOC checkpoint is expected to be naturally inactive in our arrest, allowing us to explore the remaining M-Cdk1-depending control[171,268] without interferences and without the need to inactivate it with other mutations which might also affect the mitotic exit.

The system blocks the mitotic exit machinery but does not damage it. We checked early on that it is reversible, as cells arrested by *clb2ΔN* over-expression are able to undergo cytokinesis, divide and further proliferate when the hyperstable allele *clb2ΔN* is eliminated (section 3.1.3).

As a downside, the anaphase spindle destabilises in roughly half of the cells during the high M-Cdk1 arrest after anaphase completion, as indirectly determined by the loss of maximum distance between spindle pole bodies. The observation is compatible with previous reports showing that dephosphorylation of M-Cdk1 substrates by Cdc14 promotes spindle stability[271,272]. However, we believe that this event does not hamper the objective of this study. Cells arrest after anaphase completion, and therefore the SPOC is already inactive. Still, we do not know whether SPOC signalling could be reactivated in cells where both spindle pole bodies abnormally re-localise to the mother body compartment after anaphase. In worst case scenario, the collapse does not affect all cells, and around half of them display a stable long spindle for hours. In these cells, SPOC reactivation should not be a concern. To this respect, we do not see two different phenotypes in any of the analysed variables in cells under the high M-Cdk1 arrest, either wild-type or bypass genotype.

4.1.2. Testing non-phosphorylatable alleles of mitotic exit M-Cdk1 substrates to override the block

The rationale for the choice of Cdc15, Mob1 and Dbf2 as bypass candidates was based on previously published studies. Once cells have completed anaphase successfully, mitotic exit depends on the activation of the Mitotic Exit Network (MEN). The three subunits of the two MEN kinases, Cdc15, and Mob1-Dbf2, are Cdk1 substrates[184,254]. And the phosphorylations on Cdc15 and Mob1 has been shown to result in their inhibition[184,254].

Despite several works had explored the phenotype of *cdc15(A)* strains[254] and of *cdc15(A) mob1(A)* strains[184], none had included *dbf2(A).* Yet, in a global analysis for Cdk1 substrates, Dbf2 was found to be phosphorylated in at least three sites[257]. No reports have been published on its possible biological significance, but the critical role that Dbf2 plays in mitotic exit, and the fact that its activating partner Mob1 is known to be inhibited by M-Cdk1 phosphorylation, made the inclusion of Dbf2 a sensible option.

Dbf2 has a paralog, Dbf20, that can replace to a certain extent the Dbf2 function in *dbf2* null mutants[175]. A source of concern was the possibility that if the *dbf2(A)* mutant had a lower affinity for Mob1, the bypass cells were actually run by Mob1-Dbf20. In

that case, the Dbf20 kinase might still be inhibited by M-Cdk1 and, hence, abolish entry into cytokinesis. We ruled out such a possibility based on the fact that Dbf20 is less efficient than Dbf2 to promote mitotic exit[175]. As a consequence, *dbf2* mutant cells that are run by Dbf20 show a significant phenotype, with a longer doubling time due to a longer time spent before entering cytokinesis, which results in a high dumbbell index in exponential cultures. None of the above alterations occurs in our bypass strain. We therefore rule out that Dbf20 is acting as a confounding variable.

We thus generated strains carrying the non-phosphorylatable alleles *cdc15(A), mob1(A)* and *dbf2(A)*, under their own promoters, as sole copies of the genes. We deleted the 7 CDK phosphorylation sequences present in each of the proteins, regardless of whether they were minimum or full consensus, and regardless of whether they were known to be phosphorylated *in vivo.*

The strains are viable, display the same doubling time as wild-type cells, and do not show detectable defects in mitosis, as judged by the same budding and dumbbell indexes as wild-type cells in exponentially growing cultures. The strains also show no thermosensitivity at 37ºC, ruling out major conformational alterations resulting from the 21 mutations in three proteins which are either essential (Cdc15, Mob1) or critical (Dbf2) for mitotic exit.

However, the lack of a phenotype also indicated from the onset of the project that (A) either the 3 mutant alleles were not sufficient to fully bypass the M-Cdk1 control on mitotic exit, or (B) a full bypass does not result in a significant, generalised loss of viability under normal growth conditions.

In any case, the triple mutant strain allowed us to explore in detail the role of the regulation of M-Cdk1 on the Cdc15 and Mob1-Dbf2 MEN kinases in the control of mitotic exit. It also provides a platform to check the effects resulting from the modification of additional mitotic exit players.

4.2. What does the *cdc15(A) mob1(A) dbf2(A)* bypass strain bypasses and what not

4.2.1. In bypass cells undergoing a normal cell cycle, mitotic exit does not occur prematurely

Interestingly, the early recruitment of the MEN kinases to the SPBs does not alter the timing of mitotic events, such as the time of activation of Mob1-Dbf2, as judged by the time of Cdc14 release to the cytosol (figure 3.20), or the time when a fraction of Mob1-Dbf2 localises to the bud-neck, where it triggers the contraction of the actomyosin ring (fig 3.10 and 3.14).

Also, the duration of cytokinesis, as monitored by the time that the Mob1-Dbf2 ring at the bud-neck takes to contract, is identical in the bypass strains and the corresponding isogenic wild-type cells used as control (fig 3.14).

We draw two main conclusions from these observations.

One, the lack of premature mitotic exit in the bypass strain is the result of the multiple control layers in place. First, an obvious *timer* avoids the onset of mitotic exit occurring before anaphase. The SAC keeps the APC^{Cdc20} inactive until all chromosomes are attached to the spindle and under bipolar tension. APC^{Cdc20} is required to activate the Esp1/separase activity that cleaves cohesion, triggering chromosome segregation. The second obvious *timer* is the requirement of the completion of anaphase for the SPOC to turn permissive towards MEN activation. Third, MEN activation still depends on the M-Cdk1 negative control, the focus of interest in this thesis. In an unperturbed cell cycle, the main spatiotemporal switch is expectably the inactivation of the SPOC upon the culmination of anaphase. Therefore, a premature mitotic exit is not expected in an M-Cdk1 bypass strain in wild-type cells undergoing a normal M phase. Only under sustained high M-Cdk1 activity should a bypass strain behave differently with respect to wild-type cells.

The second conclusion can be inferred from the identical duration in bypass and in wild-type cells of: (1) the time of onset of cytokinesis after anaphase completion; (2) the duration of cytokinesis; and (3) the time from the end of anaphase until the cells

are separated by independent walls. The M-Cdk1 control on Cdc15 Mob1-Dbf2 is irrelevant once MEN activates and active Mob1-Dbf2 kinase is released.

4.2.2. The recruitment of the MEN kinases to the SPBs occurs earlier and persists for longer in bypass cells undergoing a normal cell cycle

The M-Cdk1 bypass strains, carrying the non-phosphorylatable alleles of Cdc15, Mob1 and Dbf2, show a premature and extended recruitment of the mutant proteins at the SPBs. The time that Cdc15, Mob1 and Dbf2 are recruited at the SPBs in wild-type cells coincides with APC^{Cdc20}-driven decrease of M-Cdk1 activity in anaphase to around half the level of metaphase[89]. These observations indicate that in wild-type cells M-Cdk1 limits the localisation of the MEN kinases at the SPBs, therefore contributing an additional control layer in the prevention of premature mitotic exit.

The most dramatic change occurs to Cdc15. Whereas in wild-type cells the kinase is loaded at the SPBs in early anaphase, Cdc15(A) in a triple bypass is detectable at both SPBs well before anaphase (figures 3.11 and 3.15-A). In addition, while Cdc15 disappears from the SPBs shortly after anaphase completion in wild-type cells, Cdc15(A) remains detectable at both SPBs well past cell division. Inspection of individual cells in mid-exponential cultures (figure 3.15-B) shows a bright Cdc15(A)-GFP signal in all unbudded (G1 and early S phase) cells. When the progression of the cells is monitored, all of them lose the signal when they reach a small-budded morphology, compatible with the time of SPB duplication in S phase[273]. However, because the bypass strain shows a wild-type phenotype, the extended localisation of the kinase at the SPBs, both before and after normal times, does not seem to be detrimental to the cell under optimal growth conditions.

M-Cdk1 has been shown to inhibit the localisation of the MEN kinases to the SPBs[274]. Therefore, the simplest explanation for the observed extended presence of Cdc15(A) at the SPBs in the bypass strain is that, in wild-type cells, the high M-Cdk1 activity in metaphase targets Cdc15, blocking its recruitment at the SPBs. As cells enter anaphase, the reduction in the levels of M-Cdk1 activity, and the FEAR release of Cdc14, are likely to result in Cdc15 dephosphorylation, which can now bind to Nud1 at the SPBs.

Upon anaphase completion, Cdc15 is removed from the SPBs, whereas Cdc15(A) remains localised well into G1. The simplest interpretation for the loss of Cdc15 from the SPBs in wild-type cells would suggest that it is the result of direct phosphorylation by M-Cdk1. However, it is difficult to reconcile that in wild-type cells, a lower M-Cdk1/Cdc14 balance at the end of anaphase is responsible for the removal of Cdc15, whereas the higher M-Cdk1/Cdc14 activity at the onset of anaphase allows its recruitment. A more elaborate explanation contemplates two distinct Cdc15 conformations. In metaphase, a loadable conformation exposes low-affinity M-Cdk1 sites that prevent its recruitment at the SPBs. The decrease of M-Cdk1 activity by upon APC^{Cdc20} activation and the FEAR release of Cdc14 reverts the phosphorylation and allows the recruitment of Cdc15 to the SPBs. Later, MEN activation results in the Tem1-dependent conformational change in Cdc15 that activates the kinase towards Dbf2. The conformational change may expose a high-affinity M-Cdk1 phosphorylation site that the remaining M-Cdk1 activity may target to abolish the affinity of Cdc15 from the SPBs.

The behaviour of Cdc15(A) may also explain the early and extended recruitment of Mob1(A)-Dbf2(A) at the SPBs. In wild-type cells, the two proteins load in early anaphase, first at the mSPB and soon after at the dSPB, and the signal intensifies later in anaphase (figures 3.10 and 3.14). In the bypass strain the non-phosphorylatable mutant proteins load simultaneously to the two SPBs in metaphase, at a time of peak M-Cdk1 activity (figure 3.14). The specific control of the later recruitment at the dSPB is discussed in point 4.2.5 below.

The persistence of Mob1(A)-Dbf2(A) at the SPBs could be explained if the permanence of Cdc15(A) protects Nud1 from the ubiquitin ligase Dma2. Dma2 targets Nud1 for destruction in the final stages of mitosis, which is likely to result in the loss of the MEN kinases from the SPBs in wild-type cells during mitotic exit[189]. In this sense, a recent publication with a hyperactive mutant of Nud1 (Nud1-A308T) also displayed the almost continuous presence of Cdc15 in all stages of the cycle[275]. Alphafold structural prediction of Nud1 displays A308 in close proximity to K288, one of the two reported ubiquitinated residues of Nud1[276–278].

An unexpected observation, unrelated to the mitotic exit, is the consistent observation in wild-type cells of a transient localisation of Cdc15 at one point compatible with a SPB in late S / G2 cells. Such localisation is also independent of

Cdk1 control, as it is observed both in wild-type cells and in bypass cells. At that early cell cycle time, it is not possible to distinguish whether the Cdc15 signal corresponds to the mSPB or the dSPB without experiments labelling specific proteins. This early, transient presence does not result in the presence of Mob1 or Dbf2. Perhaps the Cdc15 kinase plays a role in SPB maturation independent of its role in MEN. Alternatively, it might carry out a specific licensing of one of the two SPBs. In *Saccharomyces cerevisiae*, the two SPBs are functionally distinct and carry specific factors according to their fate[279].

4.2.3. The presence of sustained high M-Cdk1 activity does not prevent the recruitment of the MEN kinases to the SPBs

Interestingly, the presence of sustained high M-Cdk1 in wild-type cells does not prevent the recruitment Cdc15, Mob1 or Dbf2 at the SPBs, indicating that even under artificially high M-Cdk1 levels that overwhelm mitotic exit, M-Cdk1 has no significant effect on this critical co-localisation. The simplest explanation is that the FEAR release of Cdc14 in anaphase prevails over the M-Cdk1 activity on Cdc15, Mob1 and Dbf2 in the nucleoplasm. Once loaded at the SPBs, the observed Cdc14 accumulation at the dSPB (Yoshida, Asakawa and Toh-e, 2002 [141] and our figure 3.20-A), locally prevails over M-Cdk1. The non-phosphorylatable mutants in the bypass strain continue to load in metaphase as in an unperturbed cell cycle.

Despite high M-Cdk1 activity not preventing the recruitment of the MEN kinases, it does block the ability of Mob1-Dbf2 to translocate to the nucleolus to trigger the cytosolic release of Cdc14 that drives mitotic exit. The high M-Cdk1 activity abolishes as well the Mob1-Dbf2 localisation to the site of cell division at the bud neck, where it is required to trigger the contraction of the actomyosin ring and the ingression promotion complex. As expected, the MEN pathway is blocked by the presence of sustained high M-Cdk1 activity.

The effect is not rescued in the triple mutant bypass strain, consistent with an incomplete bypass, as discussed in point 4.2.7 below.

4.2.4. Cdc15 activity in bypass cells under sustained high M-Cdk1 activity

A conundrum raises when two pieces of experimental evidence are confronted: (1) The MEN kinases start loading to the SPBs in early anaphase (our results and Frenz *et al.*, 2000; Visintin and Amon, 2001; Yoshida and Toh-e, 2001; König, Maekawa and Schiebel, 2010; Campbell, Zhou and Amon, 2020 [171,172,184,215,216]), when the MEN pathway is inactive and, therefore, Cdc15 is unable to activate Mob1-Dbf2 by phosphorylation[174,280]. (2) Recruitment of Mob1-Dbf2 to the SPBs requires the previous phosphorylation of the scaffold protein Nud1 by Cdc15 to create a docking site for Mob1[173].

Our results further support that the two claims are true. In the bypass strain overexpressing the hyperstable *clb2ΔN* mutant cyclin, the three proteins are loaded at the SPBs (see for instance figures 3.18, 3.21 and 3.23), indicating that Cdc15 phosphorylates Nud1. And yet, Cdc15 neither phosphorylates Dbf2 (figure 3.22), activates the Mob1-Dbf2 kinase (figure 3.20), or promotes its release (fig 3.18, 3.23). The simplest testable explanation for such an apparent paradox would be that *MEN-inactive* Cdc15 is catalytically active towards Nud1 but unable to interact with Dbf2 until Cdc15 is *MEN-activated* by Tem1. In support of this model, the over-expression of Cdc15 activates MEN in the absence of Tem1 activation[157,281], as expected for low-affinity interactions that are rescued by mass-action.

4.2.5. Nuclear release of Cdc14 in the bypass strain

All cells analysed by time-lapse microscopy in the experiment summarised in figure 3.20 show a preferential Cdc14 accumulation at the dSPB. This is evident during the FEAR-mediated release in anaphase, continues after anaphase upon the MEN-triggered Cdc14 release to the cytosol, and only disappears when Cdc14 is re-sequestered at the two nucleoli upon mitotic exit.

We do not have experimental evidence on the role of such preferential localisation. However, the fact that the two SPBs are not structurally identical, provides a basis for the specific recruitment of Cdc14 at the dSPB. In *Saccharomyces cerevisiae,* the SPBs are duplicated conservatively, and the *old* and the *new* SPBs are functionally distinct and have opposite fates[279]. As a result, the *old* SPB always migrates to the

bud[282] and distinctively carries the MEN inhibitor Bfa1-Bub2[283]. As part of the different functionality of the two SPBs, in wild-type cells undergoing a normal mitosis the loading of Mob1 and Dbf2 to the dSPB is significantly delayed with respect to the mSPB (see figure 3.10). Most significantly, Cdk1 has been shown to localise to the future dSPB until entry into anaphase[184], which may explain the later recruitment of the MEN kinases to this SPB.

Further supporting such a possibility, the delayed recruitment of the Mob1 signal at the dSPB with respect to the mSPB is erased in the bypass strains (see point 4.2.2 above). To this respect, a recently published compartmental logical model predicts that the inhibitory effect of CDK would only occur if CDK is targeted to the dSPB, whereas the forcible localisation of CDK to the mSPB would lack functional effect[284]. In that case, the dSPB would require a higher load of Cdc14 phosphatase when the time to activate the MEN cascade arrives.

The presence of sustained high M-Cdk1 by over-expression of the hyperstable *clb2ΔN* cyclin in wild-type cells has no sensible effect on the Cdc14 release to the nucleus. This is reasonable, as the FEAR release does require M-Cdk1 activity. Of note, the high M-Cdk1 activity does not suppress the accumulation of Cdc14 at the dSPB either.

4.2.6. Cytosolic release and nucleolar re-sequestration of Cdc14 in the bypass strain

Another striking phenotype in the bypass strain is the time that short Cdc14 remains in the cytosol in a normal M phase. Despite the time of cytosolic release is not altered with respect to the time of nuclear release (figure 3.20), Cdc14 remains in the cytosol for only 10 min, compared with 25 min in wild-type cells. Such a reduced time seems to be sufficient -at least in these triple bypass cells- for a timely, efficient mitotic exit (see results in section 3.5.5.1 and discussion point 4.1).

One obvious conclusion is that a short pulse of cytosolic Cdc14, instead of a sustained presence, is sufficient to fully, and efficiently drive mitotic exit. One immediate question that arises from this observation is why do wild-type cells require Cdc14 for longer at the cytosol. Aside from the control of cytokinesis, an observation from our results is the consistently larger nucleolar size in bypass cells compared to

wild-type at all times of the cell cycle (figure 3.20-A), also seen in the comparison of the final CV average values upon re-sequestration (figure 3.20-C). Nucleolar dynamics is highly dependent on the action of nuclear and cytosolic Cdc14[285,286]. Future experiments should address whether there is an increase in the frequency of deleterious events occurring stochastically in individual cells, masked by the normal behaviour of the bulk of cells in the population.

A second question resulting from the shorter time of the cytosolic release of Cdc14 is about the mechanism that underlies the prompt re-sequestering to the nucleoli. The mechanism should be dependent on the absence of phosphorylation sequences in the Mob1-Dbf2, and perhaps the Cdc15, mutant proteins, which are the only independent variables.

The short duration of the cytosolic indicates a faster switch from pro-releasing to pro-re-sequestering activities. Two possible, not necessarily excluding, scenarios may be envisioned. One, a less efficient, more labile pro-release might occur if the non-phosphorylatable mutations in Mob1(A)-Dbf2(A) result in hypomorphic activity towards the Cdc14 cytosolic release (while sparing the role in cytokinesis at the site of cell division, which appears unaffected). Despite the nuclear-to-cytosolic release occurring timely in the bypass strain (figure 3.20-A), a significant Cdc14 signal remains in the nucleus at the time of cytosolic release. Further confirming the observation, the CV quantification shows that the value does not decrease to values equivalent to the homogeneity reached in the full release seen in wild-type cells (figure 3.20-C). The inefficient release evokes the phenotype of MEN mutants that led to the discovery of FEAR. In the absence of MEN activation[128,142,170] nuclear Cdc14 is soon re-sequestered to the nucleolus.

The second scenario contemplates a faster onset of the pro-recovery activity, a process that requires that the Cdc5, M-Cdk1, and Mob1-Dbf2 phosphorylation sites on Net1 are reverted[148–150,269], a process that requires APC^{Cdh1} activation [83,121]. Although we do not have experimental evidence either supporting or discarding earlier APC^{Cdh1} activity in the bypass strain (e.g. monitoring the time of elimination of Clb2 and stabilisation of Sic1), it is hard to reconcile with the shorter, less intense presence of Cdc14 in the cytosol.

4.2.7. The non-phosphorylatable mutant does not abrogate the block of mitotic exit by sustained high M-Cdk1 activity

The strain carrying the non-phosphorylatable *cdc15(A) mob1(A) dbf2(A)* mutations abrogates in part the M-Cdk1 negative control on mitotic exit in place in wild-type cells undergoing a normal cell cycle. The three proteins that constitute the two MEN kinases localise earlier at the SPBs, the activation platform for the MEN pathway, independently of the higher M-Cdk1 activity present in metaphase.

However, the bypass strain cannot override the block of cytosolic release by sustained high M-Cdk1 and does not undergo cytokinesis (figures 3.16, 3.17, 3.23).

Therefore, the *cdc15(A) mob1(A) dbf2(A)* strain is an incomplete M-Cdk1 bypass for mitotic exit. Based on the lack of Mob1-Dbf2 localisation at the site of cell division (figures 3.17 and 3.23), and the lack of Cdc15-dependent phosphorylation on Dbf2 (figure 3.22), our results point to an additional M-Cdk1 target upstream in the MEN pathway.

4.3. Are our results consistent with previous knowledge?

A recent report published at the time this thesis work was being carried out[171], showed that cells carrying non-phosphorylatable *cdc15(A) mob1(A)* alleles can undergo mitotic exit when arrested with a thermosensitive *cdc20-1* allele. However, the genotype does not constitute a real M-Cdk1 bypass. (1) Cells take a median of 5 hours to enter mitotic exit, as they require spindle elongation to occur for the SPOC to inactivate. (2) In the absence of APC^{Cdh1} activity, cells do not enter anaphase and the spindles do not elongate timely. (3) At long times, some non-canonical spindle elongation takes place. In some cells that is enough to push one of the SPBs into the bud compartment, inactivating the SPOC.

The authors suggest that, in their experimental setting, spindle elongation is likely to depend on the eventual activation of APC^{Cdh1}. We agree, as in our laboratory we have observed other adaptative responses in which cells overcome mitotic blocks through a delayed, non-canonical activation of APC^{Cdh1} (unpublished results). (4) In that case, APC^{Cdh1} is certain to also decrease the levels of mitotic cyclins, which may certainly result in the dephosphorylation of additional M-Cdk1 targets, including the one or more is missing in our bypass strain and definitely in their bypass strain. (5) While our experimental setting is stringent, as it is aimed at identifying the minimum M-Cdk1 bypass set without interference from related pathways, the reported experimental setting is permissive, as it is aimed at identifying involvement.

It is also of interest to compare the observations in Konig, Maekawa and Schiebel, 2010[184] with our results. The authors propose that Cdk1 negatively regulates the binding of Cdc15 to the mSPB. The conclusion is based on two main observations. First, an increase in the amount of Cdc15 at the SPBs between early anaphase, when due to APC^{Cdc20} activation M-Cdk1 activity is lower than in metaphase, and late anaphase, when M-Cdk1 activity is further reduced by FEAR-released Cdc14. Second, the comparison of the Cdc15-GFP signal at the SPBs in wild-type, td-cdc14 and Cdc15(A) cells. The Cdc15 signal decreases when Cdc14 is inactivated, and the decrease is rescued by the non-phosphorylatable Cdc15(A).

Our observation in part agrees with such a regulation. In wild-type cells undergoing a normal cell cycle, we detect MEN kinases at the SPBs only upon entry in anaphase, and Mob1-Dbf2, first detected at the mSPB, is later loaded at the dSPB as well. In addition, the non-phosphorylatable Cdc15(A), Mob1(A) and Dbf2(2) mutants load before anaphase, when M-Cdk1activity is highest.

However, the over-expression of the *clb2ΔN* allele does not prevent the normal loading of the MEN kinases at the SPBs. We therefore propose that the SPBs provide a specific environment that results in a specific balance of M-Cdk1 and Cdc14 activities with respect to the general balance. In support of the model, (1) we (figure 3.20-A), and others[141] (observe that the early anaphase release of Cdc14 results in accumulation of the phosphatase at the dSPB). (2) When cells are released from the metaphase arrest, Dbf2 western blot analysis shows that the slowest electrophoretic mobility bands decrease in intensity, when cells enter anaphase in the presence of

stable high M-Cdk1 activity (figure 3.22) that prevails over Cdc14 in mitotic exit (figure 3.5).

König, Maekawa and Schiebel, 2010 also explored the phenotype of the Cdc15(A) Mob1(A) non-phosphorylatable alleles. Double mutant cells showed no phenotype. Only when combined with the deletion of the MEN regulator Bub2, the strains showed premature Cdc14 release, and defects in nucleolar division but did not undergo cytokinesis. In any case, the approach did not address the full control of MEN by M-Cdk1.

4.4. In summary

The *cdc15(A) mob1(A) dbf2(A)* bypass strain overrides to some extent the negative regulation by M-Cdk1 activity. The MEN kinases load earlier at the SPBs, the activation platform for the MEN pathway, at a time in which M-Cdk1 activity is higher.

However, the bypass strain does not abrogate the block of mitotic exit by sustained high M-Cdk1. Therefore, our results indicate that M-Cdk1 targets at least an additional substrate to block premature mitotic exit.

Based on the lack of release of active Mob1-Dbf2 from the SPBs, and given that Cdc15(A) and Mob1(A)-Dbf2(A) cannot be directly inhibited by M-Cdk1 phosphorylation, our results place the substrate upstream in the MEN pathway.

Tem1 and Lte1 are both reasonable candidates. Tem1, a small 27 kDa RAS-like GTPase, is required for Cdc15 activation. It contains 3 potential Cdk1 phosphorylation sequences, one of them, Serine 240, has been reported to be phosphorylated by Cdk1 in a global analysis *in vivo*[257], although no reports have been published on its possible biological significance.

Likewise, the MEN activator Lte1, a large 163 kDa protein at the bud cortex, contains multiple Cdk1 consensus phosphorylation sequences, two of them, Serine 212 and

Threonine 614, were reported to be phosphorylated by Cdk1 in the same global analysis *in vivo*, but again no information about a possible role has been published.

5. Conclusions

1. We designed a robust, stringent experimental system, that makes possible the identification of the minimal set of substrates through which M-Cdk1 kinase blocks premature mitotic exit.

2. Cells under sustained high M-Cdk1 by over-expression of the hyperstable *clb2ΔN* cyclin arrest after anaphase completion and M-Cdk1 prevails over Cdc14 activity on several shared substrates used as biochemical markers. The elimination of Clb2ΔN allows cells to resume the mitotic division and proliferate, indicating that the sustained high M-Cdk1 activity does not damage the ability of the cell to undergo mitotic exit.

3. At the time of arrest, the control of mitotic exit by the SPOC is not active anymore, and the block of mitotic therefore depends solely on M-Cdk1.

4. We identified three strong candidates to be part of the essential substrates that M-Cdk1 targets to block mitotic exit: the MEN kinases Cdc15 and Mob1-Dbf2.

5. We generated a strain carrying non-phosphorylatable alleles of the three proteins and the inducible *clb2ΔN* cyclin. In the absence of *clb2ΔN* induction, the fitness of the strain is undistinguishable from wild-type cells.

6. In an unperturbed cell cycle, the bypass strain shows premature and persistent localisation at the SPBs, the site of MEN activation. This observation indicates that in wild-type cells M-Cdk1 limits the assembly of the MEN kinases at the site of activation. This regulation constitutes an additional control layer in the prevention of premature mitotic exit.

7. However, the over-expression of *clb2ΔN* does not abolish the localisation of Cdc15, Mob1, and Dbf2 at the SPBs in wild-type cells, suggesting that the SPBs provide a specific microenvironment.

8. The accumulation of Cdc14 at the dSPB during the anaphase release, coincident in time with the loading of the three proteins, further supports this model. In addition, the enriched Cdc14 signal at the dSPB is not abolished by sustained high M-Cdk1 upon over-expression of *clb2ΔN.*

9. Mob1-Dbf2 is loaded at the SPBs in cells under sustained high M-Cdk1 activity, indicating that Cdc15 phosphorylates Nud1. And yet, Cdc15 fails to phosphorylate Dbf2 to activate and release the Mob1-Dbf2 kinase. We therefore propose two conformations for Cdc15. A *MEN-inactive* form, catalytically active towards Nud1 but unable to interact with Dbf2; and a *MEN-activated* form, able to interact and phosphorylate Dbf2.

10. In an unperturbed cell cycle, the bypass strain shows normal anaphase release of Cdc14 to the nucleus, but a dramatically shorter presence of Cdc14 in the cytosol, essential for mitotic exit.

11. The short pulse of cytosolic Cdc14 is notwithstanding sufficient for timely cytokinesis and mitotic exit in the bypass cells.

12. Therefore, the longer time of Cdc14 in the cytosol in wild-type cells is likely required for other Cdc14 dependent functions, such as proper nucleolar metabolism. To that respect, the bypass cells display larger nucleoli.

13. Despite the apparent hypomorphic activity of Mob1(A)-Dbf2(A) on the Cdc14 cytosolic release, the behaviour of the kinase at the site of cell division and the duration is equivalent to the wild-type kinase.

14. The normal time of onset of cytokinesis after anaphase completion, the duration of cytokinesis, and the time from the end of anaphase until the cells are separated by independent walls, indicate that the M-Cdk1 control on Cdc15 Mob1-Dbf2 is irrelevant once MEN activates and active Mob1-Dbf2 kinase is released.

15. The presence of sustained high M-Cdk1 does not affect the FEAR-dependent Cdc14 nuclear release, but completely abolishes the MEN dependent

cytosolic release required for mitotic exit. The block is not rescued in the bypass strain, indicating the existence of at least one more critical M-Cdk1 substrate.

16. Given that Mob1-Dbf2 is not released from the SPBs in the bypass strain under sustained high M-Cdk1 levels, and that Phos-tag electrophoretic analysis shows no phosphorylation in Dbf2(A), as would be expected in the Dbf2 activation by Cdc15, we propose that M-Cdk1 still blocks mitotic exit targeting a substrate upstream in the MEN pathway.

6. Bibliography

1. Mitchison, J. M. & Creanor, J. Further measurements of DNA synthesis and enzyme potential during cell cycle of fission yeast Schizosaccharomyces pombe. *Exp Cell Res* **69**, 244–247 (1971).

2. Guarente, L. UASs and enhancers: Common mechanism of transcriptional activation in yeast and mammals. *Cell* **52**, 303–305 (1988).

3. Goffeau, A. *et al.* Life with 6000 Genes. *Science (1979)* **274**, 546–567 (1996).

4. Guarente, L., Yocum, R. R. & Gifford, P. A GAL10-CYC1 hybrid yeast promoter identifies the GAL4 regulatory region as an upstream site. *Proc Natl Acad Sci U S A* **79**, 7410–7414 (1982).

5. Gierest, H., Thao, N. N. & Surdin-Kerjan, Y. Transcriptional regulation of the MET3 gene of Saccharomyces cerevisiae. *Gene* **34**, 269–281 (1985).

6. Black, S., Andrews, P. D., Sneddon, A. A. & Stark, M. J. R. A regulated MET3-GLC7 gene fusion provides evidence of a mitotic role for Saccharomyces cerevisiae protein phosphatase 1. *Yeast* **11**, 747–759 (1995).

7. Cahill, D. P., Kinzler, K. W., Vogelstein, B. & Lengauer, C. Genetic instability and darwinian selection in tumours. *Trends Cell Biol* **9**, M57–M60 (1999).

8. Hanahan, D. & Weinberg, R. A. Hallmarks of cancer: The next generation. *Cell* **144**, 646–674 (2011).

9. Reed, S. I. Ratchets and clocks: The cell cycle, ubiquitylation and protein turnover. *Nat Rev Mol Cell Biol* **4**, 855–864 (2003).

10. Evans, T., Rosenthal, E. T., Youngblom, J., Distel, D. & Hunt, T. Cyclin: A Protein Specified by Maternal mRNA in Sea Urchin Eggs That Is Destroyed at Each Cleavage Division. *Cell* **33**, 389–396 (1983).

11. Pardee, A. B. A restriction point for control of normal animal cell proliferation. *Proc Natl Acad Sci U S A* **71**, 1286–1290 (1974).

12. Haase, S. B. & Reed, S. I. Evidence that a free-running oscillator drives G1 events in the budding yeast cell cycle. *Nature 1999 401:6751* **401**, 394–397 (1999).

13. Cross, F. R., Buchler, N. E. & Skotheim, J. M. Evolution of networks and sequences in eukaryotic cell cycle control. *Philos Trans R Soc Lond B Biol Sci* **366**, 3532–3544 (2011).

14. Gilberto, S. & Peter, M. Dynamic ubiquitin signaling in cell cycle regulation. *Journal of Cell Biology* **216**, 2259–2271 (2017).

15. Bassermann, F., Eichner, R. & Pagano, M. The ubiquitin proteasome system – Implications for cell cycle control and the targeted treatment of cancer. *Biochim Biophys Acta* **1843**, 150–162 (2014).

16. Hartwell, L. H. & Weinert, T. A. Checkpoints: Controls That Ensure the Order of Cell Cycle Events. *Science (1979)* **246**, 629–634 (1989).

17. O Morgan, D. *Cell Cycle: Principles of Control*. *Oxford University Press* (2007).

18. Hartwell, L. H., Culotti, J. & Reid, B. Genetic control of the cell-division cycle in yeast. I. Detection of mutants. *Proc Natl Acad Sci U S A* **66**, 352–359 (1970).

19. Nurse, P. Genetic control of cell size at cell division in yeast. *Nature* **256**, 547–551 (1975).

20. Meyerson, M., Faha, B., Su, L. K., Harlow, E. & Tsai, L. H. The cyclin-dependent kinase family. *Cold Spring Harb Symp Quant Biol* **56**, 177–186 (1991).

21. Malumbres, M. Cyclin-dependent kinases. *Genome Biol* **15**, 1–10 (2014).

22. Hartwell, L. H., Mortimer, R. K., Culotti, J. & Culotti, M. Genetic Control of the Cell Division Cycle in Yeast: V. Genetic Analysis of cdc Mutants. *Genetics* **74**, 267–286 (1973).

23. de Lichtenberg, U., Jensen, L. J., Brunak, S. & Bork, P. Dynamic complex formation during the yeast cell cycle. *Science (1979)* **307**, 724–727 (2005).

24. Jallepalli, P. v. & Kelly, T. J. Cyclin-dependent kinase and initiation at eukaryotic origins: a replication switch? *Curr Opin Cell Biol* **9**, 358–363 (1997).

25. Songyang, Z. *et al.* Use of an oriented peptide library to determine the optimal substrates of protein kinases. *Current Biology* **4**, 973–982 (1994).

26. Palou, R. *et al.* G1 cyclin driven DNA replication. *Cell Cycle* **14**, 3842–3850 (2015).

27. Swaffer, M. P., Jones, A. W., Flynn, H. R., Snijders, A. P. & Nurse, P. CDK Substrate Phosphorylation and Ordering the Cell Cycle. *Cell* **167**, 1750-1761.e16 (2016).

28. Coudreuse, D. & Nurse, P. Driving the cell cycle with a minimal CDK control network. *Nature* **468**, 1074–1080 (2010).

29. Fisher, D. L. & Nurse, P. A single fission yeast mitotic cyclin B p34cdc2 kinase promotes both S-phase and mitosis in the absence of G1 cyclins. *EMBO J* **15**, 850–860 (1996).

30. Stern, B. & Nurse, P. A quantitative model for the cdc2 control of S phase and mitosis in fission yeast. *Trends in Genetics* **12**, 345–350 (1996).

31. Kõivomägi, M. *et al.* Dynamics of Cdk1 substrate specificity during the cell cycle. *Mol Cell* **42**, 610–623 (2011).

32. Morgan, D. O. Principles of CDK regulation. *Nature 1995 374:6518* **374**, 131–134 (1995).

33. Pines, J. Cyclins and cyclin-dependent kinases: a biochemical view. *Biochemical Journal* **308**, 697 (1995).

34. Tyers, M., Tokiwa, G. & Futcher, B. Comparison of the Saccharomyces cerevisiae G1 cyclins: Cln3 may be an upstream activator of Cln1, Cln2 and other cyclins. *EMBO J* **12**, 1955–1968 (1993).

35. Yahya, G., Parisi, E., Flores, A., Gallego, C. & Aldea, M. A Whi7-Anchored Loop Controls the G1 Cdk-Cyclin Complex at Start. *Mol Cell* **53**, 115–126 (2014).

36. Vergés, E., Colomina, N., Garí, E., Gallego, C. & Aldea, M. Cyclin Cln3 Is Retained at the ER and Released by the J Chaperone Ydj1 in Late G1 to Trigger Cell Cycle Entry. *Mol Cell* **26**, 649–662 (2007).

37. Dirick, L., Böhm, T. & Nasmyth, K. Roles and regulation of Cln-Cdc28 kinases at the start of the cell cycle of Saccharomyces cerevisiae. *EMBO J* **14**, 4803 (1995).

38. Epstein, C. B. & Cross, F. R. CLB5: a novel B cyclin from budding yeast with a role in S phase. *Genes Dev* **6**, 1695–1706 (1992).

39. McIntosh, E. M. MCB elements and the regulation of DNA replication genes in yeast. *Curr Genet* **24**, 185–192 (1993).

40. Dirick, L., Böhm, T. & Nasmyth, K. Roles and regulation of Cln-Cdc28 kinases at the start of the cell cycle of Saccharomyces cerevisiae. *EMBO J* **14**, 4803 (1995).

41. Schwob, E. & Nasmyth, K. CLB5 and CLB6, a new pair of B cyclins involved in DNA replication in Saccharomyces cerevisiae. *Genes Dev* **7**, 1160–1175 (1993).

42. Fitch, I. *et al.* Characterization of four B-type cyclin genes of the budding yeast Saccharomyces cerevisiae. *Mol Biol Cell* **3**, 805–818 (1992).

43. Richardson, H., Lew, D. J., Henze, M., Sugimoto, K. & Reed, S. I. Cyclin-B homologs in Saccharomyces cerevisiae function in S phase and in G2. *Genes Dev* **6**, 2021–2034 (1992).

44. Spellman, P. T. *et al.* Comprehensive Identification of Cell Cycle–regulated Genes of the Yeast Saccharomyces cerevisiae by Microarray Hybridization. *Mol Biol Cell* **9**, 3273 (1998).

45. Cho, R. J. *et al.* A genome-wide transcriptional analysis of the mitotic cell cycle. *Mol Cell* **2**, 65–73 (1998).

46. Ghiara, J. B. *et al.* A cyclin B homolog in S. cerevisiae: Chronic activation of the Cdc28 protein kinase by cyclin prevents exit from mitosis. *Cell* **65**, 163–174 (1991).

47. Surana, U. *et al.* The role of CDC28 and cyclins during mitosis in the budding yeast S. cerevisiae. *Cell* **65**, 145–161 (1991).

48. Wäsch, R. & Cross, F. R. APC-dependent proteolysis of the mitotic cyclin Clb2 is essential for mitotic exit. *Nature 2002 418:6897* **418**, 556–562 (2002).

49. Zeng, F. & Garcia Quintana, D. Novel Modes of Regulation of Cyclin Dependent Kinase Cdk1. *TDX (Tesis Doctorals en Xarxa)* (2014).

50. Thuret, J. Y., Valay, J. G., Faye, G. & Mann, C. Civ1 (CAK in vivo), a novel Cdk-activating kinase. *Cell* **86**, 565–576 (1996).

51. Ross, K. E., Kaldis, P. & Solomon, M. J. Activating phosphorylation of the Saccharomyces cerevisiae cyclin-dependent kinase, cdc28p, precedes cyclin binding. *Mol Biol Cell* **11**, 1597–1609 (2000).

52. Espinoza, F. H., Farrell, A., Erdjument-Bromage, H., Tempst, P. & Morgan, D. O. A Cyclin-Dependent Kinase-Activating Kinase (CAK) in Budding Yeast Unrelated to Vertebrate CAK. *Science (1979)* **273**, 1714–1717 (1996).

53. Schwob, E., Böhm, T., Mendenhall, M. D. & Nasmyth, K. The B-type cyclin kinase inhibitor p40SIC1 controls the G1 to S transition in S. cerevisiae. *Cell* **79**, 233–244 (1994).

54. Epstein, C. B. & Cross, F. R. CLB5: a novel B cyclin from budding yeast with a role in S phase. *Genes Dev* **6**, 1695–1706 (1992).

55. Schwob, E. & Nasmyth, K. CLB5 and CLB6, a new pair of B cyclins involved in DNA replication in Saccharomyces cerevisiae. *Genes Dev* **7**, 1160–1175 (1993).

56. Palou, G. *et al.* Three Different Pathways Prevent Chromosome Segregation in the Presence of DNA Damage or Replication Stress in Budding Yeast. *PLoS Genet* **11**, (2015).

57. Booher, R. N., Deshales, R. J. & Kirschner, M. W. Properties of Saccharomyces cerevisiae wee1 and its differential regulation of p34CDC28 in response to G1 and G2 cyclins. *EMBO J* **12**, 3417 (1993).

58. Dirick, L., Böhm, T. & Nasmyth, K. Roles and regulation of Cln-Cdc28 kinases at the start of the cell cycle of Saccharomyces cerevisiae. *EMBO Journal* **14**, 4803–4813 (1995).

59. Tyers, M., Tokiwa, G. & Futcher, B. Comparison of the Saccharomyces cerevisiae G1 cyclins: Cln3 may be an upstream activator of Cln1, Cln2 and other cyclins. *EMBO J* **12**, 1955–1968 (1993).

60. Stuart, D. & Wittenberg, C. CLN3, not positive feedback, determines the timing of CLN2 transcription in cycling cells. *Genes Dev* **9**, 2780–2794 (1995).

61. Parviz, F., Hall, D. D., Markwardt, D. D. & Heideman, W. Transcriptional Regulation of CLN3 Expression by Glucose in Saccharomyces cerevisiae. *J Bacteriol* **180**, 4508 (1998).

62. McInerny, C. J., Partridge, J. F., Mikesell, G. E., Creemer, D. P. & Breeden, L. L. A novel Mcm1-dependent element in the SWI4, CLN3, CDC6, and CDC47 promoters activates M/G1-specific transcription. *Genes Dev* **11**, 1277–1288 (1997).

63. Nash, R. S., Volpe, T. & Futcher, B. Isolation and characterization of WHI3, a size-control gene of Saccharomyces cerevisiae. *Genetics* **157**, 1469–1480 (2001).

64. Wang, H., Garí, E., Vergés, E., Gallego, C. & Aldea, M. Recruitment of Cdc28 by Whi3 restricts nuclear accumulation of the G1 cyclin-Cdk complex to late G1. *EMBO J* **23**, 180–190 (2004).

65. Garí, E. *et al.* Whi3 binds the mRNA of the G1 cyclin CLN3 to modulate cell fate in budding yeast. *Genes Dev* **15**, 2803–2808 (2001).

66. Costanzo, M. *et al.* CDK activity antagonizes Whi5, an inhibitor of G1/S transcription in yeast. *Cell* **117**, 899–913 (2004).

67. de Bruin, R. A. M., McDonald, W. H., Kalashnikova, T. I., Yates, J. & Wittenberg, C. Cln3 activates G1-specific transcription via phosphorylation of the SBF bound repressor Whi5. *Cell* **117**, 887–898 (2004).

68. Iyer, V. R. *et al.* Genomic binding sites of the yeast cell-cycle transcription factors SBF and MBF. *Nature 2001 409:6819* **409**, 533–538 (2001).

69. Koch, C. & Nasmyth, K. Cell cycle regulated transcription in yeast. *Curr Opin Cell Biol* **6**, 451–459 (1994).

70. Quilis, I. & Igual, J. C. A comparative study of the degradation of yeast cyclins Cln1 and Cln2. *FEBS Open Bio* **7**, 74–87 (2017).

71. Lanker, S., Valdivieso, M. H. & Wittenberg, C. Rapid Degradation of the G1 Cyclin Cln2 Induced by CDK-Dependent Phosphorylation. *Science (1979)* **271**, 1597–1601 (1996).

72. Johnston, L. H. & Lowndes, N. F. Cell cycle control of DNA synthesis in budding yeast. *Nucleic Acids Res* **20**, 2403–2410 (1992).

73. Koch, C., Moll, T., Neuberg, M., Ahorn, H. & Nasmyth, K. A role for the transcription factors Mbp1 and Swi4 in progression from G1 to S phase. *Science* **261**, 1551–1557 (1993).

74. Jackson, L. P., Reed, S. I. & Haase, S. B. Distinct Mechanisms Control the Stability of the Related S-Phase Cyclins Clb5 and Clb6. *Mol Cell Biol* **26**, 2456–2466 (2006).

75. Shirayama, M., Tóth, A., Gálová, M. & Nasmyth, K. APC(Cdc20) promotes exit from mitosis by destroying the anaphase inhibitor Pds1 and cyclin Clb5. *Nature* **402**, 203–207 (1999).

76. Irniger, S. & Nasmyth, K. The anaphase-promoting complex is required in G1 arrested yeast cells to inhibit B-type cyclin accumulation and to prevent uncontrolled entry into S-phase. *J Cell Sci* **110 (Pt 13)**, 1523–1531 (1997).

77. Koranda, M., Schleiffer, A., Endler, L. & Ammerer, G. Forkhead-like transcription factors recruit Ndd1 to the chromatin of G2/M-specific promoters. *Nature* **406**, 94–98 (2000).

78. Pecani, K. & Cross, F. R. Degradation of the Mitotic Cyclin Clb3 Is not Required for Mitotic Exit but Is Necessary for G1 Cyclin Control of the Succeeding Cell Cycle. *Genetics* **204**, 1479 (2016).

79. Yeong, F. M., Lim, H. H., Wang, Y. & Surana, U. Early Expressed Clb Proteins Allow Accumulation of Mitotic Cyclin by Inactivating Proteolytic Machinery during S Phase. *Mol Cell Biol* **21**, 5071 (2001).

80. Zachariae, W., Schwab, M., Nasmyth, K. & Seufert, W. Control of cyclin ubiquitination by CDK-regulated binding of Hct1 to the anaphase promoting complex. *Science* **282**, 1721–1724 (1998).

81. Hendrickson, C., Meyn, M. A., Morabito, L. & Holloway, S. L. The KEN box regulates Clb2 proteolysis in G1 and at the metaphase-to-anaphase transition. *Current Biology* **11**, 1781–1787 (2001).

82. Hyun, S. Y., Sarantuya, B., Lee, H. J. & Jang, Y. J. APC/CCdh1-dependent degradation of Cdc20 requires a phosphorylation on CRY-box by Polo-like kinase-1 during somatic cell cycle. *Biochem Biophys Res Commun* **436**, 12–18 (2013).

83. Visintin, R., Prinz, S. & Amon, A. CDC20 and CDH1: A family of substrate-specific activators of APC- dependent proteolysis. *Science (1979)* **278**, 460–463 (1997).

84. Sudakin, V. *et al.* The cyclosome, a large complex containing cyclin-selective ubiquitin ligase activity, targets cyclins for destruction at the end of mitosis. *Mol Biol Cell* **6**, 185 (1995).

85. Burton, J. L. & Solomon, M. J. D box and KEN box motifs in budding yeast Hsl1p are required for APC-mediated degradation and direct binding to Cdc20p and Cdh1p. *Genes Dev* **15**, 2381 (2001).

86. Amon, A. A decade of Cdc14 – a personal perspective Delivered on 9 July 2007 at the 32nd FEBS Congress in Vienna, Austria. *FEBS J* **275**, 5774–5784 (2008).

87. Pfleger, C. M. & Kirschner, M. W. The KEN box: an APC recognition signal distinct from the D box targeted by Cdh1. *Genes Dev* **14**, 655–665 (2000).

88. Surana, U. *et al.* Destruction of the CDC28/CLB mitotic kinase is not required for the metaphase to anaphase transition in budding yeast. *EMBO J* **12**, 1969–1978 (1993).

89. Wäsch, R. & Cross, F. R. APC-dependent proteolysis of the mitotic cyclin Clb2 is essential for mitotic exit. *Nature* **418**, 556–562 (2002).

90. Orlando, D. A. *et al.* Global control of cell-cycle transcription by coupled CDK and network oscillators. *Nature* **453**, 944–947 (2008).

91. Nasmyth, K. & Dirick, L. The role of SWI4 and SWI6 in the activity of G1 cyclins in yeast. *Cell* **66**, 995–1013 (1991).

92. Primig, M., Sockanathan, S., Auer, H. & Nasmyth, K. Anatomy of a transcription factor important for the start of the cell cycle in Saccharomyces cerevisiae. *Nature* **358**, 593–597 (1992).

93. Ogas, J., Andrews, B. J. & Herskowitz, I. Transcriptional activation of CLN1, CLN2, and a putative new G1 cyclin (HCS26) by SWI4, a positive regulator of G1-specific transcription. *Cell* **66**, 1015–1026 (1991).

94. Spellman, P. T. *et al.* Comprehensive Identification of Cell Cycle–regulated Genes of the Yeast Saccharomyces cerevisiae by Microarray Hybridization. *Mol Biol Cell* **9**, 3273 (1998).

95. Pramila, T., Wu, W., Miles, S., Noble, W. S. & Breeden, L. L. The Forkhead transcription factor Hcm1 regulates chromosome segregation genes and fills the S-phase gap in the transcriptional circuitry of the cell cycle. *Genes Dev* **20**, 2266–2278 (2006).

96. Cho, R. J. *et al.* A genome-wide transcriptional analysis of the mitotic cell cycle. *Mol Cell* **2**, 65–73 (1998).

97. Toyn, J. H., Johnson, A. L., Donovan, J. D., Toone, W. M. & Johnston, L. H. The Swi5 transcription factor of Saccharomyces cerevisiae has a role in exit from mitosis through induction of the cdk-inhibitor Sic1 in telophase. *Genetics* **145**, 85–96 (1997).

98. Zhou, P. & Howley, P. M. Ubiquitination and degradation of the substrate recognition subunits of SCF ubiquitin-protein ligases. *Mol Cell* **2**, 571–580 (1998).

99. Feldman, R. M. R., Correll, C. C., Kaplan, K. B. & Deshaies, R. J. A complex of Cdc4p, Skp1p, and Cdc53p/cullin catalyzes ubiquitination of the phosphorylated CDK inhibitor Sic1p. *Cell* **91**, 221–230 (1997).

100. Rudner, A. D. & Murray, A. W. Phosphorylation by Cdc28 activates the Cdc20-dependent activity of the anaphase-promoting complex. *J Cell Biol* **149**, 1377–1390 (2000).

101. Alberts, B. *et al.* An Overview of M Phase. (2002).

102. Gupta, A., Evans, R. K., Koch, L. B., Littleton, A. J. & Biggins, S. Purification of kinetochores from the budding yeast Saccharomyces cerevisiae. *Methods Cell Biol* **144**, 349 (2018).

103. Nannas, N. J., O'Toole, E. T., Winey, M. & Murray, A. W. Chromosomal attachments set length and microtubule number in the Saccharomyces cerevisiae mitotic spindle. *Mol Biol Cell* **25**, 4034 (2014).

104. Uhlmann, F., Lottspelch, F. & Nasmyth, K. Sister-chromatid separation at anaphase onset is promoted by cleavage of the cohesin subunit Scc1. *Nature* **400**, 37–42 (1999).

105. Ciosk, R. *et al.* An ESP1/PDS1 complex regulates loss of sister chromatid cohesion at the metaphase to anaphase transition in yeast. *Cell* **93**, 1067–1076 (1998).

106. Sudakin, V., Chan, G. K. T. & Yen, T. J. Checkpoint inhibition of the APC/C in HeLa cells is mediated by a complex of BUBR1, BUB3, CDC20, and MAD2. *J Cell Biol* **154**, 925 (2001).

107. Ditchfield, C. *et al.* Aurora B couples chromosome alignment with anaphase by targeting BubR1, Mad2, and Cenp-E to kinetochores. *J Cell Biol* **161**, 267–280 (2003).

108. Chung, E. & Chen, R. H. Spindle Checkpoint Requires Mad1-bound and Mad1-free Mad2. *Mol Biol Cell* **13**, 1501 (2002).

109. Weiss, E. & Winey, M. The Saccharomyces cerevisiae spindle pole body duplication gene MPS1 is part of a mitotic checkpoint. *J Cell Biol* **132**, 111–123 (1996).

110. Morrow, C. J. *et al.* Bub1 and aurora B cooperate to maintain BubR1-mediated inhibition of APC/CCdc20. *J Cell Sci* **118**, 3639–3652 (2005).

111. Musacchio, A. & Salmon, E. D. The spindle-assembly checkpoint in space and time. *Nature Reviews Molecular Cell Biology 2007 8:5* **8**, 379–393 (2007).

112. Rieder, C. L., Cole, R. W., Khodjakov, A. & Sluder, G. The checkpoint delaying anaphase in response to chromosome monoorientation is mediated by an inhibitory signal produced by unattached kinetochores. *J Cell Biol* **130**, 941–948 (1995).

113. Nicklas, R. B. How Cells Get the Right Chromosomes. *Science (1979)* **275**, (1997).

114. Nicklas, R. B., Waters, J. C., Salmon, E. D. & Ward, S. C. Checkpoint signals in grasshopper meiosis are sensitive to microtubule attachment, but tension is still essential. *J Cell Sci* **114**, 4173–4183 (2001).

115. Hauf, S. *et al.* The small molecule Hesperadin reveals a role for Aurora B in correcting kinetochore-microtubule attachment and in maintaining the spindle assembly checkpoint. *J Cell Biol* **161**, 281–294 (2003).

116. Tanaka, T. U. *et al.* Evidence that the Ipl1-Sli15 (Aurora Kinase-INCENP) complex promotes chromosome bi-orientation by altering kinetochore-spindle pole connections. *Cell* **108**, 317–329 (2002).

117. Biggins, S. & Murray, A. W. The budding yeast protein kinase Ipl1/Aurora allows the absence of tension to activate the spindle checkpoint. *Genes Dev* **15**, 3118–3129 (2001).

118. Cohen-Fix, O., Peters, J. M., Kirschner, M. W. & Koshland, D. Anaphase initiation in Saccharomyces cerevisiae is controlled by the APC-dependent degradation of the anaphase inhibitor Pds1p. *Genes Dev* **10**, 3081–3093 (1996).

119. Prinz, S., Hwang, E. S., Visintin, R. & Amon, A. The regulation of Cdc20 proteolysis reveals a role for the APC components Cdc23 and Cdc27 during S phase and early mitosis. *Current Biology* **8**, 750–760 (1998).

120. Jaspersen, S. L., Charles, J. F. & Morgan, D. O. Inhibitory phosphorylation of the APC regulator Hct1 is controlled by the kinase Cdc28 and the phosphatase Cdc14. *Current Biology* **9**, 227–236 (1999).

121. Visintin, C. *et al.* APC/C-Cdh1-mediated degradation of the Polo kinase Cdc5 promotes the return of Cdc14 into the nucleolus. *Genes Dev* **22**, 79–90 (2008).

122. Jensen, S., Segal, M., Clarke, D. J. & Reed, S. I. A Novel Role of the Budding Yeast Separin Esp1 in Anaphase Spindle ElongationEvidence That Proper Spindle Association of Esp1 Is Regulated by Pds1. *Journal of Cell Biology* **152**, 27–40 (2001).

123. Sullivan, M., Lehane, C. & Uhlmann, F. Orchestrating anaphase and mitotic exit: Separase cleavage and localization of Slk19. *Nat Cell Biol* **3**, 771–777 (2001).

124. Zeng, X. *et al.* Slk19p is a centromere protein that functions to stabilize mitotic spindles. *J Cell Biol* **146**, 415–425 (1999).

125. Havens, K. A., Gardner, M. K., Kamieniecki, R. J., Dresser, M. E. & Dawson, D. S. Slk19p of Saccharomyces cerevisiae Regulates Anaphase Spindle

Dynamics Through Two Independent Mechanisms. *Genetics* **186**, 1247 (2010).

126. Zhang, T., Lim, H. H., Cheng, C. S. & Surana, U. Deficiency of centromere-associated protein Slk19 causes premature nuclear migration and loss of centromeric elasticity. *J Cell Sci* **119**, 519–531 (2006).

127. Richmond, D., Rizkallah, R., Liang, F., Hurt, M. M. & Wang, Y. Slk19 clusters kinetochores and facilitates chromosome bipolar attachment. *Mol Biol Cell* **24**, 566–577 (2013).

128. Stegmeier, F., Visintin, R. & Amon, A. Separase, polo kinase, the kinetochore protein Slk19, and Spo12 function in a network that controls Cdc14 localization during early anaphase. *Cell* **108**, 207–220 (2002).

129. Queralt, E., Lehane, C., Novak, B. & Uhlmann, F. Downregulation of PP2ACdc55 Phosphatase by Separase Initiates Mitotic Exit in Budding Yeast. *Cell* **125**, 719–732 (2006).

130. Agarwal, R. & Cohen-Fix, O. Phosphorylation of the mitotic regulator Pds1/securin by Cdc28 is required for efficient nuclear localization of Esp1/separase. *Genes Dev* **16**, 1371–1382 (2002).

131. Lianga, N. *et al.* Cdk1 phosphorylation of Esp1/Separase functions with PP2A and Slk19 to regulate pericentric Cohesin and anaphase onset. *PLoS Genet* **14**, (2018).

132. Visintin, R. *et al.* The phosphatase Cdc14 triggers mitotic exit by reversal of Cdk-dependent phosphorylation. *Mol Cell* **2**, 709–718 (1998).

133. Rock, J. M. & Amon, A. The FEAR network. *Current Biology* **19**, R1063–R1068 (2009).

134. Baro, B., Queralt, E. & Monje-Casas, F. Regulation of Mitotic Exit in Saccharomyces cerevisiae. *Methods Mol Biol* **1505**, 3–17 (2017).

135. Shou, W. *et al.* Cdc5 influences phosphorylation of Net1 and disassembly of the RENT complex. *BMC Mol Biol* **3**, (2002).

136. Azzam, R. *et al.* Phosphorylation by cyclin B-Cdk underlies release of mitotic exit activator Cdc14 from the nucleolus. *Science* **305**, 516–519 (2004).

137. Ptacek, J. *et al.* Global analysis of protein phosphorylation in yeast. *Nature* **438**, 679–684 (2005).

138. Queralt, E., Lehane, C., Novak, B. & Uhlmann, F. Downregulation of PP2A(Cdc55) phosphatase by separase initiates mitotic exit in budding yeast. *Cell* **125**, 719–732 (2006).

139. Queralt, E. & Uhlmann, F. Separase cooperates with Zds1 and Zds2 to activate Cdc14 phosphatase in early anaphase. *J Cell Biol* **182**, 873–883 (2008).

140. Rossio, V. & Yoshida, S. Spatial regulation of Cdc55-PP2A by Zds1/Zds2 controls mitotic entry and mitotic exit in budding yeast. *Journal of Cell Biology* **193**, 445–454 (2011).

141. Yoshida, S., Asakawa, K. & Toh-e, A. Mitotic Exit Network controls the localization of Cdc14 to the Spindle Pole Body in Saccharomyces cerevisiae. *Current Biology* **12**, 944–950 (2002).

142. Yellman, C. M. & Roeder, G. S. Cdc14 Early Anaphase Release, FEAR, Is Limited to the Nucleus and Dispensable for Efficient Mitotic Exit. *PLoS One* **10**, (2015).

143. Holt, L. J., Krutchinsky, A. N. & Morgan, D. O. Positive feedback sharpens the anaphase switch. *Nature* **454**, 353–357 (2008).

144. Hwang, W. W. & Madhani, H. D. Nonredundant requirement for multiple histone modifications for the early anaphase release of the mitotic exit regulator Cdc14 from nucleolar chromatin. *PLoS Genet* **5**, (2009).

145. Khmelinskii, A., Lawrence, C., Roostalu, J. & Schiebel, E. Cdc14-regulated midzone assembly controls anaphase B. *J Cell Biol* **177**, 981 (2007).

146. Roccuzzo, M., Visintin, C., Tili, F. & Visintin, R. FEAR-mediated activation of Cdc14 is the limiting step for spindle elongation and anaphase progression. *Nat Cell Biol* **17**, 251–261 (2015).

147. Simpson-Lavy, K. J. & Brandeis, M. Phosphorylation of Cdc5 regulates its accumulation. *Cell Div* **6**, 1–6 (2011).

148. Zhou, X., Li, W., Liu, Y. & Amon, A. Cross-compartment signal propagation in the mitotic exit network. *Elife* **10**, 1–30 (2021).

149. Yoshida, S. & Toh-e, A. Budding yeast Cdc5 phosphorylates Net1 and assists Cdc14 release from the nucleolus. *Biochem Biophys Res Commun* **294**, 687–691 (2002).

150. Játiva, S., Calabria, I., Moyano-Rodriguez, Y., Garcia, P. & Queralt, E. Cdc14 activation requires coordinated Cdk1-dependent phosphorylation of Net1 and PP2A–Cdc55 at anaphase onset. *Cellular and Molecular Life Sciences* **76**, 3601–3620 (2019).

151. Bi, E. & Pringle, J. R. ZDS1 and ZDS2, genes whose products may regulate Cdc42p in Saccharomyces cerevisiae. *Mol Cell Biol* **16**, 5264 (1996).

152. Stegmeier, F. *et al.* The replication fork block protein Fob1 functions as a negative regulator of the FEAR network. *Current Biology* **14**, 467–480 (2004).

153. Valerio-Santiago, M. & Monje-Casas, F. Tem1 localization to the spindle pole bodies is essential for mitotic exit and impairs spindle checkpoint function. *Journal of Cell Biology* **192**, 599–614 (2011).

154. Molk, J. N. *et al.* The Differential Roles of Budding Yeast Tem1p, Cdc15p, and Bub2p Protein Dynamics in Mitotic Exit. *Mol Biol Cell* **15**, 1519–1532 (2004).

155. Fraschini, R., Formenti, E., Lucchini, G. & Piatti, S. Budding yeast Bub2 is localized at spindle pole bodies and activates the mitotic checkpoint via a different pathway from Mad2. *J Cell Biol* **145**, 979–991 (1999).

156. Fraschini, R., D'Ambrosio, C., Venturetti, M., Lucchini, G. & Piatti, S. Disappearance of the budding yeast Bub2-Bfa1 complex from the mother-bound spindle pole contributes to mitotic exit. *J Cell Biol* **172**, 335–346 (2006).

157. Pereira, G., Höfken, T., Grindlay, J., Manson, C. & Schiebel, E. The Bub2p spindle checkpoint links nuclear migration with mitotic exit. *Mol Cell* **6**, 1–10 (2000).

158. Pereira, G. & Schiebel, E. Kin4 kinase delays mitotic exit in response to spindle alignment defects. *Mol Cell* **19**, 209–221 (2005).

159. Maekawa, H., Priest, C., Lechner, J., Pereira, G. & Schiebel, E. The yeast centrosome translates the positional information of the anaphase spindle into a cell cycle signal. *Journal of Cell Biology* **179**, 423–436 (2007).

160. Hu, F. *et al.* Regulation of the Bub2/Bfa1 GAP complex by Cdc5 and cell cycle checkpoints. *Cell* **107**, 655–665 (2001).

161. Yeh, E., Skibbens, R. v., Cheng, J. W., Salmon, E. D. & Bloom, K. Spindle dynamics and cell cycle regulation of dynein in the budding yeast, Saccharomyces cerevisiae. *J Cell Biol* **130**, 687–700 (1995).

162. Falk, J. E. *et al.* LTE1 promotes exit from mitosis by multiple mechanisms. *Mol Biol Cell* **27**, 3991–4001 (2016).

163. Bertazzi, D. T., Kurtulmus, B. & Pereira, G. The cortical protein Lte1 promotes mitotic exit by inhibiting the spindle position checkpoint kinase Kin4. *J Cell Biol* **193**, 1033 (2011).

164. Geymonat, M., Spanos, A., de Bettignies, G. & Sedgwick, S. G. Lte1 contributes to Bfa1 localization rather than stimulating nucleotide exchange by Tem1. *Journal of Cell Biology* **187**, 497–511 (2009).

165. Geymonat, M. *et al.* Control of mitotic exit in budding yeast. In vitro regulation of Tem1 GTPase by Bub2 and Bfa1. *J Biol Chem* **277**, 28439–28445 (2002).

166. Furge, K. A., Wong, K., Armstrong, J., Balasubramanian, M. & Albright, C. F. Byr4 and Cdc16 form a two-component GTPase-activating protein for the

Spg1 GTPase that controls septation in fission yeast. *Curr Biol* **8**, 947–954 (1998).

167. Visintin, R., Hwang, E. S. & Amon, A. Cfi1 prevents premature exit from mitosis by anchoring Cdc14 phosphatase in the nucleolus. *Nature* **398**, 818–823 (1999).

168. Lee, S. E., Frenz, L. M., Wells, N. J., Johnson, A. L. & Johnston, L. H. Order of function of the budding-yeast mitotic exit-network proteins Tem1, Cdc15, Mob1, Dbf2, and Cdc5. *Curr Biol* **11**, 784–788 (2001).

169. Mohl, D. A., Huddleston, M. J., Collingwood, T. S., Annan, R. S. & Deshaies, R. J. Dbf2-Mob1 drives relocalization of protein phosphatase Cdc14 to the cytoplasm during exit from mitosis. *J Cell Biol* **184**, 527–539 (2009).

170. Manzoni, R. *et al.* Oscillations in Cdc14 release and sequestration reveal a circuit underlying mitotic exit. *J Cell Biol* **190**, 209–222 (2010).

171. Campbell, I. W., Zhou, X. & Amon, A. Spindle pole bodies function as signal amplifiers in the Mitotic Exit Network. *Mol Biol Cell* **31**, 906–916 (2020).

172. Visintin, R. & Amon, A. Regulation of the Mitotic Exit Protein Kinases Cdc15 and Dbf2. *Mol Biol Cell* **12**, 2961 (2001).

173. Rock, J. M. *et al.* Activation of the yeast Hippo pathway by phosphorylation-dependent assembly of signaling complexes. *Science* **340**, 871–875 (2013).

174. Mah, A. S., Jang, J. & Deshaies, R. J. Protein kinase Cdc15 activates the Dbf2-Mob1 kinase complex. *Proc Natl Acad Sci U S A* **98**, 7325–7330 (2001).

175. Toyn, J. H., Hiroyuki, A., Akio, S. & Johnston, L. H. The cell-cycle-regulated budding yeast gene DBF2, encoding a putative protein kinase, has a homologue that is not under cell-cycle control. *Gene* **104**, 63–70 (1991).

176. Luca, F. C. & Winey, M. MOB1, an Essential Yeast Gene Required for Completion of Mitosis and Maintenance of Ploidy. *Mol Biol Cell* **9**, 29 (1998).

177. Naylor, S. G. & Morgan, D. O. Cdk1-dependent phosphorylation of iqg1 governs actomyosin ring assembly prior to cytokinesis. *J Cell Sci* **127**, 1128–1137 (2014).

178. Zhang, G., Kashimshetty, R., Kwee, E. N., Heng, B. T. & Foong, M. Y. Exit from mitosis triggers Chs2p transport from the endoplasmic reticulum to mother-daughter neck via the secretory pathway in budding yeast. *Journal of Cell Biology* **174**, 207–220 (2006).

179. Meitinger, F. *et al.* Targeted localization of Inn1, Cyk3 and Chs2 by the mitotic-exit network regulates cytokinesis in budding yeast. *J Cell Sci* **123**, 1851–1861 (2010).

180. Meitinger, F., Palani, S., Hub, B. & Pereira, G. Dual function of the NDR-kinase Dbf2 in the regulation of the F-BAR protein Hof1 during cytokinesis. *Mol Biol Cell* **24**, 1290–1304 (2013).

181. Cabib, E., Mol, P. C., Shaw, J. A. & Choi, W. J. Biosynthesis of cell wall and septum during yeast growth. *Arch Med Res* **24**, 301–303 (1993).

182. Nishihama, R. *et al.* Role of Inn1 and its interactions with Hof1 and Cyk3 in promoting cleavage furrow and septum formation in S. cerevisiae. *Journal of Cell Biology* **185**, 995–1012 (2009).

183. Oh, Y. *et al.* Mitotic exit kinase Dbf2 directly phosphorylates chitin synthase Chs2 to regulate cytokinesis in budding yeast. *Mol Biol Cell* **23**, 2445–2456 (2012).

184. König, C., Maekawa, H. & Schiebel, E. Mutual regulation of cyclin-dependent kinase and the mitotic exit network. *J Cell Biol* **188**, 351–368 (2010).

185. Kuilman, T. *et al.* Identification of Cdk targets that control cytokinesis. *EMBO J* **34**, 81 (2015).

186. Jaspersen, S. L., Charles, J. F., Tinker-Kulberg, R. L. & Morgan, D. O. A late mitotic regulatory network controlling cyclin destruction in Saccharomyces cerevisiae. *Mol Biol Cell* **9**, 2803–2817 (1998).

187. Frenz, L. M., Lee, S. E., Fesquet, D. & Johnston, L. H. The budding yeast Dbf2 protein kinase localises to the centrosome and moves to the bud neck in late mitosis. *J Cell Sci* **113 Pt 19**, 3399–3408 (2000).

188. Schmidt, M., Bowers, B., Varma, A., Roh, D. H. & Cabib, E. In budding yeast, contraction of the actomyosin ring and formation of the primary septum at cytokinesis depend on each other. *J Cell Sci* **115**, 293–302 (2002).

189. Tamborrini, D., Juanes, M. A., Ibanes, S., Rancati, G. & Piatti, S. Recruitment of the mitotic exit network to yeast centrosomes couples septin displacement to actomyosin constriction. *Nature Communications 2018 9:1* **9**, 1–15 (2018).

190. Sburlatil, A. & Cabibg, E. Chitin synthetase 2, a presumptive participant in septum formation in Saccharomyces cerevisiae. **261**, 15147–15152 (1986).

191. Shaw, J. A. *et al.* The function of chitin synthases 2 and 3 in the Saccharomyces cerevisiae cell cycle. *J Cell Biol* **114**, 111–123 (1991).

192. Wloka, C. & Bi, E. Mechanisms of cytokinesis in budding yeast. *Cytoskeleton* **69**, 710–726 (2012).

193. Onishi, M., Nolan, K., Nishihama, R. & Pringle, J. R. Distinct roles of Rho1, Cdc42, and Cyk3 in septum formation and abscission during yeast cytokinesis. *J Cell Biol* **202**, 311–329 (2013).

194. Foltman, M. *et al.* Ingression Progression Complexes Control Extracellular Matrix Remodelling during Cytokinesis in Budding Yeast. *PLoS Genet* **12**, e1005864 (2016).

195. Meitinger, F. & Palani, S. Actomyosin ring driven cytokinesis in budding yeast. *Semin Cell Dev Biol* **53**, 19–27 (2016).

196. Chin, C. F., Bennett, A. M., Ma, W. K., Hall, M. C. & Yeong, F. M. Dependence of Chs2 ER export on dephosphorylation by cytoplasmic Cdc14 ensures that septum formation follows mitosis. *Mol Biol Cell* **23**, 45–58 (2012).

197. Devrekanli, A., Foltman, M., Roncero, C., Sanchez-Diaz, A. & Labib, K. Inn1 and Cyk3 regulate chitin synthase during cytokinesis in budding yeasts. *J Cell Sci* **125**, 5453–5466 (2012).

198. Weiss, E. L. Mitotic exit and separation of mother and daughter cells. *Genetics* **192**, 1165–1202 (2012).

199. Wloka, C. *et al.* Immobile myosin-II plays a scaffolding role during cytokinesis in budding yeast. *J Cell Biol* **200**, 271–286 (2013).

200. Gladfelter, A. S., Pringle, J. R. & Lew, D. J. The septin cortex at the yeast mother–bud neck. *Curr Opin Microbiol* **4**, 681–689 (2001).

201. McMurray, M. A. & Thorner, J. Biochemical Properties and Supramolecular Architecture of Septin Hetero-Oligomers and Septin Filaments. *The Septins* 47–100 (2008) doi:10.1002/9780470779705.CH3.

202. Byers, B. & Goetsch, L. E. A highly ordered ring of membrane-associated filaments in budding yeast. *J Cell Biol* **69**, 717–721 (1976).

203. Cid, V. J., Adamiková, L., Sánchez, M., Molina, M. & Nombela, C. Cell cycle control of septin ring dynamics in the budding yeast. *Microbiology (Reading)* **147**, 1437–1450 (2001).

204. McMurray, M. A. *et al.* Septin Filament Formation Is Essential in Budding Yeast. *Dev Cell* **20**, 540–549 (2011).

205. Patasi, C. *et al.* The role of Bni5 in the regulation of septin higher-order structure formation. *Biol Chem* **396**, 1325–1337 (2015).

206. Luedeke, C. *et al.* Septin-dependent compartmentalization of the endoplasmic reticulum during yeast polarized growth. *J Cell Biol* **169**, 897–908 (2005).

207. Takizawa, P. A., DeRisi, J. L., Wilhelm, J. E. & Vale, R. D. Plasma membrane compartmentalization in yeast by messenger RNA transport and a septin diffusion barrier. *Science* **290**, 341–344 (2000).

208. Barral, Y., Mermall, V., Mooseker, M. S. & Snyder, M. Compartmentalization of the cell cortex by septins is required for maintenance of cell polarity in yeast. *Mol Cell* **5**, 841–851 (2000).

209. Lee, P. R. *et al.* Bni5p, a Septin-Interacting Protein, Is Required for Normal Septin Function and Cytokinesis in Saccharomyces cerevisiae . *Mol Cell Biol* **22**, 6906–6920 (2002).

210. Boyne, J. R., Yosuf, H. M., Bieganowski, P., Brenner, C. & Price, C. Yeast myosin light chain, Mlc1p, interacts with both IQGAP and class II myosin to effect cytokinesis. *J Cell Sci* **113 Pt 24**, 4533–4543 (2000).

211. Miller, D. P. *et al.* Dephosphorylation of Iqg1 by Cdc14 regulates cytokinesis in budding yeast. *Mol Biol Cell* **26**, 2913–2926 (2015).

212. Duran, A., Cabib, E. & Bowers, B. Chitin synthetase distribution on the yeast plasma membrane. *Science* **203**, 363–365 (1979).

213. Ee, M. T., Chuan, C. C. & Foong, M. Y. Retention of Chs2p in the ER requires N-terminal CDK1-phosphorylation sites. *Cell Cycle* **8**, 2964–2974 (2009).

214. Oh, Y., Schreiter, J., Nishihama, R., Wloka, C. & Bi, E. Targeting and functional mechanisms of the cytokinesis-related F-BAR protein Hof1 during the cell cycle. *Mol Biol Cell* **24**, 1305–1320 (2013).

215. Yoshida, S. & Toh-e, A. Regulation of the localization of Dbf2 and Mob1 during cell division of Saccharomyces cerevisiae. *Genes Genet Syst* **76**, 141–147 (2001).

216. Frenz, L. M., Lee, S. E., Fesquet, D. & Johnston, L. H. The budding yeast Dbf2 protein kinase localises to the centrosome and moves to the bud neck in late mitosis. *J Cell Sci* **113 Pt 19**, 3399–3408 (2000).

217. Douglas, C. M. *et al.* The Saccharomyces cerevisiae FKS1 (ETG1) gene encodes an integral membrane protein which is a subunit of 1,3-beta-D-glucan synthase. *Proc Natl Acad Sci U S A* **91**, 12907 (1994).

218. Mazur, P. *et al.* Differential expression and function of two homologous subunits of yeast 1,3-beta-D-glucan synthase. *Mol Cell Biol* **15**, 5671–5681 (1995).

219. Kuranda, M. J. & Robbins, P. W. Chitinase is required for cell separation during growth of Saccharomyces cerevisiae. *Journal of Biological Chemistry* **266**, 19758–19767 (1991).

220. Mendoza, M. *et al.* A mechanism for chromosome segregation sensing by the NoCut checkpoint. *Nature Cell Biology 2009 11:4* **11**, 477–483 (2009).

221. Fujiwara, T. *et al.* Cytokinesis failure generating tetraploids promotes tumorigenesis in p53-null cells. *Nature* **437**, 1043–1047 (2005).

222. Steigemann, P. *et al.* Aurora B-mediated abscission checkpoint protects against tetraploidization. *Cell* **136**, 473–484 (2009).

223. Ganem, N. J., Storchova, Z. & Pellman, D. Tetraploidy, aneuploidy and cancer. *Curr Opin Genet Dev* **17**, 157–162 (2007).

224. Gatenby, R. A. & Gillies, R. J. A microenvironmental model of carcinogenesis. *Nat Rev Cancer* **8**, 56–61 (2008).

225. Charles, J. F. *et al.* The Polo-related kinase Cdc5 activates and is destroyed by the mitotic cyclin destruction machinery in S. cerevisiae. *Curr Biol* **8**, 497–507 (1998).

226. Dischinger, S., Krapp, A., Xie, L., Paulson, J. R. & Simanis, V. Chemical genetic analysis of the regulatory role of Cdc2p in the S. pombe septation initiation network. *J Cell Sci* **121**, 843–853 (2008).

227. Niiya, F., Xie, X., Lee, K. S., Inoue, H. & Miki, T. Inhibition of cyclin-dependent kinase 1 induces cytokinesis without chromosome segregation in an ECT2 and MgcRacGAP-dependent manner. *Journal of Biological Chemistry* **280**, 36502–36509 (2005).

228. Sanchez-Diaz, A., Nkosi, P. J., Murray, S. & Labib, K. The Mitotic Exit Network and Cdc14 phosphatase initiate cytokinesis by counteracting CDK

phosphorylations and blocking polarised growth. *EMBO J* **31**, 3620–3634 (2012).

229. Prendergast, J. A. *et al.* Size selection identifies new genes that regulate Saccharomyces cerevisiae cell proliferation. *Genetics* **124**, 81–90 (1990).

230. Ghiara, J. B. *et al.* A cyclin B homolog in S. cerevisiae: chronic activation of the Cdc28 protein kinase by cyclin prevents exit from mitosis. *Cell* **65**, 163–174 (1991).

231. Dahmann, C., Diffley, J. F. X. & Nasmyth, K. A. S-phase-promoting cyclin-dependent kinases prevent re-replication by inhibiting the transition of replication origins to a pre-replicative state. *Curr Biol* **5**, 1257–1269 (1995).

232. Thomas, B. J. & Rothstein, R. Elevated recombination rates in transcriptionally active DNA. *Cell* **56**, 619–630 (1989).

233. Louvion, J. F., Havaux-Copf, B. & Picard, D. Fusion of GAL4-VP16 to a steroid-binding domain provides a tool for gratuitous induction of galactose-responsive genes in yeast. *Gene* **131**, 129–134 (1993).

234. Morawska, M. & Ulrich, H. D. An expanded tool kit for the auxin-inducible degron system in budding yeast. *Yeast* **30**, 341–351 (2013).

235. Nishimura, K., Fukagawa, T., Takisawa, H., Kakimoto, T. & Kanemaki, M. An auxin-based degron system for the rapid depletion of proteins in nonplant cells. *Nat Methods* **6**, 917–922 (2009).

236. Nishimura, K. & Kanemaki, M. T. Rapid Depletion of Budding Yeast Proteins via the Fusion of an Auxin-Inducible Degron (AID). *Curr Protoc Cell Biol* **64**, 20.9.1-20.9.16 (2014).

237. Gietz, R. D., Schiestl, R. H., Willems, A. R. & Woods, R. A. Studies on the transformation of intact yeast cells by the LiAc/SS-DNA/PEG procedure. *Yeast* **11**, 355–360 (1995).

238. Schiestl, R. H. & Gietz, R. D. High efficiency transformation of intact yeast cells using single stranded nucleic acids as a carrier. *Curr Genet* **16**, 339–346 (1989).

239. Rothstein, R. J. One-step gene disruption in yeast. *Methods Enzymol* **101**, 202–211 (1983).

240. Bähler, J. *et al.* Heterologous modules for efficient and versatile PCR-based gene targeting in Schizosaccharomyces pombe. *Yeast* **14**, 943–951 (1998).

241. Chee, M. K. & Haase, S. B. New and redesigned pRS plasmid shuttle vectors for genetic manipulation of saccharomyces cerevisiae. *G3: Genes, Genomes, Genetics* **2**, 515–526 (2012).

242. Janke, C. *et al.* A versatile toolbox for PCR-based tagging of yeast genes: new fluorescent proteins, more markers and promoter substitution cassettes. *Yeast* **21**, 947–962 (2004).

243. Ye, J. *et al.* Primer-BLAST: a tool to design target-specific primers for polymerase chain reaction. *BMC Bioinformatics* **13**, 134 (2012).

244. Gibson, D. G. *et al.* Enzymatic assembly of DNA molecules up to several hundred kilobases. *Nat Methods* **6**, 343–345 (2009).

245. Zhang, T. *et al.* An improved method for whole protein extraction from yeast Saccharomyces cerevisiae. *Yeast* **28**, 795–798 (2011).

246. Laemmli, U. K. Cleavage of structural proteins during the assembly of the head of bacteriophage T4. *Nature* **227**, 680–685 (1970).

247. Foiani, M., Liberi, G., Lucchini, G. & Plevani, P. Cell Cycle-Dependent Phosphorylation and Dephosphorylation of the Yeast DNA Polymerase-Primase B Subunit. *Mol Cell Biol* **15**, 883–891 (1995).

248. Sanchez-Diaz, A. *et al.* Inn1 couples contraction of the actomyosin ring to membrane ingression during cytokinesis in budding yeast. *Nat Cell Biol* **10**, 395–406 (2008).

249. Neurohr, G. & Mendoza, M. Cdc14 Localization as a Marker for Mitotic Exit: In Vivo Quantitative Analysis of Cdc14 Release. *Methods Mol Biol* **1505**, 59–67 (2017).

250. Bousset, K. & Diffley, J. F. X. The Cdc7 protein kinase is required for origin firing during S phase. *Genes Dev* **12**, 480–490 (1998).

251. Geymonat, M. *et al.* Orderly assembly underpinning built-in asymmetry in the yeast centrosome duplication cycle requires cyclin-dependent kinase. *Elife* **9**, 1–29 (2020).

252. Labib, K., Diffley, J. F. X. & Kearsey, S. E. G1-phase and B-type cyclins exclude the DNA-replication factor Mcm4 from the nucleus. *Nature Cell Biology 1999 1:7* **1**, 415–422 (1999).

253. Nakanishi, H., de Los Santos, P. & Neiman, A. M. Positive and negative regulation of a SNARE protein by control of intracellular localization. *Mol Biol Cell* **15**, 1802–1815 (2004).

254. Jaspersen, S. L. & Morgan, D. O. Cdc14 activates Cdc15 to promote mitotic exit in budding yeast. *Current Biology* **10**, 615–618 (2000).

255. Nadal-Ribelles, M. *et al.* Control of Cdc28 CDK1 by a stress-induced lncRNA. *Mol Cell* **53**, 549–561 (2014).

256. Jin, F. *et al.* Temporal control of the dephosphorylation of Cdk substrates by mitotic exit pathways in budding yeast. *Proc Natl Acad Sci U S A* **105**, 16177–16182 (2008).

257. Holt, L. J. *et al.* Global analysis of cdk1 substrate phosphorylation sites provides insiqhts into evolution. *Science (1979)* **325**, 1682–1686 (2009).

258. Stegmeier, F. & Amon, A. Closing Mitosis: The Functions of the Cdc14 Phosphatase and Its Regulation. *https://doi.org/10.1146/annurev.genet.38.072902.093051* **38**, 203–232 (2004).

259. Valerio-Santiago, M., de los Santos-Velázquez, A. I. & Monje-Casas, F. Inhibition of the Mitotic Exit Network in Response to Damaged Telomeres. *PLoS Genet* **9**, e1003859 (2013).

260. Komarnitsky, S. I. *et al.* DBF2 Protein Kinase Binds to and Acts through the Cell Cycle-Regulated MOB1 Protein. *Mol Cell Biol* **18**, 2100–2107 (1998).

261. Visintin, R. & Amon, A. Regulation of the Mitotic Exit Protein Kinases Cdc15 and Dbf2. *Mol Biol Cell* **12**, 2961 (2001).

262. Frenz, L. M., Lee, S. E., Fesquet, D. & Johnston, L. H. The budding yeast Dbf2 protein kinase localises to the centrosome and moves to the bud neck in late mitosis. *J Cell Sci* **113 Pt 19**, 3399–3408 (2000).

263. Yoshida, S. & Toh-e, A. Regulation of the localization of Dbf2 and mob1 during cell division of saccharomyces cerevisiae. *Genes Genet Syst* **76**, 141–147 (2001).

264. Rock, J. M. *et al.* Activation of the Yeast Hippo Pathway by Phosphorylation-Dependent Assembly of Signaling Complexes. *Science* **340**, 871–875 (2013).

265. Higuchi, T. & Uhlmann, F. Stabilization of microtubule dynamics at anaphase onset promotes chromosome segregation. *Nature* **433**, 171 (2005).

266. Pereira, G. & Schiebel, E. Separase Regulates INCENP-Aurora B Anaphase Spindle Function Through Cdc14. *Science (1979)* **302**, 2120–2124 (2003).

267. Cavanaugh, A. M. & Jaspersen, S. L. Big Lessons from Little Yeast: Budding and Fission Yeast Centrosome Structure, Duplication, and Function. *Annu Rev Genet* **51**, 361–383 (2017).

268. Campbell, I. W., Zhou, X. & Amon, A. The Mitotic Exit Network integrates temporal and spatial signals by distributing regulation across multiple components. *Elife* **8**, (2019).

269. Visintin, R., Stegmeier, F. & Amon, A. The role of the polo kinase Cdc5 in controlling Cdc14 localization. *Mol Biol Cell* **14**, 4486–4498 (2003).

270. Almeida, A. de, Raccurt, I., Peyrol, S. & Charbonneau, M. The Saccharomyces cerevisiae Cdc14 phosphatase is implicated in the structural organization of the nucleolus. *Biol Cell* **91**, 649–663 (1999).

271. Pereira, G. & Schiebel, E. Separase Regulates INCENP-Aurora B Anaphase Spindle Function Through Cdc14. *Science (1979)* **302**, 2120–2124 (2003).

272. Higuchi, T. & Uhlmann, F. Stabilization of microtubule dynamics at anaphase onset promotes chromosome segregation. *Nature* **433**, 171 (2005).

273. Cavanaugh, A. M. & Jaspersen, S. L. Big Lessons from Little Yeast: Budding and Fission Yeast Centrosome Structure, Duplication, and Function. *Annu Rev Genet* **51**, 361–383 (2017).

274. König, C., Maekawa, H. & Schiebel, E. Mutual regulation of cyclin-dependent kinase and the mitotic exit network. *Journal of Cell Biology* **188**, 351–368 (2010).

275. Vannini, M. *et al.* A Novel Hyperactive Nud1 Mitotic Exit Network Scaffold Causes Spindle Position Checkpoint Bypass in Budding Yeast. *Cells* **11**, (2021).

276. Swaney, D. L. *et al.* Global analysis of phosphorylation and ubiquitylation cross-talk in protein degradation. *Nat Methods* **10**, 676–682 (2013).

277. Jumper, J. *et al.* Highly accurate protein structure prediction with AlphaFold. *Nature 2021 596:7873* **596**, 583–589 (2021).

278. Varadi, M. *et al.* AlphaFold Protein Structure Database: massively expanding the structural coverage of protein-sequence space with high-accuracy models. *Nucleic Acids Res* **50**, D439–D444 (2022).

279. Howell, R. S. M., Klemm, C., Thorpe, P. H. & Csikasz-Nagy, A. Unifying the mechanism of mitotic exit control in a spatiotemporal logical model. *PLoS Biol* **18**, (2020).

280. Visintin, R. & Amon, A. Regulation of the mitotic exit protein kinases CDc15 and Dbf2. *Mol Biol Cell* **12**, 2961–2974 (2001).

281. Rock, J. M. & Amon, A. Cdc15 integrates Tem1 GTPase-mediated spatial signals with Polo kinase-mediated temporal cues to activate mitotic exit. *Genes Dev* **25**, 1943–1954 (2011).

282. Pereira, G., Tanaka, T. U., Nasmyth, K. & Schiebel, E. Modes of spindle pole body inheritance and segregation of the Bfa1p–Bub2p checkpoint protein complex. *EMBO J* **20**, 6359–6370 (2001).

283. Pereira, G., Höfken, T., Grindlay, J., Manson, C. & Schiebel, E. The Bub2p spindle checkpoint links nuclear migration with mitotic exit. *Mol Cell* **6**, 1–10 (2000).

284. Howell, R. S. M., Klemm, C., Thorpe, P. H. & Csikasz-Nagy, A. Unifying the mechanism of mitotic exit control in a spatiotemporal logical model. *PLoS Biol* **18**, (2020).

285. Sullivan, M., Higuchi, T., Katis, V. L. & Uhlmann, F. Cdc14 phosphatase induces rDNA condensation and resolves cohesin-independent cohesion during budding yeast anaphase. *Cell* **117**, 471–482 (2004).

286. D'Amours, D., Stegmeier, F. & Amon, A. Cdc14 and condensin control the dissolution of cohesin-independent chromosome linkages at repeated DNA. *Cell* **117**, 455–469 (2004).

7. Annexes

7.1. Figures table

7.2. Table of abbreviations

Abbrevation	Meaning
AMR	Actomyosin Ring
APC	Anaphase Promoting Complex
CDC	Cell Division Cycle
CDK	Cyclin Dependent Kinase
Con A	Concanavalin A
CV	Coefficient of Variation
DAPI	4′,6-diamidino-2-phenylindole
EDTA	Ethylenediaminetetraacetic acid
ER	Endoplasmic Reticulum
EtBr	Ethidium Bromide
FEAR	cdc Fourteen Early Release
GAP	GTPase Activating Protein
GEF	Guanine nucleotide Exchange Factor
IPC	Ingression Progression Complex
LB	Luria Broth
LLB	Laemmli Loading Buffer
MBF	Mlu I Cell-cycle Box Binding Factor
MCC	Mitotic Checkpoint Complex
MCS	Multiple Cloning Site
MEN	Mitotic Exit Network
ORF	Open Reading Frame
PS	Primary Septum
SAC	Spindle Assembly Checkpoint
SBF	Swi4/6 Cell-Cycle Box Binding Factor
SC	Synthetic Complete
SCD	Synthetic Complete Dextrose
SCGal	Synthetic Complete Galactose
SCRaff	Synthetic Complete Raffinose
SDS	Sodium Dodecyl Sulfate
SFF	Swi five Factor
SPB	Spindle Pole Body (m for *mother*, d for *daughter*)
SPOC	Spindle Position Checkpoint
TEMED	Tetramethylethylenediamine
TSAP	Thermosensitive Alkaline Phosphatase
YP	Yeast extract Peptone
YPD	Yeast Extract Peptone Dextrose
YPGal	Yeast extract Peptone Galactose
YPRaff	Yeast extract Peptone Raffinose

7.3. Acknowledgements

This thesis has been, without any shade of a doubt, the hardest project I have ever undertaken in my life. I think that, if I have been able to finish it, it is thanks to an enormous amount of help from good and caring people.

I would like to thank my boss and mentor, David Garcia Quintana. I am forever in debt to your teachings over these years. If my previous mentors showed me a tiny glimpse of what science is about, you have shown me what it really means to be a scientist. For your passion, your ideas, the opportunities you have given me and your unquestioned trust in me, thank you.

I would also like to thank the members of my yearly thesis review committee, Francesc Posas, Martí Aldea and Javier Jiménez, for their attention and challenging discussions over the years, as well as the opportunities given to work in their facilities, especially Javier.

Besides them, I would like to thank the people with whom I have spent the last 6 years at the Biophysics Unit. Thank you, Alex, Ramon, Pep, Núria, Mireia, and Elena. You are all good people and have always been kind and friendly to me. I would also like to thank Gloria, without whom I would not have learned how to properly work in a lab. Finally, I would like to dedicate a special mention to Elodia, our lab technician. Without her work, her support, and her company, none of us in the lab (particularly me) would be able to achieve nearly as much.

Finally, special thanks to Dr Karim Labib and his lab (Cristian, Ryo, Tasha, Johanna, Cécile, Fabrizio and Remi) and all the people in Dundee for the opportunity given to work in their lab this last summer, for my greatest of times doing and learning science and for being so helpful and friendly to me. I will visit you again soon.

On a more personal note, I would like to remember the people that are not in the lab anymore but have been under my responsibility, as well as people that briefly joined the lab. Thank you, Biel, Viviana, Pep, Ainoa, Adrià and Miguel. You have no idea how much it helped me having someone around, someone to teach and someone to share a laugh with. I hope you had as much fun in the lab with me as I had with you.

And thank you Èric, David and Mario for those Padel matches. I really needed those.

Para acabar, me gustaría, en mi lengua materna, dar las gracias a mi familia. A mi padre Ernesto y mi madre, Conchita. A mi hermana María i Carles. A mis tíos Antonio y Gloria. Y a mi abuela María y mi tía Luisa, que sé que les habría encantado estar aquí para verlo. Aun cuando no siempre he estado, vosotros me habéis animado a seguir adelante. Y para mi pareja, Isa, por todo el apoyo y amor que me has dado estos años.